5-2018

Accounting for Uncertainty in Process Optimization Initiatives with Statistical Convolutions and Stochastic Programming Techniques

Russell William Krenek
Clemson University, rkrenek@clemson.edu

ACCOUNTING FOR UNCERTAINTY IN PROCESS OPTIMIZATION INITIATIVES WITH STATISTICAL CONVOLUTIONS AND STOCHASTIC PROGRAMMING TECHNIQUES

A Dissertation
Presented to
the Graduate School of
Clemson University

In Partial Fulfillment
of the Requirements for the Degree
Doctor of Philosophy
Industrial Engineering

---

by
Russell William Krenek
May 2018

Accepted by:
Dr. Byung Rae Cho, Committee Chair
Dr. Sandra D. Ekşioğlu
Dr. David M. Neyens
Dr. Robert Riggs

ABSTRACT

The purpose of this dissertation is to explore the uncertainty of process means and variances in order to improve processes with stochastic characteristics due to the complex nature of the underlying probability distributions. First, the gap between the existing conceptual notion of defects per million opportunities (DPMO) as part of process improvement initiatives and its applications to real-world engineering processes is explored. This is important because the current way of obtaining the DPMOs documented in the literature is problematic since it strictly assumes that there will be a shift in the process mean over time, while process variability remains unchanged. Accordingly, it does not account for shifting process standard deviation. This may not be the case in real-world practices. Several unique contributions to the Six Sigma body of knowledge are offered by expanding the existing DPMO and process fallout concepts, ultimately leading to process improvement. Second, convolutions of normal random variables are explored. Convolutions often arise in engineering problems, and the probability densities of the sums of these random variables are known in the literature. There are practical situations where specification limits on a process are imposed externally, and the product is typically scrapped if its performance does not fall in the specification range. The actual distribution after inspection is therefore truncated. Despite the practical importance of the role of truncated distributions, there has been little work on the theoretical foundation of convolutions associated with truncated random variables. This is paramount, since

convolutions are often used as an important standard in statistical tolerance analysis. The convolutions of the combinations of truncated normal and truncated skew normal random variables on double and triple truncations are developed. This allows for a more accurate assessment of the mean and variance for a given process. Furthermore, it may not always be possible to define the specification limits and tolerances precisely within the limits of a probability density function for a process due to a relatively inaccurate or unstable process. This situation will be addressed through stochastic constrained programming.

DEDICATION

This dissertation is dedicated to my family. Without their support none of this would have been possible.

ACKNOWLEDGMENTS

I acknowledge my committee chair Dr. Byung Rae Cho for teaching me how to write and never giving up on me. I am further grateful for my committee members Dr. Sandra D. Ekşioğlu, Dr. David M. Neyens, and Dr. Robert Riggs for all of their valuable input and council. I would also like to recognize the Industrial Engineering Department at Clemson University, for without their support in helping me none of this would have been possible. In particular, I would like to thank Dr. Sandra D. Ekşioğlu, Dr. David M. Neyens, Dr. Tugce Isik and Dr. Laura Stanley for helping me prepare for job interviews and providing me with advice to help me sell myself better. In addition, I would have been lost without the support of Martin Clark, Jenny Wirtz, and Debra Smith. I would also like to thank Dr. Cole Smith for providing me with excellent advice over the course of my studies. I realize that it took a small army of people to help me complete my dissertation, and I am forever grateful.

TABLE OF CONTENTS

Page

Table of Contents (Continued)

Page

Table of Contents (Continued)

LIST OF TABLES

List of Tables (Continued)

LIST OF FIGURES

List of Figures (Continued)

Figure Page

List of Figures (Continued)

Figure Page

List of Figures (Continued)

Figure Page

List of Figures (Continued)

Figure Page

CHAPTER ONE

INTRODUCTION

The purpose of this dissertation is to explore the uncertainty of process means and variances in order to improve processes with stochastic characteristics due to the complex nature of the underlying probability distributions. This will be done by first exploring combined effect of shifted process mean and changing process variance to explore the consequences of process fallout when the normal distribution is used in a complex system. Here, process fallout is defined as the violation of the upper or lower specification limits that could result in a product being scrapped or reworked. Second, various combinations of truncated normal and truncated skew normal random variables will be used as a way to more accurately assess the mean, variance and underlying probability distribution of complex systems, such as a multistage production process. Third, stochastic programming techniques will be used to help optimize tolerances in systems where there is a great amount of uncertainty.

1.1 Analyzing the combined effect of shifted process mean and changing process variance to explore the consequences of process fallout when the normal distribution is used in a production process.

To the author's knowledge the compounding effect of changing variability as the process mean shifts overtime on product or service defect rates has not been explored prior to this study. This is a critical issue since production processes do not all have centered process means and equal variances. Therefore, assumptions underlying process fallout may be grievously incorrect in many situations in which processes shift and change over long periods of time.

The long term shifted mean of a product or service production process is also an important assumption within the Six Sigma framework that has not been thoroughly evaluated. Although the literature mentioning the 1.5 sigma shift assumption within the Six Sigma framework is vast, very few comprehensive quantitative studies have been done validating this assumption which has caused much controversy. Furthermore, the compounding effect of changing variability as the process mean shifts overtime on product or service defect rates has not been explored at all. This is a critical issue since production processes do not all have centered process means and equal variances. Therefore assumptions underlying process fallout within the Six Sigma framework may be grievously incorrect in many situations. This study aims to rectify this knowledge gap by exploring process fallout under different variances and mean shifts. A mathematical framework will also be developed in order to provide insight into optimizing these processes under various mean and variance assumptions so that operating conditions will provide minimum process fallout.

1.2 Using covolutions to assess uncertainty and predict outcomes in complex systems by examining the convolutions of truncated normal and truncated skew normal random variables

Convolutions of normal random variables often arise in engineering problems, and the probability densities of the sums of these random variables are known in the literature. There are practical situations where specification limits on a process are imposed externally, and the product is typically scrapped if its performance does not fall in the specification range. As such, the actual distribution after inspection is truncated. Despite the practical importance of the role of truncated distributions, there has been little work on the theoretical foundation of convolutions associated with truncated random variables. This is paramount, since convolutions are often used as an important standard in statistical tolerance analysis. In this paper, the convolutions of the combinations of truncated normal and truncated skew normal random variables on double and triple truncations are developed. The successful completion of this research task on convolution could help obtain a better understanding of integrated effects of statistical tolerance analysis in engineering design, leading to process and quality improvement.

The analysis of convolutions on these distributions can also lead to minimizing waste in manufacturing processes. This is paramount in promoting sustainability and saving companies' time, money and physical resources in the process. This can be particularly useful in many common manufacturing processes which involve casting, molding, forming, machining, joining or other additive manufacturing processes such as stereolithography, which produce products in multiple steps, one layer at a time. Accurate screening inspections may also contribute to a more efficient use of resources in the production process. Scraping and reuse of wasted raw materials as part of a production process can be analyzed more precisely through truncated normal distributions, and their associated convolutions. This section of the manuscript will also explore the mathematical foundations of various truncated normal distributions and the convolutions of these distributions in order to offer insights into noteworthy methods used to meticulously account for material use.

1.3 Developing a Two-Stage Stochastic Programming Model in Tolerance Optimization using a Guard Band Approach

Parts cannot be manufactured to exact nominal dimensions due to variation in materials, machines and the people that control the manufacturing process. As a result, the specification limits and their associated tolerances can have a vast impact on the quality, performance and cost of the finished product. This has created a large research interest in obtaining optimal tolerances and specification limits in order to not only reduce manufacturing costs, but also to minimize the expected quality loss of a product. The expected quality loss of a product includes not only scrap and rework costs, but also incorporates costs as a part or product deviates from a nominal value. Furthermore, unnecessarily tight tolerances may result in a complicated and costly manufacturing process, while low tolerances mean a lower manufacturing cost, but weaker product performance.

One of the key difficulties of any process is defining the specification limits and tolerances precisely within the limits of a probability density function. This may not always be possible, however, since the production process may not be sophisticated or accurate enough to manufacture a product within the specification limits. Under this situation, where the production process is not stable enough to be able to calculate the probability that the product falls outside of the specification limits exactly, one could guarantee that the product is within the specification limit or outside the specification limits with a certain probability. This would allow practitioners to have the maximum amount of control over setting specifications and tolerances of their product within their inherently unstable process. This could be done by incorporating a technique known as chance constrained programming into tolerance optimization.

Chance constrained or stochastic programming is an approach for modeling problems that have uncertain parameters. This is opposed to deterministic programming approaches that have known parameters and are usually tractable, however most deterministic approaches often do not accurately account for real world variables and parameters which are often uncertain at the time of making a decision. Subject pioneers Charnes and Cooper define chance constrained programming as the process of selecting certain random variables as functions of random variables in order to maximize a functional of random variables subject to constraints that must be maintained at prescribed levels of certainty represented by a probabilistic value (Charnes & Cooper, 1959). They illustrate this idea by comparing the deterministic and chance constrained forms of an inventory model involving oil tankage facilities supplied by a refinery, where expected profit is maximized subject to specified probability constraints where a certain minimum inventory must be maintained with a certain probability and inventory must not exceed a certain maximum with a certain specified probability. Other prominent examples of chance constrained programming include situations in which decisions are made repeatedly within a similar set of circumstances and the objective is to formulate a solution that will perform well on average, such as designing truck routes for package carriers, whose customers have random demand for packages. Chance constrained programming can also be applied to situations in which a one-time decision must be made such as the initial investments in a financial portfolio, activity analysis and technology planning, capital budgeting, dietary planning, and material composition selection.

The overarching goal in this section is to present ways of managing chance constrained programming problems by utilizing the Normal distribution in order to make constraints relatively manageable by improving tractability in difficult tolerance optimization problems. In particular, that practitioners can benefit from the results illustrated in this manuscript, which has a particular focus on tolerance optimization.

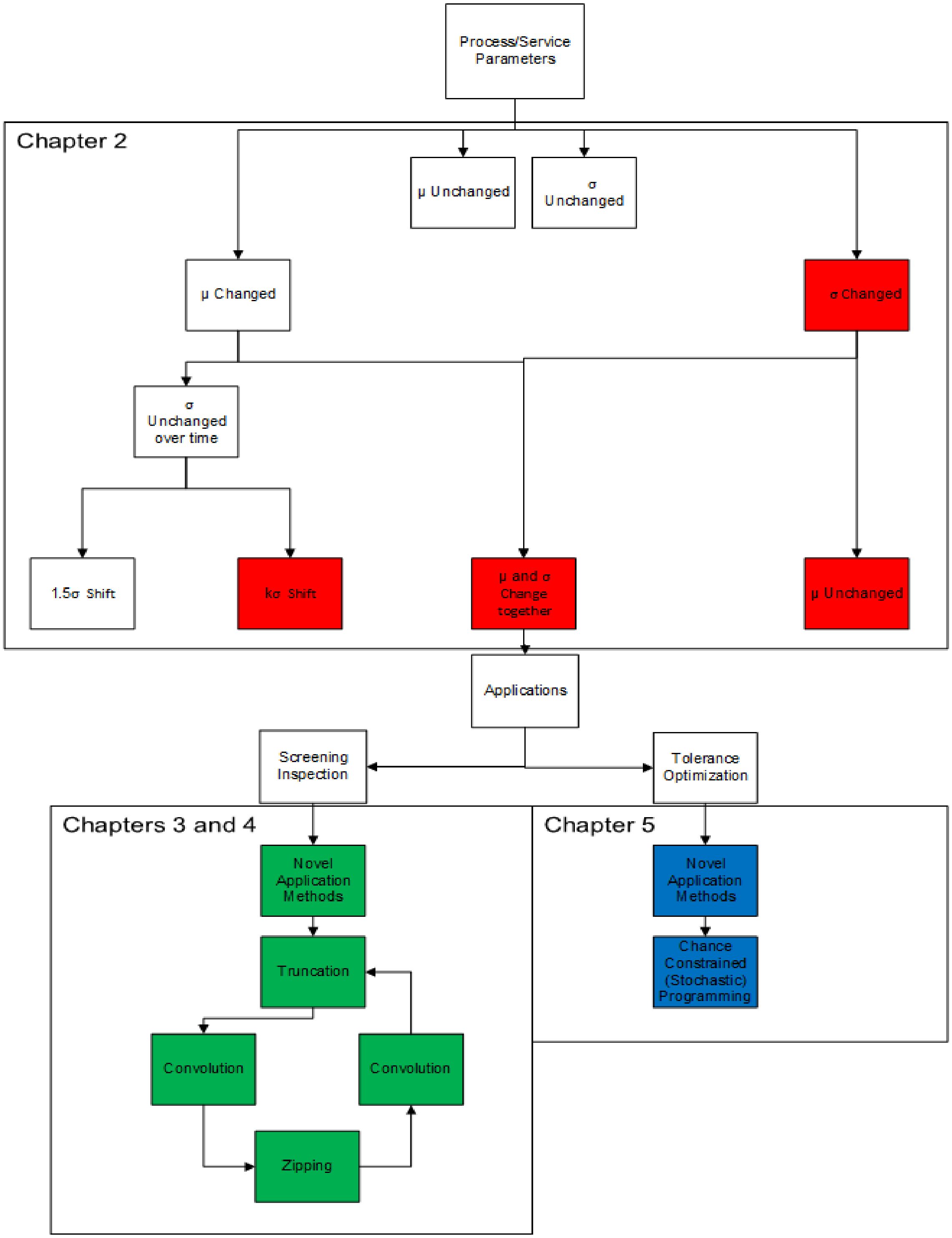

1.1 The Relationship of the Dissertation Components. The shaded boxes represent contributions to the literature

CHAPTER TWO

THE EXPANDED DPMO INTERFACE FOR CAPTURING THE COMPOUNDING EFFECT OF PROCESS MEAN AND VARIABILITY AS A NEW PARADIGM FOR PROCESS EVALUATION AND IMPROVEMENT

This chapter has been published in the International Journal of Six Sigma and Competitive Advantage and should be cited as:

Krenek, R. and Cho, B.R. (2015) 'The expanded DPMO interface for capturing the compounding effect of process mean and variability as a new paradigm for process evaluation and improvement', Int. J. Six Sigma and Competitive Advantage, Vol. 9, Nos. 2/3/4, pp.174–207.

2.1 Introduction

In an industrial manufacturing environment, less product fallout typically leads to more efficient production with less work stoppage and greater profits with more conserved raw materials. A more accurate assessment of process fallout allows companies to better assess true process performance, thereby better allocating resources to improve the process and reduce costs simultaneously. Industrial examples are numerous. Consider a company that manufactures a metal connector that has to be reworked if it falls outside its upper or lower specification limit. Understanding process fallout and performance in this case will allow the company to better allocate resources to improve the manufacturing process as well as pinpoint the area of rework for the metal connector. This includes machining the metal connector if it falls outside the upper specification limit (USL) and remolding the connector if it falls outside the lower specification limit (LSL). In a service environment, time and money are saved. In endocrinology, suppose a patient's insulin levels are out of control. Being able to better assess insulin levels could be paramount to a better diabetes treatment and help prevent excessive medical costs, both financially and physically, to the patient.

Current Six Sigma techniques do not account for a shifting process standard deviation over time. This standard deviation shift, coupled with the process mean shift has also not been explored. This article aims to rectify this knowledge gap by illuminating the mean and standard deviation shift issue and then show examples of how these shifts can be applied to several dependent quality characteristics at one time.

2.2 Literature Review

In process improvement initiatives, defects per million opportunities, or DPMO, serves as a conceptual cornerstone for measuring process performance. DPMO is implemented primarily in the manufacturing sector; however, it has also been successfully linked to other service industries, including healthcare. In healthcare, for example, (Taner, Kagan, Celik, Erbas, & Kagan, 2013) used DPMOs to measure the number of complications that occurred, while trying to improve a coronary stent insertion process. They also used DPMO to measure the number of repeat scans in evaluating the effectiveness of a diagnostic imaging department in a private hospital (Taner, Sezen, & Atwat, 2011). In the construction industry, (Gijo & Sarkar, 2012) used DPMO to measure the number of defects in wind farm roads in order to help improve the road quality for wind turbine installation. In a call center, DPMO were used to measure the number of unresolved queries after the first phone call (Laureani, Antony, & Douglas, 2010). DPMO have also been used to evaluate the effectiveness of government electronic services through website and computer system quality

(Alhyari, Alazab, Venkatraman, Alazab, & Alazab, 2012). Other application areas of the DPMO concept include printed circuit board assembly (Santos et al., 1997; Tsai, 2012), microbiology (Elder, 2008), aircraft design (Maleyeff and Krayenvenger, 2004; Gijo and Ashok, 2014), supply chain (Lanier, 2012), billing operation (Levlzow, 2013), healthcare operations (Carrign and Kujwa, 2006; Pocha, 2010), information technology (Chiao, 2006), material handling (Das, 2005), pharmaceuticals (Kamberi, 2011), and process control (Yang, 2009).

The DPMO and process fallout concepts also play an important conceptual role in Six Sigma. The Six Sigma concept introduces an assumption that when a process reaches the six sigma quality level, the process mean is subject to disturbances that could cause it to shift by up to 1.5 standard deviations off target, resulting in 3.4 DPMO. This assumption accounts for a long-term variation in a production or service process mean. This assumption about the mean shift has been a source of controversy within the Six Sigma literature. (Stevenson, 2009) had conducted a comprehensive study assessing the validity of the 1.5 sigma shift. This was performed on an industrial company that makes off-highway vehicles. Some have argued that if the mean drifts, the process might be unstable and predictions can only be made when the process is stable, while others argue that the 3.4 DPMO assumption might not be reliable, since the mean could be shifted by more than 1.5 standard deviations (Montgomery & Woodall, 2008). Furthermore, little research work has been done on the 1.5 sigma shift assumption and this issue should become a major thrust for future research (Antony, 2004). Bothe (2002) provided a statistically based reason for the 1.5 shift in the process means by examining the sensitivity of control charts to detect changes of various magnitudes and developed the corresponding Cpk process capability index (PCI). Note that process capability indices are defined as the ability of a process to produce outputs within specification limits. Cpk in particular depends inversely on the process standard deviation and becomes large as the standard deviation approaches zero; hence, the Cpk can be a poor measure of process centering. In order to address this issue, Cpm can be used as a better measure of process centering. Estimators and sampling properties associated with the Cpm are discussed in (Chan, Cheng, & Spiring, 1988). Along the same line, Cpm's usefulness in process centering was explored in (Boyles, 1991) which discussed the fact that Cpk and Cpm are equivalent to Cp, when the mean value of the process is on target and decrease as the mean value moves away from the target. However, these values need increased sensitivity to account for departures of the process mean from the desired target value. Consequently, Cpkm, was introduced by (Pearn, Kotz, & Johnson, 1992). The majority of the industrial uses of process capability ratios are used for estimating and interpreting the point estimates of process capability indices. Also, the confidence intervals for process capability ratios and associated statistical hypothesis tests may be important methods to describe the processes. It is noted that since the standard deviation for a process is being estimated, only approximate confidence intervals can be used. (Zhang, Stenback, & Wardrop, 1990), for example, developed a confidence interval for the Cpk index. Other authors that have developed approximate confidence intervals for capability indices include (Kushler & Hurley, 1992), (Bissell, 1990), and (Pearn et al., 1992). For non-normal data, the Cpc index with its confidence interval developed by (Luceño, 1996) can be employed.

The long-term shifted mean of a product or service production process is an important assumption within the Six Sigma framework that has not been thoroughly evaluated. Although the literature mentioning the 1.5 sigma shift assumption within the Six Sigma framework is vast, very few comprehensive quantitative studies have been done validating this assumption which has caused much controversy. Furthermore, the compounding effect of changing variability as the process mean shifts over time on product or service defect rates has not been explored for stable processes at all. This is a critical issue since production processes do not all have centered process means and constant variances. Therefore, assumptions underlying process fallout may be incorrect in many situations. The examination of mean and variability shifts also needs to be explored in the context of process capability analysis, since it is an important part of an overall process improvement program that can help reduce the variability in a manufacturing process. Mean and variability shifts can also help to predict how well processes will hold the tolerances, and assist product developers in selecting or modifying processes. Exploring this notion will also help in establishing a sampling interval for process monitoring, specify performance requirements for new equipment, and help a company select between competing suppliers on a quality basis. In addition, this gives process designers' insights into planning the sequence of production processes when there is an interactive effect on process tolerances. This paper aims to rectify this knowledge gap by exploring process fallout under different variances and mean shifts with the consideration of single and dual quality characteristics. In addition, the process capability indices are also augmented with a standard deviation shift factor for improved accuracy.

This paper is organized as follows. In the next section, a brief review of existing DPMO and PCI concepts is given. In Section 2.3, two proposed models for DPMO evaluations are provided by considering process variability shifts and joint process mean and variability shifts. Section 4 extends these concepts to dual quality characteristics and evaluates DPMO values, followed by numerical examples in Section 2.5. Conclusions and future study are discussed in Section 2.6.

2.3 Review of Existing DPMO and PCIs

Six Sigma programs define Six Sigma Quality of a product or service as having LSL and USL falling within 6 standard deviations of the mean but incorporate a 1.5 sigma shift to calculate the DPMO (Montgomery, 2013). This assumption accounts for long term variation in a production or service process mean. This is needed because special or assignable causes can result in deterioration of process performance over time. The 1.5 sigma shift within the six sigma framework helps prevent underestimation of defect levels likely to be seen within real processes; however, not much research work has been done to explore the consequences of this assumption. The 1.5 sigma shift results in about 3.4 DPMO (Bothe, 2002). The basic mathematical framework is presented as follows.

The cumulative normal distribution function is defined as $f(z)=\int_{-\infty}^{z}\frac{1}{\sqrt{2\pi\sigma^2}}e^{-\frac{1}{2}\left(\frac{x-\mu}{\sigma}\right)^2}dx$. The standard normal cumulative probabilities can be evaluated to any prescribed accuracy using the standard cumulative normal distribution function $\Phi(z)=\int_{-\infty}^{z}\frac{1}{\sqrt{2\pi}}e^{-\frac{1}{2}x^2}dx$ and the Lagrange remainder for the error bounds of the Taylor series polynomial, since the above integral has no closed-form expression. Standard examples of numerical integration include the trapezoid rule or Simpson's rule. Using the definition of the standard normal cumulative distribution function, one can now formally define what is referred to as the DPMO for the left standard deviation shift size for the mean as $\left(1-P\left(\frac{(\mu-6\sigma-x\sigma)-\mu}{\sigma}<z<\frac{(\mu+6\sigma-x\sigma)-\mu}{\sigma}\right)\right)10^6$ which simplifies to $\left(1-\left(\Phi(6-x)-\Phi(-6-x)\right)\right)10^6$ where x represents the shift size in standard deviation. Similarly, the DMPO for the right standard deviation shift size is given by $\left(1-P\left(\frac{(\mu-6\sigma+x\sigma)-\mu}{\sigma}<z<\frac{(\mu+6\sigma+x\sigma)-\mu}{\sigma}\right)\right)10^6$ or $\left(1-\left(\Phi(6+x)-\Phi(-6+x)\right)\right)10^6$. From this mathematical framework the concept of defects per unit can also be defined. Defects per unit, or DPU, is the number of defects found in a sample divided by the number of units sampled.

It should be noted that process shift and drift over time also affects the capability of a process. This is important since, the process capability indices measure how much variation due to common causes affects the process relative the specific process's specification limits. This allows for different processes to be compared with respect to how well an organization can control them, and these statistics are tracked over time. PCIs, such as Cp, are widely used in industry, but are unfortunately misused and misinterpreted quite frequently (Kotz & Lovelace, 1998). Various non-normal distributions have been investigated with regards to Cp and it was found that errors of several orders of magnitude were made when predicting process fallout by incorrectly making the normal distribution assumption. Even with using a t-distribution with as many as 30 degrees of freedom resulted in substantial errors (Somerville & Montgomery, 1996). Note that a t-distribution is approximately normal for 30 degrees of freedom, but the heavier tails of the t-distribution make a significant difference when determining process fallout. Therefore, it is important to check the normality assumption of the data. If the data is non-normal, transformation techniques such as the Box-Cox transformation (Box & Cox, 1964) or the Johnson transformation (Hernandez & Johnson, 1980) should be used.

PCIs are only useful if the process is in statistical control, so the value of computing PCIs from historical data may be greatly diminished or useless if the process is out of control. This is because process capability indices measure how much the variation from common causes affect the process relative to the process's specification limits. Finally, what is observed in practice is actually only an estimate of true process capability. The estimate is subject to error in estimation, since it is dependent on sample statistics. Large errors in estimating PCIs from sample data can occur, so that the estimates obtained are not very accurate (English & Taylor, 1993). With respect to the

Six Sigma framework, a centered process with no shifting mean and a constant standard deviation has a sigma level of 3 if the process capability index is 1, and a sigma level of 6 if the process capability index is 2 (Montgomery, 2013). Common univariate process capability indices are given in Table 2.1.

Table 2.1: Common process capability indices as defined in Montgomery (2013).

Index	**Description**
$C_p = \frac{USL - LSL}{6\sigma}$	Estimates the process capability by assuming a centered mean
$C_{p,lower} = \frac{\mu - LSL}{3\sigma}$	Estimates the process capability for a process that has a lower limit only.
$C_{p,upper} = \frac{USL - \mu}{3\sigma}$	Estimates the process capability for a process that has an upper limit only.
$C_{pk} = \min\left(C_{p,upper}, C_{p,lower}\right)$	Estimates the process capability for a process by taking into account that the process mean may not be centered between the specification limits. If this capability index is less than zero then the process mean falls outside of specification limits.
$C_{pm} = \frac{C_p}{\sqrt{1+\left(\frac{\mu - T}{\sigma}\right)^2}}$	Estimates the process capability around a specified production target, T. This index assumes that the process mean is centered between the specification limits.
$C_{pkm} = \frac{C_{pk}}{\sqrt{1+\left(\frac{\mu - T}{\sigma}\right)^2}}$	Estimates the process capability around a specified production target, T. This index accounts for an off-center process mean.

Since the standard normal distribution is symmetric about its mean, the DPMO calculations for the left shifted and right shifted means will be the same. Sample DPMO and PCIs resulting from various sigma shifts are found in Table 2. Note that the Cpm and Cpkm values assume that the process was originally on target and has shifted over time. Notice that the Cp capability index is extremely poor since it does not account for process "shift and drift". Notice also that these DPMO are the same for both the left sigma shifts and the right sigma shifts since

$$\left(1-\left(\Phi\left(6-x\right)-\Phi\left(-6-x\right)\right)\right)10^6 = (1-((1-\Phi(-6+x))-(1-\Phi(6+x)))10^6$$

$$=\left(1-\left(\Phi\left(6+x\right)-\Phi\left(-6+x\right)\right)\right)10^6.$$

If the process mean stays centered and only the process standard deviation changes, then the standard deviation resulting in 3.4 DPMO would be $P\left(\frac{-6}{\sigma}\le z\le\frac{6}{\sigma}\right)=\Phi\left(4.5\right)-\Phi\left(-7.5\right)$ which results in

$$\sigma=\frac{6}{\Phi^{-1}\left(\frac{\Phi\left(4.5\right)-\Phi\left(-7.5\right)+1}{2}\right)}=1.291659.$$

This is depicted graphically in Figure 1.

2.4 Proposed Models for Single Quality Characteristics

According to the notation defined earlier, the resultant DPMO from k_1 and k_2 can be defined from a standard normal random variable with mean $\mu_{current}$ and standard deviation $\sigma_{current}/k_2$. Mathematically, for a left shift of the normal distribution that is:

$$DPMO = \left(1 - P\left(\frac{\left(\mu_{current} - 6\sigma_{current} - k_1\sigma_{current}\right) - \mu_{current}}{\left(\frac{\sigma_{current}}{k_2}\right)} \le z \le \frac{\left(\mu_{current} + 6\sigma_{current} - k_1\sigma_{current}\right) - \mu_{current}}{\left(\frac{\sigma_{current}}{k_2}\right)} \right) \right) 10^6$$

where $k_1, k_2 \ge 0$, for the left shift above. This simplifies to

$$DPMO = \left(1 - \left(\Phi\left(\left(6 - k_1\right)k_2\right) - \Phi\left(\left(-6 - k_1\right)k_2\right)\right)\right)10^6,$$ where

$$\Phi(z) = \int_{-\infty}^{z} \frac{1}{\sqrt{2\pi}} e^{-\frac{1}{2}z^2} dz.$$

Figure 2.1: Standard Normal Distribution vs. Normal Distribution with Standard Deviation of 1.292 and mean zero

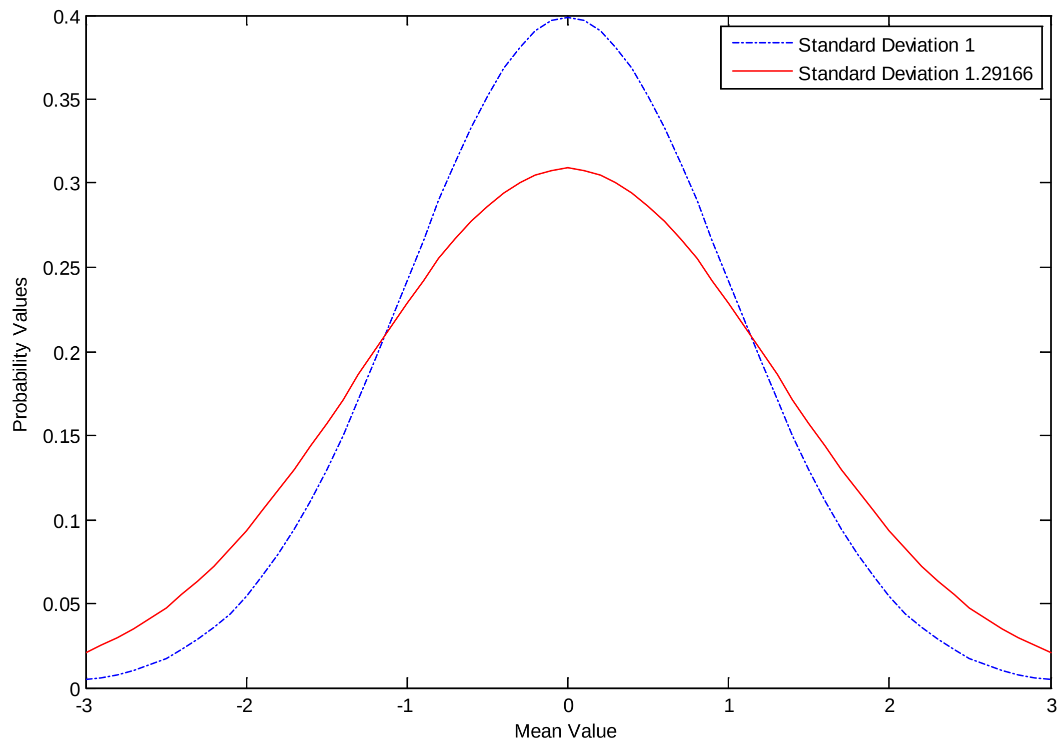

Notice that

$$
\begin{aligned}
DPMO &= \Big(1-\big(\Phi\big((6-k_1)k_2\big)-\Phi\big((-6-k_1)k_2\big)\big)\Big)10^6 \\
&= \Big(1-\Big(\big(1-\Phi\big(-(6-k_1)k_2\big)\big)-\big(1-\Phi\big((6+k_1)k_2\big)\big)\Big)\Big)10^6 \\
&= \Big(1-\Big(\big(\Phi\big((6+k_1)k_2\big)\big)-\Phi\big(-(6-k_1)k_2\big)\Big)\Big)10^6 \\
&= \Big(1-\Big(\big(\Phi\big((6+k_1)k_2\big)\big)-\Phi\big((-6+k_1)k_2\big)\Big)\Big)10^6 \\
&= \left(1-P\left(\frac{(\mu_{current}-6\sigma_{current}+k_1\sigma_{current})-\mu_{current}}{\left(\frac{\sigma_{current}}{k_2}\right)} \le z \le \frac{(\mu_{current}+6\sigma_{current}+k_1\sigma_{current})-\mu_{current}}{\left(\frac{\sigma_{current}}{k_2}\right)}\right)\right)10^6
\end{aligned}
$$

This means that the same DPMO values result from a left or a right k_1 shifted mean. Two cases are studied.

2.4.1 Sigma shifts while mean remains unchanged

Setting $k_1=0$ (process mean is unchanged), the DPMO equation above simplifies to

$$
DPMO = \big(1-\big(\Phi(6k_2)-\Phi(-6k_2)\big)\big)*10^6 = \Big(1-\big(\Phi(6k_2)-\big(1-\Phi(6k_2)\big)\big)\Big)10^6 = \Big(1-\big(2\Phi(6k_2)-1\big)\Big)10^6
$$

$$
=\big(2-2\Phi(6k_2)\big)10^6
$$

Finally, solving for k_2 as a function of DPMO, one has $DPMO = \big(2-2*\Phi(6k_2)\big)*10^6$ where $\Phi(6k_2) = 1-\frac{DPMO}{2(10^6)}$ or $k_2 = \frac{\Phi^{-1}\left(1-\frac{DPMO}{2(10^6)}\right)}{6}$. Table 2 shows some DPMO values for six sigma and higher quality processes. Here note that as K2 increases from 0.7742 to

1 and the shift variability decreases, the DPMO value also decreases from 3.39767 to 0.00197.

Table 2.2: Variability Shift and Process Fallout with no Mean Shift

k_2 variability shift	0.7742	0.790	0.806	0.822	0.8390	0.8553	0.8716	0.8878
DPMO	3.3976	2.112	1.300	0.793	0.4791	0.2866	0.1698	0.0996
k_2 variability shift	0.9041	0.920	0.936	0.952	0.9688	0.98361	0.99528	1
DPMO	0.0579	0.033	0.019	0.010	0.0061	0.0036	0.0023	0.001

2.4.2 Mean and sigma shift at the same time

As both mean and standard deviation shift over time, the contour plots resulting from various DPMOs are as follows for k_2 and k_1 shifts:

Figure 2.2: Variability Shift vs. Mean Shift Process Fallout Contour Plot

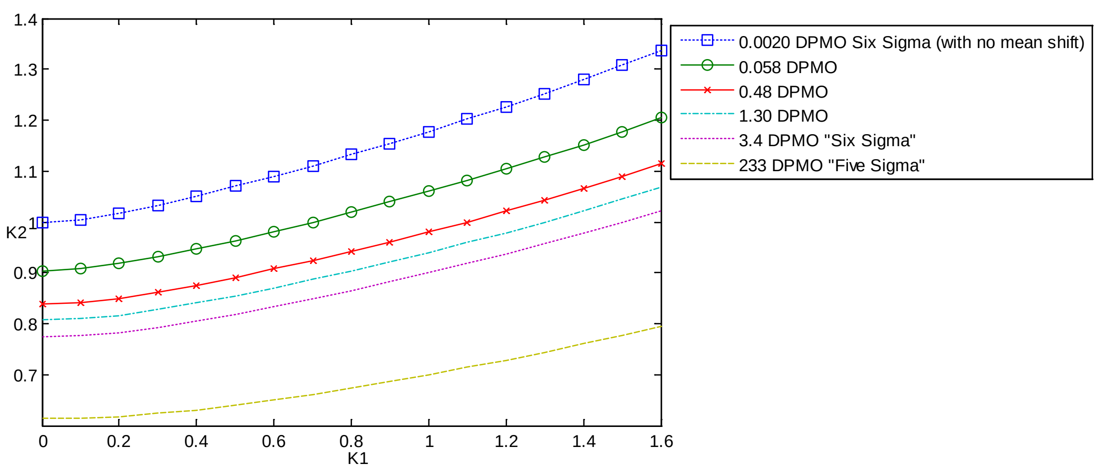

In terms of k_1 and k_2, using $\sigma_{\text{shifted}} = \pm\, \sigma_{\text{current}}/k_2$, and the specification limits defined as (LSL, USL) = ($\mu_{\text{current}} - 6\sigma_{\text{current}}$, $\mu_{\text{current}} + 6\sigma_{\text{current}}$), the PCIs can be computed as

$$C_p = \frac{USL-LSL}{6\sigma_{shifted}} = \frac{(\mu_{current}+6\sigma_{current})-(\mu_{current}-6\sigma_{current})}{6\left(\frac{\sigma_{current}}{k_2}\right)} = \frac{12\sigma_{current}}{6\left(\frac{\sigma_{current}}{k_2}\right)} = 2k_2,$$

$$C_{p,lower} = \frac{\mu-LSL}{3\sigma_{shifted}} = \frac{(\mu-k_1\sigma_{current})-(\mu-6\sigma_{current})}{3\left(\frac{\sigma_{current}}{k_2}\right)} = \frac{(6-k_1)\sigma_{current}}{3\left(\frac{\sigma_{current}}{k_2}\right)} = \frac{k_2(6-k_1)}{3}, \text{ and}$$

$$C_{p,upper} = \frac{USL-\mu}{3\sigma_{shifted}} = \frac{(\mu+6\sigma_{current})-(\mu-k_1\sigma_{current})}{3\left(\frac{\sigma_{current}}{k_2}\right)} = \frac{(6+k_1)\sigma_{current}}{3\left(\frac{\sigma_{current}}{k_2}\right)} = \frac{k_2(6+k_1)}{3}.$$

Now note that $C_{p,lower}$ and $C_{p,upper}$ were computed for left shifts where $k_1 > 0$. If $k_1 < 0$ in the above, that would correspond to a right shift so that $C_{p,lower}$ and $C_{p,upper}$ would switch signs making $C_{p,upper} = \frac{k_2(6-k_1)}{3}$ and $C_{p,lower} = \frac{k_2(6+k_1)}{3}$. This means that for either a left or right shift $C_{pk} = \min(C_{p,upper}, C_{p,lower}) = \frac{k_2(6-k_1)}{3}$. Similarly, if one assumes that a process was on target with the original unshifted mean, implying that $T = \mu_{current}$, where T is defined as a target value, and is subject to process "shift and drift" over time, one has

$$C_{pm} = \frac{C_p}{\sqrt{1+\left(\frac{\mu-T}{\sigma}\right)^2}} = \frac{2k_2}{\sqrt{1+\left(\frac{\mu_{current}\pm k_1\sigma_{current}-\mu_{current}}{\left(\frac{\sigma_{current}}{k_2}\right)}\right)^2}} = \frac{2k_2}{\sqrt{1+(\pm k_2k_1)^2}} = \frac{2k_2}{\sqrt{1+(k_2k_1)^2}}.$$

Similarly, for C_{pkm}, one has $C_{pkm} = \frac{C_{pk}}{\sqrt{1+\left(\frac{\mu-T}{\sigma}\right)^2}} = \frac{\frac{k_2(6-k_1)}{3}}{\sqrt{1+(k_2k_1)^2}} = \frac{k_2(6-k_1)}{3\sqrt{1+(k_2k_1)^2}}.$

2.5 Proposed Models for Dual Quality Characteristics

The univariate case can be extended to the bivariate normal distribution with mean and variance shifts. The bivariate normal distribution is defined as the multivariate normal distribution, $f(\mathbf{x}) = \frac{1}{(2\pi)^{\frac{p}{2}} |\Sigma|^{\frac{1}{2}}} e^{-\frac{1}{2}(\mathbf{x}-\boldsymbol{\mu})^T \Sigma^{-1}(\mathbf{x}-\boldsymbol{\mu})}$, where $p = 2$. In the bivariate case where the variances are shifted by k_{2x_i} factors, the variance-covariance matrix can be described by:

$$\Sigma = \begin{pmatrix} \frac{\sigma_1^2}{k_{2x_1}{}^2} & \frac{Cov(X_1, X_2)}{k_{2x_1} k_{2x_2}} \\ \frac{Cov(X_1, X_2)}{k_{2x_1} k_{2x_2}} & \frac{\sigma_2^2}{k_{2x_2}{}^2} \end{pmatrix}$$

Noting that the correlation coefficient ρ is defined as $\rho = \frac{Cov(X_1, X_2)}{\sigma_1 \sigma_2}$ for $\sigma_1, \sigma_2 > 0$, one has $Cov(X_1, X_2) = \rho \sigma_1 \sigma_2$; hence, the variance-covariance matrix can be rewritten as

$$\Sigma = \begin{pmatrix} \frac{\sigma_1^2}{k_{2x_1}{}^2} & \frac{\rho \sigma_1 \sigma_2}{k_{2x_1} k_{2x_2}} \\ \frac{\rho \sigma_1 \sigma_2}{k_{2x_1} k_{2x_2}} & \frac{\sigma_2^2}{k_{2x_2}{}^2} \end{pmatrix}.$$

The determinant of the variance-covariance matrix is given by $|\Sigma| = \frac{\sigma_1^2 \sigma_2^2}{k_{2x_1}{}^2 k_{2x_2}{}^2}(1-\rho^2)$, so that $|\Sigma|^{\frac{1}{2}} = \frac{\sigma_1 \sigma_2}{k_{2x_1} k_{2x_2}} \sqrt{(1-\rho^2)}$ and $\Sigma^{-1} = \frac{1}{1-\rho^2} \begin{pmatrix} \frac{k_{2x_1}{}^2}{\sigma_1^2} & -\frac{\rho k_{2x_1} k_{2x_2}}{\sigma_1 \sigma_2} \\ -\frac{\rho k_{2x_1} k_{2x_2}}{\sigma_1 \sigma_2} & \frac{k_{2x_2}{}^2}{\sigma_2^2} \end{pmatrix}$

Plugging the above into multivariate normal distribution where p=2, and noting that $\mathbf{x} = [x_1\ x_2]$ and $\boldsymbol{\mu} = [\mu_1\ \mu_2]$, one finally arrives at

$$f(x_1, x_2) = \frac{k_{2x_1} k_{2x_2}}{2\pi\sigma_1\sigma_2\sqrt{1-\rho^2}} e^{-\frac{1}{2}(q(x_1,x_2))}$$

(1)

$$q(x_1, x_2) = \frac{1}{1-\rho^2}\left(\left(k_{2x_1}\left(\frac{x_1-\mu_1}{\sigma_1}\right)\right)^2 - 2\rho\left(k_{2x_1}\left(\frac{x_1-\mu_1}{\sigma_1}\right)\right)\left(k_{2x_2}\left(\frac{x_2-\mu_2}{\sigma_2}\right)\right) + \left(k_{2x_2}\left(\frac{x_2-\mu_2}{\sigma_2}\right)\right)^2\right)$$

(2)

for the bivariate normal distribution function. Here, process fallout in terms of DPMO can be described by the following two functions:

$$DPMO = \left(1 - P\begin{pmatrix} \mu_{current} - 6\sigma_{current} + k_{1x_1}\sigma_{current} \le x_1 \le \mu_{current} + 6\sigma_{current} + k_{1x_1}\sigma_{current}, \\ \mu_{current} - 6\sigma_{current} + k_{1x_2}\sigma_{current} \le x_2 \le \mu_{current} + 6\sigma_{current} + k_{1x_2}\sigma_{current} \end{pmatrix}\right)10^6$$

$$\begin{aligned} DPMO &= \left(1 - \int_{\mu_{2current}-6\sigma_{2current}+k_{1x_2}\sigma_{2current}}^{\mu_{2current}+6\sigma_{2current}+k_{1x_2}\sigma_{2current}} \int_{\mu_{1current}-6\sigma_{1current}+k_{1x_1}\sigma_{1current}}^{\mu_{1current}+6\sigma_{1current}+k_{1x_1}\sigma_{1current}} f(x_1, x_2)\, dx_1 dx_2\right)10^6 \\ &= \left(1 - \int_{\mu_{2current}-6\sigma_{2current}+k_{1x_2}\sigma_{2current}}^{\mu_{2current}+6\sigma_{2current}+k_{1x_2}\sigma_{2current}} \int_{\mu_{1current}-6\sigma_{1current}+k_{1x_1}\sigma_{1current}}^{\mu_{1current}+6\sigma_{1current}+k_{1x_1}\sigma_{1current}} \frac{k_{2x_1} k_{2x_2}}{2\pi\sigma_1\sigma_2\sqrt{1-\rho^2}} e^{-\frac{1}{2}(q(x_1,x_2))} dx_1 dx_2\right)10^6 \end{aligned}$$

for the various k_{1x_i} sigma shifts. Here note that $k_{1x_i} \in \mathbb{R}$, where $k_{1x_i} < 0$ indicates a left sigma shift of the μ_i^{th} mean and $k_{1x_i} > 0$ indicates a right sigma shift of the μ_i^{th} mean. The process fallout DPMO level for two quality characteristics originally performing within 6 standard deviations of the mean without shift is 0.00395 DPMO. With the 1.5 sigma shift assumption from the Six Sigma framework, the fallout changes to 6.7953 DPMO. This is the same for any positive or negative combination of a $1.5k_{1_{xi}}$ DPMO shift. Furthermore, it should be noted that these fallout numbers are different from the univariate case since the bivariate normal distribution is radially symmetric about the $[x_1\ x_2] = [\mu_1\ \ \mu_2]$ axis. This means that a rectangular region can be defined by (LSL1, USL1) and (LSL2, USL2) for the two quality characteristics and yield different standard DPMO numbers than the univariate case. The contours outside the dashed rectangle represent the process fallout percentage. If two quality characteristics are independent of each other, this means that $\rho = 0$. Thus, Eqs (1) and (2) simplify to

$$f\left(x_1, x_2\right) = \frac{k_{2x_1} k_{2x_2}}{2\pi\sigma_1\sigma_2} e^{-\frac{1}{2}\left(q\left(x_1, x_2\right)\right)} \tag{3}$$

$$q\left(x_1, x_2\right) = \left(\left(k_{2x_1}\left(\frac{x_1 - \mu_1}{\sigma_1}\right)\right)^2 + \left(k_{2x_2}\left(\frac{x_2 - \mu_2}{\sigma_2}\right)\right)^2\right) \tag{4}$$

If there is a shift in process variability while the process mean remains unchanged, this implies that $k_{1x_1} = k_{1x_2} = 0$, so that the process fallout can be described as:

$$\begin{aligned} DPMO &= \left(1 - P\left(\begin{matrix} \mu_{1current} - 6\sigma_{1current} \le x_1 \le \mu_{1current} + 6\sigma_{1current}, \mu_{2current} - 6\sigma_{2current} \le x_2 \\ \le \mu_{2current} + 6\sigma_{2current} \end{matrix}\right)\right)10^6 \\ &= \left(1 - \int_{\mu_{2current} - 6\sigma_{2current}}^{\mu_{2current} + 6\sigma_{2current}} \int_{\mu_{1current} - 6\sigma_{1current}}^{\mu_{1current} + 6\sigma_{1current}} f\left(x_1, x_2\right) dx_1 dx_2\right)10^6 \\ &= \left(1 - \int_{\mu_{2current} - 6\sigma_{2current}}^{\mu_{2current} + 6\sigma_{2current}} \int_{\mu_{1current} - 6\sigma_{1current}}^{\mu_{1current} + 6\sigma_{1current}} \frac{k_{2x_1} k_{2x_2}}{2\pi\sigma_1\sigma_2\sqrt{1-\rho^2}} e^{-\frac{1}{2}\left(q\left(x_1, x_2\right)\right)} dx_1 dx_2\right)10^6 \end{aligned}$$

(5)

2.6 Numerical examples

2.6.1 The single quality characteristic case

Looking at the raw data for the various DPMO values below, it can be seen that the process capability indices can vary substantially, depending on the combination of mean and standard deviation shift sizes k_1 and k_2, while resulting in equivalent process fallout. This can be seen in Tables 2.3-2.8 where the Cpm and Cpkm values assume that the process was originally on target and shifted over time.

Table 2.3: PCIs for 3.40 DPMO level incorporating joint mean and standard deviation shifts

DPMO	**3.39767**	**6 sigma level**			
k1	k2	Cp	Cpk	Cpm	Cpkm
0.0000	0.7742	1.5484	1.5484	1.5484	1.5484
0.1000	0.7765	1.5530	1.5271	1.5483	1.5225
0.2000	0.7830	1.5660	1.5138	1.5471	1.4956
0.3000	0.7929	1.5857	1.5064	1.5427	1.4655
0.4000	0.8050	1.6101	1.5027	1.5326	1.4304
0.5000	0.8188	1.6375	1.5011	1.5155	1.3892
0.6000	0.8336	1.6671	1.5004	1.4910	1.3419
0.7000	0.8491	1.6983	1.5001	1.4599	1.2895
0.8000	0.8654	1.7308	1.5000	1.4231	1.2333
0.9000	0.8824	1.7647	1.5000	1.3820	1.1747
1.0000	0.9000	1.8000	1.5000	1.3379	1.1149
1.1000	0.9184	1.8367	1.5000	1.2922	1.0553
1.2000	0.9375	1.8750	1.5000	1.2457	0.9965
1.3000	0.9574	1.9149	1.5000	1.1993	0.9395
1.4000	0.9783	1.9565	1.5000	1.1538	0.8845
1.5000	1.0000	2.0000	1.5000	1.1094	0.8321
1.6000	1.0227	2.0455	1.5000	1.0666	0.7822

Table 2.4: PCIs for 233 DPMO level incorporating joint mean and standard deviation shifts

DPMO	**233**	**5 sigma level**			
k1	k2	Cp	Cpk	Cpm	Cpkm
0.0000	0.6133	1.2266	1.2266	1.2266	1.2266
0.1000	0.6145	1.2290	1.2085	1.2267	1.2062
0.2000	0.6179	1.2358	1.1946	1.2265	1.1856
0.3000	0.6234	1.2468	1.1844	1.2255	1.1643
0.4000	0.6307	1.2614	1.1773	1.2231	1.1415
0.5000	0.6397	1.2794	1.1728	1.2186	1.1170
0.6000	0.6499	1.2998	1.1698	1.2110	1.0899
0.7000	0.6613	1.3225	1.1682	1.2002	1.0601
0.8000	0.6735	1.3469	1.1673	1.1858	1.0277
0.9000	0.6863	1.3727	1.1668	1.1678	0.9927
1.0000	0.6999	1.3999	1.1666	1.1468	0.9557
1.1000	0.7141	1.4283	1.1664	1.1232	0.9173
1.2000	0.7290	1.4580	1.1664	1.0974	0.8779
1.3000	0.7445	1.4890	1.1664	1.0699	0.8381
1.4000	0.7607	1.5213	1.1663	1.0414	0.7984
1.5000	0.7776	1.5552	1.1664	1.0122	0.7592
1.6000	0.7953	1.5905	1.1664	0.9828	0.7207

Table 2.5: PCIs for 1.30 DPMO level incorporating joint mean and standard deviation shifts

DPMO	**1.30081**	**Better than 6 sigma level**			
k1	k2	Cp	Cpk	Cpm	Cpkm
0.0000	0.8066	1.6132	1.6132	1.6132	1.6132
0.1000	0.8092	1.6184	1.5914	1.6131	1.5862
0.2000	0.8165	1.6329	1.5785	1.6116	1.5578
0.3000	0.8272	1.6545	1.5718	1.6058	1.5255
0.4000	0.8404	1.6807	1.5687	1.5931	1.4869
0.5000	0.8549	1.7099	1.5674	1.5723	1.4412
0.6000	0.8705	1.7410	1.5669	1.5432	1.3889
0.7000	0.8868	1.7737	1.5668	1.5069	1.3311
0.8000	0.9039	1.8077	1.5667	1.4649	1.2696
0.9000	0.9216	1.8431	1.5667	1.4187	1.2059
1.0000	0.9400	1.8800	1.5667	1.3698	1.1415
1.1000	0.9592	1.9184	1.5667	1.3197	1.0777
1.2000	0.9792	1.9583	1.5667	1.2692	1.0154
1.3000	1.0000	2.0000	1.5667	1.2194	0.9552
1.4000	1.0217	2.0435	1.5667	1.1708	0.8976
1.5000	1.0445	2.0889	1.5667	1.1239	0.8429

1.6000	1.0682	2.1364	1.5667	1.0789	0.7912

Table 2.6: PCIs for 0.479 DPMO level incorporating joint mean and standard deviation shifts

DPMO	**0.47918**	**Better than 6 sigma level**			
k1	k2	Cp	Cpk	Cpm	Cpkm
0.0000	0.8391	1.6782	1.6782	1.6782	1.6782
0.1000	0.8420	1.6839	1.6559	1.6780	1.6500
0.2000	0.8500	1.7000	1.6433	1.6760	1.6201
0.3000	0.8618	1.7235	1.6373	1.6686	1.5852
0.4000	0.8758	1.7515	1.6348	1.6530	1.5428
0.5000	0.8912	1.7823	1.6338	1.6280	1.4924
0.6000	0.9075	1.8150	1.6335	1.5940	1.4346
0.7000	0.9245	1.8491	1.6334	1.5523	1.3712
0.8000	0.9423	1.8846	1.6333	1.5049	1.3042
0.9000	0.9608	1.9216	1.6333	1.4535	1.2355
1.0000	0.9800	1.9600	1.6333	1.3999	1.1665
1.1000	1.0000	2.0000	1.6333	1.3453	1.0987
1.2000	1.0208	2.0416	1.6333	1.2911	1.0329
1.3000	1.0425	2.0851	1.6333	1.2380	0.9697
1.4000	1.0652	2.1305	1.6334	1.1865	0.9097
1.5000	1.0889	2.1778	1.6334	1.1371	0.8529
1.6000	1.1137	2.2273	1.6334	1.0901	0.7994

Table 2.7: PCIs for 0.0579 DPMO level incorporating joint mean and standard deviation shifts

DPMO	**0.05791**	**Better than 6 sigma level**			
k1	k2	Cp	Cpk	Cpm	Cpkm
0.0000	0.9042	1.8084	1.8084	1.8084	1.8084
0.1000	0.9078	1.8156	1.7853	1.8081	1.7780
0.2000	0.9175	1.8349	1.7738	1.8048	1.7446
0.3000	0.9311	1.8621	1.7690	1.7935	1.7038
0.4000	0.9468	1.8936	1.7674	1.7709	1.6528
0.5000	0.9637	1.9275	1.7668	1.7364	1.5917
0.6000	0.9815	1.9630	1.7667	1.6915	1.5223
0.7000	1.0000	2.0000	1.7667	1.6385	1.4473
0.8000	1.0192	2.0384	1.7666	1.5798	1.3692
0.9000	1.0392	2.0784	1.7666	1.5180	1.2903
1.0000	1.0600	2.1200	1.7667	1.4548	1.2123
1.1000	1.0816	2.1632	1.7666	1.3919	1.1367
1.2000	1.1042	2.2083	1.7666	1.3303	1.0642

1.3000	1.1276	2.2553	1.7666	1.2709	0.9956
1.4000	1.1522	2.3043	1.7666	1.2142	0.9309
1.5000	1.1778	2.3555	1.7667	1.1603	0.8703
1.6000	1.2045	2.4090	1.7666	1.1095	0.8137

Table 2.8: PCIs for 0.00197 DPMO level incorporating joint mean and standard deviation shifts

DPMO	**0.00197**	**Better than 6 sigma level**			
k1	k2	Cp	Cpk	Cpm	Cpkm
0.0000	1.0000	2.0000	2.0000	2.0000	2.0000
0.1000	1.0048	2.0096	1.9761	1.9995	1.9662
0.2000	1.0171	2.0342	1.9664	1.9934	1.9269
0.3000	1.0333	2.0666	1.9633	1.9739	1.8752
0.4000	1.0513	2.1026	1.9624	1.9382	1.8090
0.5000	1.0703	2.1406	1.9622	1.8873	1.7300
0.6000	1.0901	2.1802	1.9622	1.8246	1.6421
0.7000	1.1107	2.2214	1.9622	1.7537	1.5491
0.8000	1.1320	2.2640	1.9621	1.6781	1.4544
0.9000	1.1542	2.3084	1.9621	1.6009	1.3608
1.0000	1.1773	2.3546	1.9622	1.5243	1.2703
1.1000	1.2013	2.4026	1.9621	1.4498	1.1840
1.2000	1.2264	2.4528	1.9622	1.3785	1.1028
1.3000	1.2524	2.5049	1.9622	1.3109	1.0269
1.4000	1.2797	2.5594	1.9622	1.2474	0.9563
1.5000	1.3081	2.6162	1.9622	1.1880	0.8910
1.6000	1.3378	2.6756	1.9621	1.1325	0.8305

2.6.2 The dual quality characteristic case

DPMO values are obtained for various combinations of k_{2x_1} and k_{2x_2} under different assumptions about the variances of the two quality characteristics. The results are shown in Table 2.9, where the DPMO values for $\left[k_{2x_1}, k_{2x_2}\right]$shifts and $\left[\mu_1,\ \mu_2\right]=\left[a,\ b\right]$, $\left[\sigma_1,\ \sigma_2\right]=\left[c,\ d\right]$ where $a,b\in\mathbb{R}$, $c,d\in\mathbb{R}^+$, and $\left[k_{1x_1},\ k_{1x_2}\right]=\left[0,\ 0\right]$.

Table 2.9: DPMOs resulting from variance shifts, with fixed means and uncorrelated variables obtained by using equations 3-5

k_{2x_2}	$k_{2x_1}=0.5$	$k_{2x_1}=0.7$	$k_{2x_1}=0.9$	$k_{2x_1}=1.1$	$k_{2x_1}=1.3$	$k_{2x_1}=1.5$
0.5000	5392.3000	2726.4200	2699.8600	2699.8000	2699.8000	2699.8000
0.7000	2726.4200	53.3823	26.7581	26.6915	26.6915	26.6915
0.9000	2699.8600	26.7581	0.1333	0.0667	0.0666	0.0666
1.1000	2699.8000	26.6915	0.0667	0.0001	0.0000	0.0000
1.3000	2699.8000	26.6915	0.0666	0.0000	0.0000	0.0000
1.5000	2699.8000	26.6915	0.0666	0.0000	0.0000	0.0000

Notice that as the k_2 values increase, the DPMO decrease. These values will always be the same for any starting mean vectors and standard deviation with no mean shifts since the bivariate random variables are standardized and uncorrelated. This matrix is also symmetric due to the symmetry of the multivariate normal random variable. DPMO plots incorporating various mean and standard deviation shifts, while setting $\rho = 0$, are depicted in Figures 2.3.1 – 2.3.6.

2.6.2.1 *Equal means, equal standard deviations:* $[\mu_1,\ \mu_2]=[0,\ 0],[\sigma_1,\ \sigma_2]=[1,1]$:

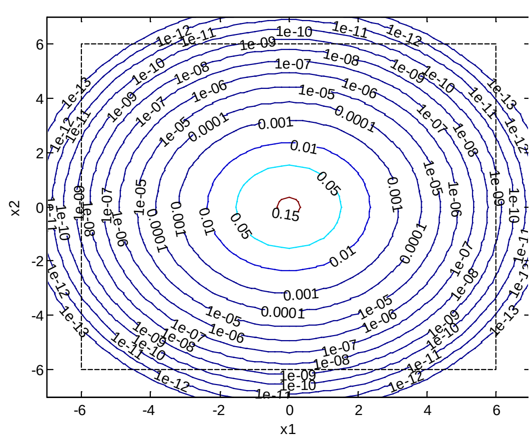

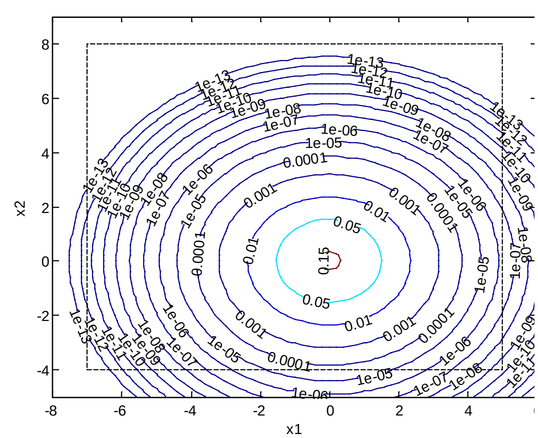

Figure 2.3.1: (no mean shift) $\left[k_{1x_1}, k_{1x_2}\right] = [0,\ 0]$, (no standard deviation shift) $\left[k_{2x_1}, k_{2x_2}\right] = [1,1]$
DPMO= 0.0039464 (Baseline Contour Plot)

Figure 2.3.2: (mean shift) $\left[k_{1x_1}, k_{1x_2}\right] = [-1,\ 2]$, (no standard deviation shift) $\left[k_{2x_1}, k_{2x_2}\right] = [1,1]$
DPMO=31.958

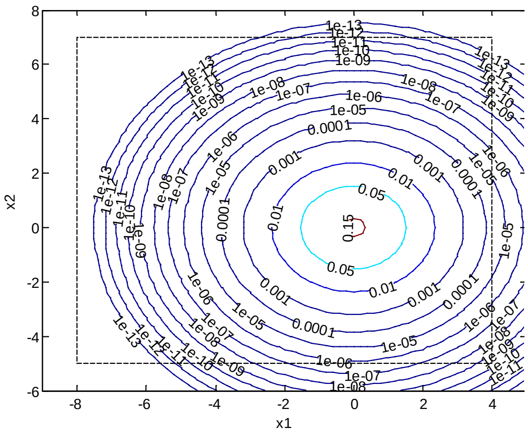

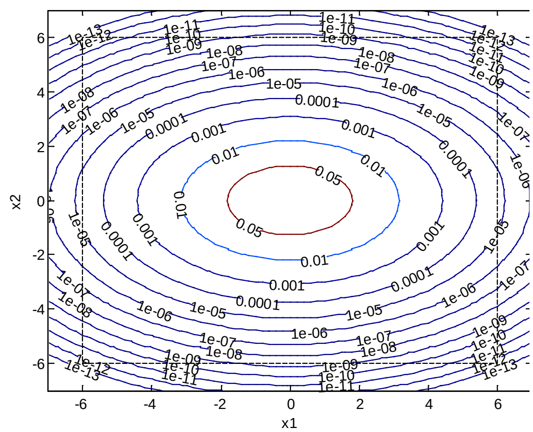

Figure 2.3.3: (mean shift) $\left[k_{1x_1}, k_{1x_2}\right] = [-2,\ 1]$, (no standard deviation shift) $\left[k_{2x_1}, k_{2x_2}\right] = [1,1]$
DPMO=31.958

Figure 2.3.4: (no mean shift) $\left[k_{1x_1}, k_{1x_2}\right] = [0,\ 0]$, (standard deviation shift) $\left[k_{2x_1}, k_{2x_2}\right] = [0.693177,\ 1]$
DPMO=31.958

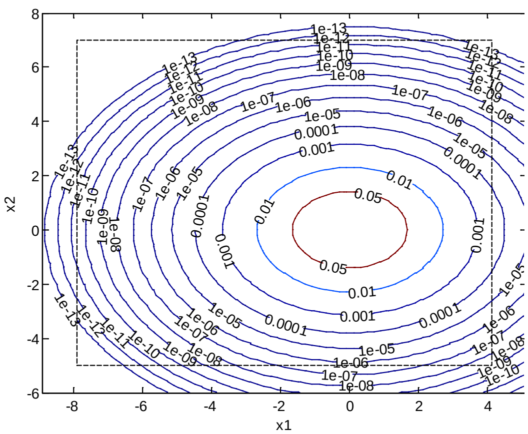

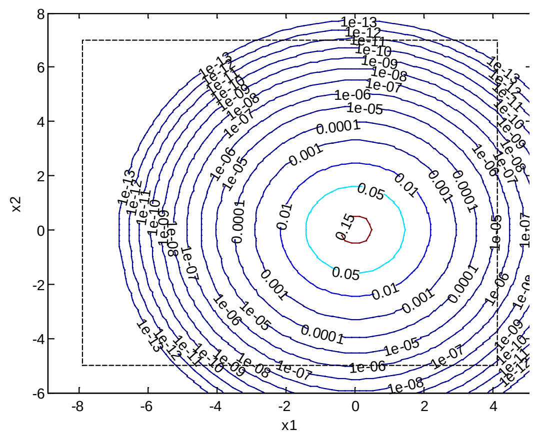

Figure 2.3.5: (mean shift) $\left[k_{1x_1}, k_{1x_2}\right] = [-1.9,\ 1]$, (standard deviation shift) $\left[k_{2x_1}, k_{2x_2}\right] = [1,\ 0.847507]$
DPMO=31.958

Figure 2.3.6: (mean shift) $\left[k_{1x_1}, k_{1x_2}\right] = [-1.9,\ 1]$, (standard deviation shift) $\left[k_{2x_1}, k_{2x_2}\right] = [0.975124,\ 1.1]$
DPMO=31.958

Figure 3.1 represents a baseline for comparison for all contour plots in case 1. Figures 2.3.2-2.3.6 represent various mean shifts and standard deviation shifts resulting in a process fallout of 31.958 DPMO. Figures 2.3.2 and 2.3.3 result in the same process fallout due to the symmetry of the standard bivariate normal distribution about the origin**.** Figures 2.3.2- 2.3.6 illustrate the concept that an equal process fallout can result by either shifting the process mean over time, shifting the process standard deviation over time or both. Looking at Figures 2.3.3, 2.3.5 and 2.3.6 one can see that the standard deviation shifts are highly sensitive to even small changes in the shifted means.

2.6.2.2 *Unequal means, unequal standard deviations:* $[\mu_1,\ \mu_2]=[5,\ 1]$**,** $[\sigma_1,\ \sigma_2]=[0.5,\ 1]$

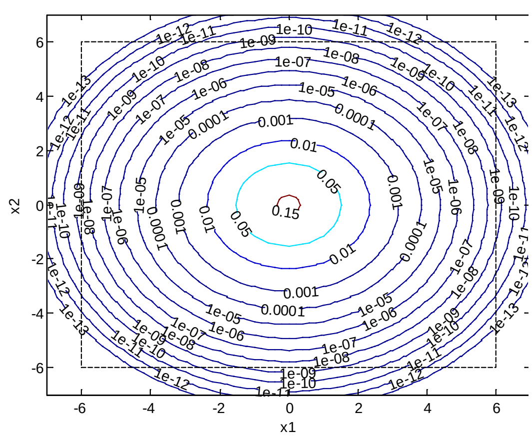

Figure 2.4.1: (no mean shift) $\left[k_{1x_1},\ k_{1x_2}\right]=[0,\ 0]$, (no standard deviation shift) $\left[k_{2x_1},\ k_{2x_2}\right]=[1,\ 1]$
DPMO= 0.0039464 (Baseline Contour Plot)

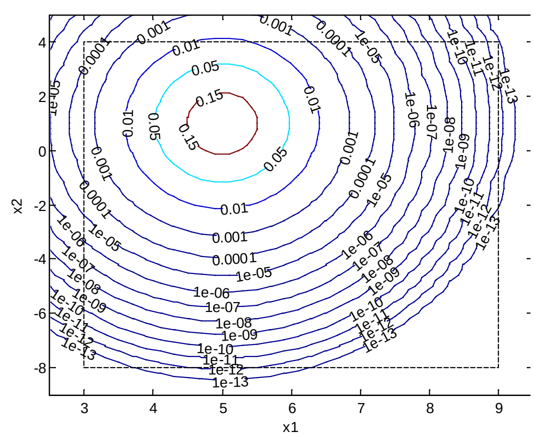

Figure 2.4.2: (mean shift) $\left[k_{1x_1},\ k_{1x_2}\right]=[2,\ -3]$, (standard deviation shift) $\left[k_{2x_1},\ k_{2x_2}\right]=[0.9,\ 0.8]$
DPMO= 8355.3

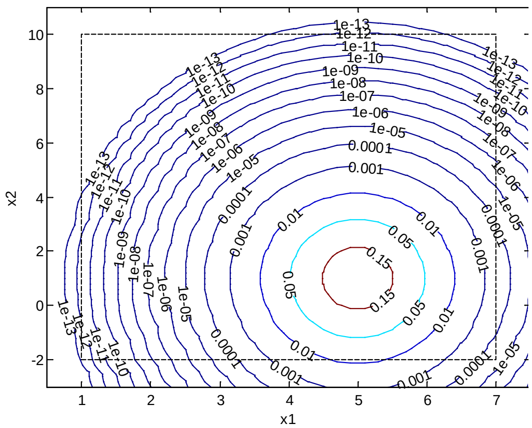

Figure 2.4.3: (mean shift) $\left[k_{1x_1}, k_{1x_2}\right] = [-2, 3]$, (standard deviation shift) $\left[k_{2x_1}, k_{2x_2}\right] = [0.9, 0.8]$
DPMO= 8355.3

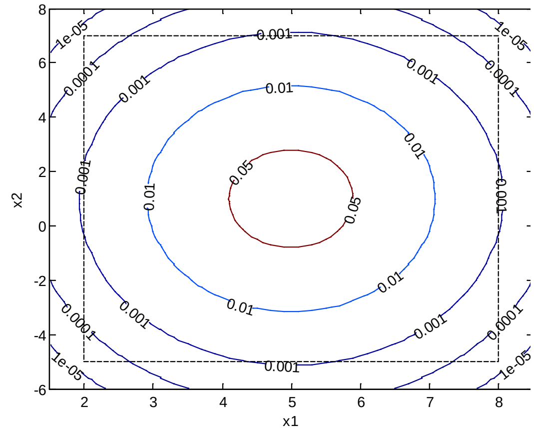

Figure 2.4.4: (no mean shift) $\left[k_{1x_1}, k_{1x_2}\right] = [0, 0]$, (standard deviation shift) $\left[k_{2x_1}, k_{2x_2}\right] = [.4772935, .4772935]$
DPMO= 8355.3

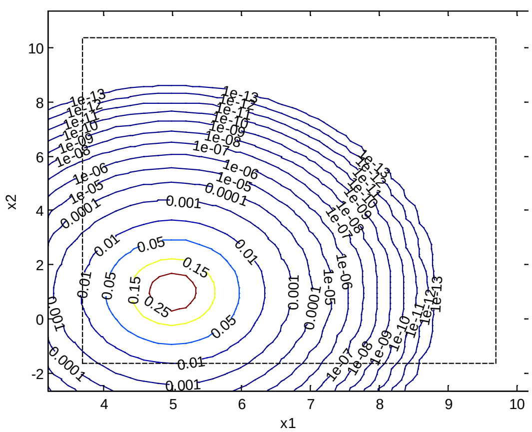

Figure 2.4.5: (mean shift) $\left[k_{1x_1}, k_{1x_2}\right] = [3.363345, 3.363345]$, (no standard deviation shift) $\left[k_{2x_1}, k_{2x_2}\right] = [1, 1]$
DPMO= 8355.3

Figure 4.1 shows a baseline for comparison for all contour plots in Figure 4. Figures 2.4.2-2.4.5 represent various mean and standard deviation shifts resulting in a process fallout of 8355.3 DPMO. Figures 2.4.2 and 2.4.3 result in the same process fallout because of the symmetry of the standard bivariate normal distribution about the origin. Figures 2.4.2- 2.4.5 show the concept that an equal process fallout can result by either shifting the process mean over time, shifting the process standard deviation overtime or both. The investigation of Figures 2.4.3 and 2.4.4 reveals that the standard deviation shifts are highly sensitive to changes in the shifted means.

If two quality characteristics are correlated with each other, this means that $0 < |\rho| < 1$. Furthermore, since the original means are not shifting, this implies $k_{1x_1} = k_{1x_2} = 0$. The DPMO function can therefore be written as:

$$DPMO = \left(1 - \int_{\mu_{2current}-6\sigma_{2current}}^{\mu_{2current}+6\sigma_{2current}} \int_{\mu_{1current}-6\sigma_{1current}}^{\mu_{1current}+6\sigma_{1current}} f\left(x_1, x_2\right) dx_1 dx_2\right) 10^6 \tag{6}$$

$$= \left(1 - \int_{\mu_{2current}-6\sigma_{2current}}^{\mu_{2current}+6\sigma_{2current}} \int_{\mu_{1current}-6\sigma_{1current}}^{\mu_{1current}+6\sigma_{1current}} \frac{k_{2x_1} k_{2x_2}}{2\pi\sigma_1\sigma_2\sqrt{1-\rho^2}} e^{-\frac{1}{2}\left(q\left(x_1, x_2\right)\right)} dx_1 dx_2\right) 10^6$$

where

$$q\left(x_1, x_2\right) = \frac{1}{1-\rho^2}\left(\left(k_{2x_1}\left(\frac{x_1-\mu_1}{\sigma_1}\right)\right)^2 - 2\rho\left(k_{2x_1}\left(\frac{x_1-\mu_1}{\sigma_1}\right)\right)\left(k_{2x_2}\left(\frac{x_2-\mu_2}{\sigma_2}\right)\right) + \left(k_{2x_2}\left(\frac{x_2-\mu_2}{\sigma_2}\right)\right)^2\right) \tag{7}$$

Table 2.10 illustrates DPMO values for $\left[k_{2x_1} \;\; k_{2x_2}\right]$ shifts: $\left[\mu_1 \;\; \mu_2\right] = \left[a \;\; b\right]$, $\left[\sigma_1 \;\; \sigma_2\right] = \left[c \;\; d\right]$ where $a, b \in \mathbb{R}, c, d \in \mathbb{R}^+$.

Table 2.10: DPMOs resulting from variance shifts, with fixed means and correlated variables

(k_{2x_1}, k_{2x_2})	$\rho = -0.9$	$\rho = -0.5$	$\rho = 0$	$\rho = 0.5$	$\rho = 0.9$	$\rho = 0.99999999$
$(0.5, 0.5)$	4178.78	5235.81	5392.303	5235.813	4178.78	2700.2960
$(0.5, 1)$	2699.79	2699.79	2699.79	2699.79	2699.79	2699.7960
$(0.5, 1.5)$	2699.79	2699.79	2699.79	2699.79	2699.79	2699.7960
$(1, 0.5)$	2699.79	2699.79	2699.79	2699.79	2699.79	2699.7960
$(1, 1)$	0.0036	0.0039	0.0039	0.0039	0.0036	0.0020
$(1, 1.5)$	0.0020	0.0020	0.0020	0.0020	0.0020	0.0020
$(1.5, 0.5)$	2699.79	2699.79	2699.79	2699.79	2699.79	2699.7960
$(1.5, 1)$	0.0020	0.0020	0.0020	0.0020	0.0020	0.0020
$(1.5, 1.5)$	0.0000	0.0000	0.0000	0.0000	0.0000	0.0000

A few key insights can be drawn as follows. As the k_2 values increase, the DPMO decrease. These values will always be the same for any starting mean vectors and standard deviation with no mean shifts since the bivariate random variables are standardized. Process fallout in terms of DPMO only depends on $|\rho|$. As $|\rho| \to 1$, the process fallout decreases dramatically. It should also be noted that as $|\rho|$ increases, the k_2 values that result in the highest DPMO decrease the most dramatically. This is due to the scaling factor $\frac{1}{1-\rho^2}$ in the exponent and $\frac{1}{\sqrt{1-\rho^2}}$ in the integrand. Relatively speaking $|\rho|$ has a minimal impact on DPMO compared to $[\mu_1, \mu_2]$, $[\sigma_1, \sigma_2]$ and their respective shifts. $|\rho|$ has a larger impact on DPMO only when $\left[k_{2x_1}, k_{2x_2}\right]$ are small (e.g., $0 < k_{2x_1}, k_{2x_2} \le 0.5$). DPMO plots incorporating various mean and standard deviation shifts, while $\rho \neq 0$ are shown in figures 2.5.1.1 to 2.5.5.3. These examples will mirror Figure 4 and be referred to as Figure 5:

2.6.2.3 *Unequal means, unequal standard deviations:* $[\mu_1, \mu_2] = [5, 1]$, $[\sigma_1, \sigma_2] = [0.5, 1]$

Note that Figure 2.4.1.0 can be referred to with $\rho = 0$ as a baseline for DPMO comparison.

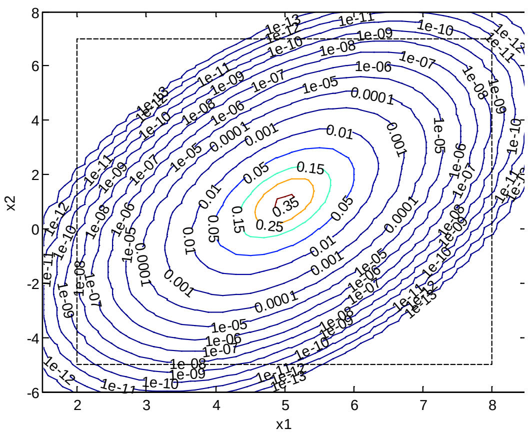

Figure 2.5.1.1: (no mean shift) $\left[k_{1x_1}, k_{1x_2}\right] = [0, 0]$, (no standard deviation shift) $\left[k_{2x_1}, k_{2x_2}\right] = [1, 1]$ DPMO= 0.0039456, $\rho = 0.5$

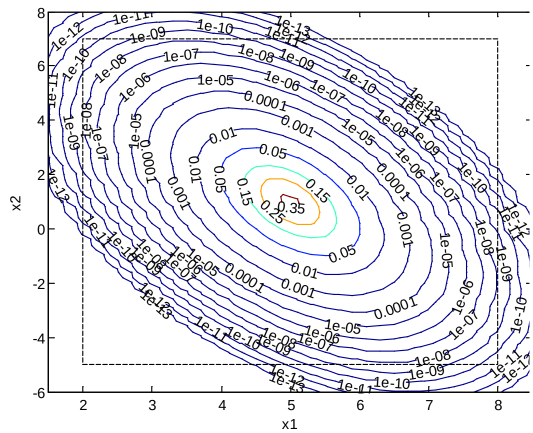

Figure 2.5.1.2: (no mean shift) $\left[k_{1x_1}, k_{1x_2}\right] = [0, 0]$, (no standard deviation shift) $\left[k_{2x_1}, k_{2x_2}\right] = [1, 1]$ DPMO= 0.0039456, $\rho = -0.5$

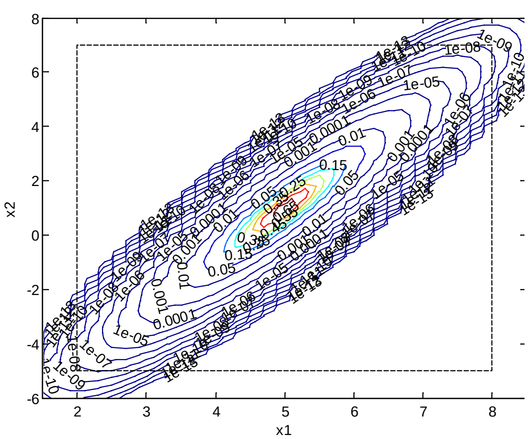

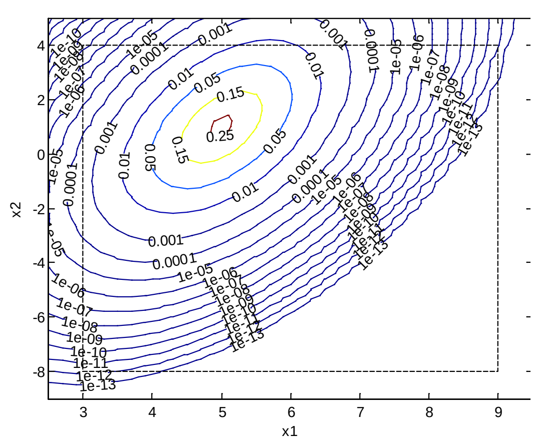

Figure 2.5.1.3: (no mean shift) $\left[k_{1x_1}, k_{1x_2}\right]=[0,\ 0]$, (no standard deviation shift) $\left[k_{2x_1}, k_{2x_2}\right]=[1,\ 1]$
DPMO= 0.0036347, $\rho=0.9$

Figure 2.5.2.1: (mean shift) $\left[k_{1x_1}, k_{1x_2}\right]=[2,\ -3]$, (standard deviation shift) $\left[k_{2x_1}, k_{2x_2}\right]=[0.9,\ 0.8]$
DPMO= 8356.6, $\rho=0.5$

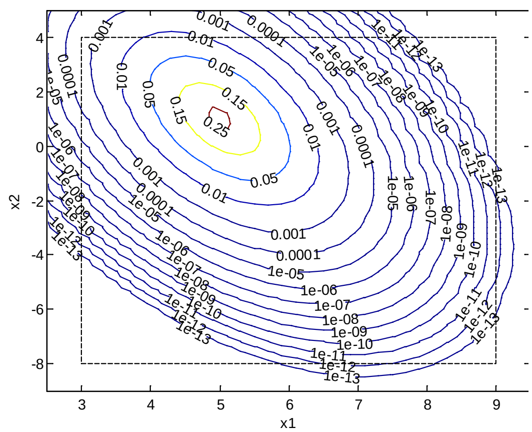

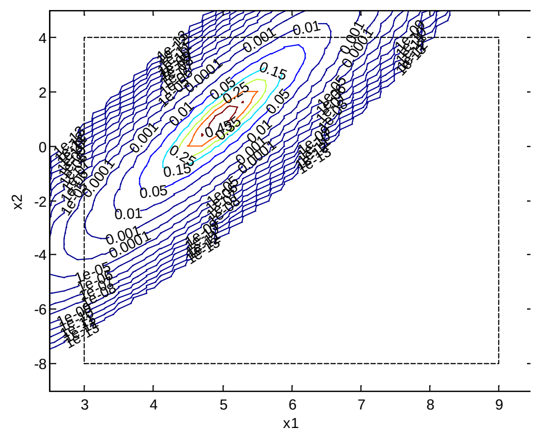

Figure 2.5.2.2: (mean shift) $\left[k_{1x_1}, k_{1x_2}\right]=[2,\ -3]$, (standard deviation shift) $\left[k_{2x_1}, k_{2x_2}\right]=[0.9,\ 0.8]$
DPMO= 8310.1, $\rho=-0.5$

Figure 2.5.2.3: (mean shift) $\left[k_{1x_1}, k_{1x_2}\right]=[2,\ -3]$, (standard deviation shift) $\left[k_{2x_1}, k_{2x_2}\right]=[0.9,\ 0.8]$
DPMO= 8356.6, $\rho=0.9$

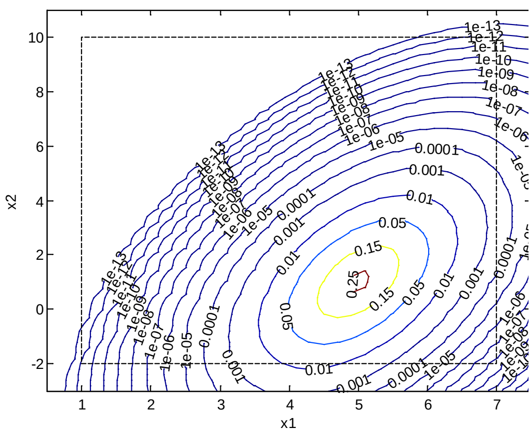

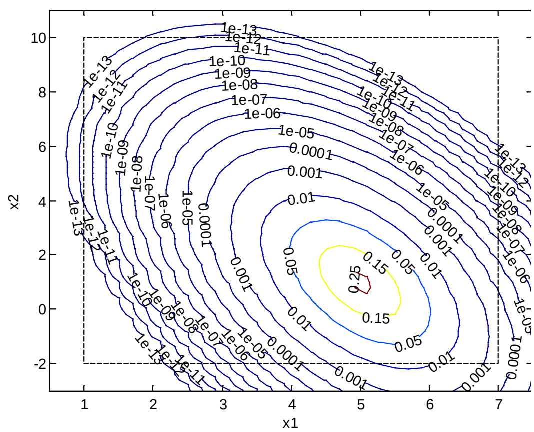

Figure 2.5.3.1: (mean shift) $\left[k_{1x_1}, k_{1x_2}\right]=[-2,\ 3]$, (standard deviation shift) $\left[k_{2x_1}, k_{2x_2}\right]=[0.9,\ 0.8]$
DPMO= 8356.6, $\rho=0.5$

Figure 2.5.3.2: (mean shift) $\left[k_{1x_1}, k_{1x_2}\right]=[-2,\ 3]$, (standard deviation shift) $\left[k_{2x_1}, k_{2x_2}\right]=[0.9,\ 0.8]$
DPMO= 8310.1, $\rho=-0.5$

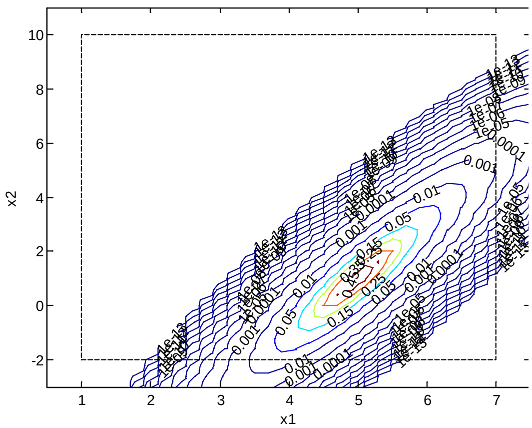

Figure 2.5.3.3: (mean shift) $\left[k_{1x_1}, k_{1x_2}\right]=\left[-2, 3\right]$, (standard deviation shift) $\left[k_{2x_1}, k_{2x_2}\right]=\left[0.9, 0.8\right]$
DPMO= 8356.6, $\rho = 0.9$

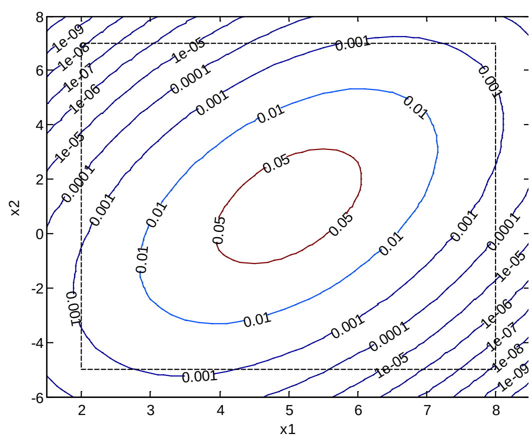

Figure 2.5.4.1: (no mean shift) $\left[k_{1x_1}, k_{1x_2}\right]=\left[0, 0\right]$, (standard deviation shift)
$\left[k_{2x_1}, k_{2x_2}\right]=\left[0.4772935, 0.4772935\right]$
DPMO= 8073.7, $\rho = 0.5$

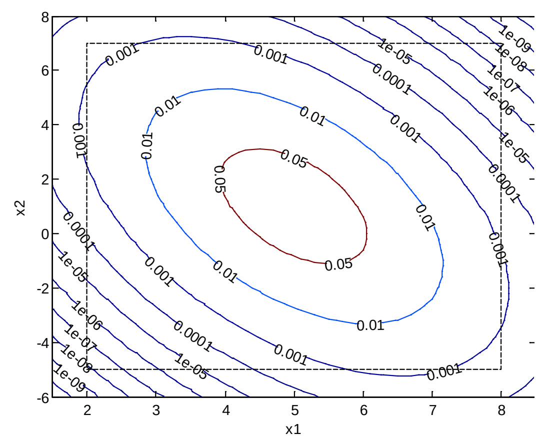

Figure 2.5.4.2 (no mean shift) $\left[k_{1x_1}, k_{1x_2}\right]=\left[0, 0\right]$, (standard deviation shift)
$\left[k_{2x_1}, k_{2x_2}\right]=\left[0.4772935, 0.4772935\right]$
DPMO= 8073.7, $\rho = -0.5$

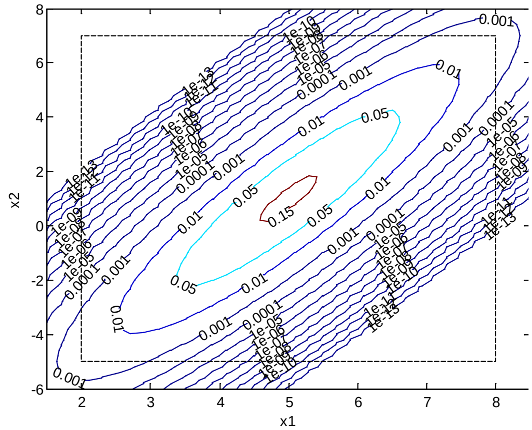

Figure 2.5.4.3: (no mean shift) $\left[k_{1x_1}, k_{1x_2}\right] = [0,\ 0]$, (standard deviation shift) $\left[k_{2x_1}, k_{2x_2}\right] = [0.4772935,\ 0.4772935]$ DPMO= 6406, $\rho = 0.9$

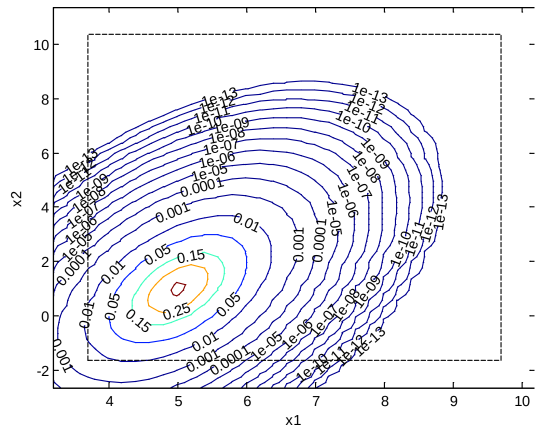

Figure 2.5.5.1: (mean shift) $\left[k_{1x_1}, k_{1x_2}\right] = [3.363345,\ 3.363345]$, (no standard deviation shift) $\left[k_{2x_1}, k_{2x_2}\right] = [1,\ 1]$ DPMO= 7984.3, $\rho = 0.5$

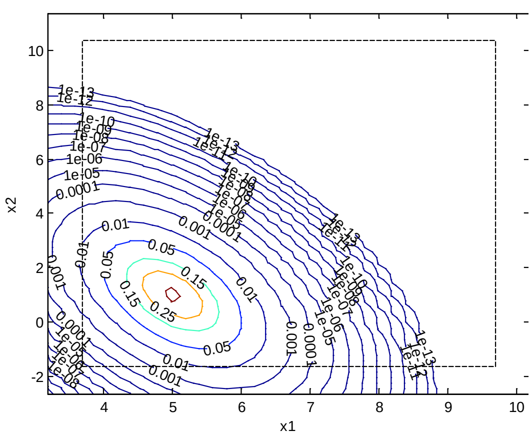

Figure 2.5.5.2: (mean shift) $\left[k_{1x_1}, k_{1x_2}\right] = [3.363345,\ 3.363345]$, (no standard deviation shift) $\left[k_{2x_1}, k_{2x_2}\right] = [1,\ 1]$ DPMO= 8372.8, $\rho = -0.5$

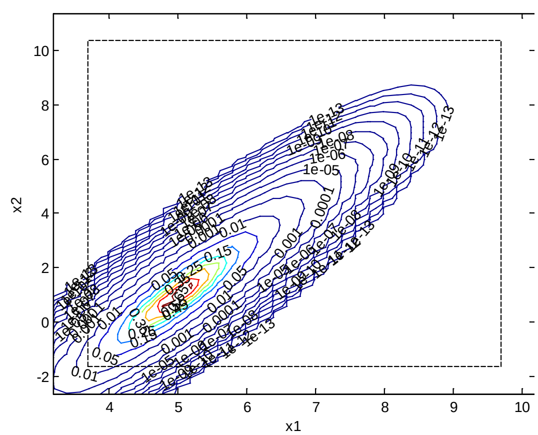

Figure 2.5.5.3: (mean shift) $\left[k_{1x_1}, k_{1x_2}\right] = [3.363345,\ 3.363345]$, (no standard deviation shift) $\left[k_{2x_1}, k_{2x_2}\right] = [1,\ 1]$ DPMO= 6280.2, $\rho = 0.9$

Figure 4.1 represents a baseline for comparison for all contour plots in Figure 5.

Figures 2.5.1.1-2.5.1.3 demonstrate that as $|\rho|$ increases, the process fallout decreases for the bivariate normal distribution with no shifting. Since $k_{2x_1}, k_{2x_2} > 0.5$, the magnitude of the process fallout decrease is negligible as $|\rho|$ increases. Figures 2.5.2.1-2.5.2.3 show that at certain combinations of high k_{2x_1}, k_{2x_2} standard deviation shift values and k_{1x_1}, k_{1x_2} mean shift values the impact of having high correlation coefficient values is negligible for a DPMO decrease. Moreover this example also demonstrates that the sign of ρ can make a larger impact on DPMO decrease than its magnitude. Figures 2.5.2.1-2.5.2.3 and 2.5.3.1-2.5.3.3 combine to illustrate the symmetry of the standard bivariate normal distribution about the origin, regardless of the value of ρ, as they result in the same DPMO. This is shown in the figures by the shifting of the dashed rectangle bounds. Figures 2.5.4.1-2.5.4.3 clearly show that $|\rho|$ has a large impact on DPMO when the $\left[k_{2x_1}, k_{2x_2}\right]$ (Standard deviation) shift values are small, especially with no shifted means. Again notice that $0 < k_{2x_1}, k_{2x_2} \le 0.5$. Looking at Figures 5.5.1-5.5.3, one can see that the sign and magnitude of ρ can have a large impact on DPMOs when relatively large mean shifts occur. This is because the mean shifts that occur are functions of the original standard deviations of the bivariate normal distribution.

2.7 Conclusion and Further Study

This study illustrates the importance of understanding how process variability shifts over time is just as important as mean shifts over time. This means that practitioners need to take special care in understanding the root causes of change in not only their process means, but also the variability, if process fallout is to be minimized. In section 4, process capability indices were developed analytically that show this shift. Numerical results displaying process capability indicies were shown in section 5. This paper has also demonstrated that the importance of understanding the interaction of correlation coefficients, shifting means and shifting variances on several quality characteristics is critical to minimizing process fallout. This can be seen analytically in section 5 and numerically in section 6. To the authors' knowledge, the compounding effect of changing variability as the process mean shifts over time on product or service defect rates had not been explored prior to this study. This is a critical issue since production processes do not all have centered process means and constant variances. Therefore, assumptions underlying process fallout within the Six Sigma framework may be grievously incorrect in many situations in which relatively stable processes exhibit shifts and drifts over a long period of time. This study has examined that processes can have the same process fallout over time but have vastly different process capability indices as the mean and standard deviation of the process shift over time. This highlights the critical need for practitioners to consider calculating process fallout in terms of DPMO by considering both the mean and variability shifts of their processes. Otherwise, their incorrect assumptions about their processes will lead to costly errors in manufacturing and service defects. Evaluation of process fallout for dual quality characteristics demonstrated the importance of the effects of correlation of two different CTQs on process fallout.

One logical extension of this study would be to evaluate expected quality loss functions to illustrate the importance of preventing underestimation of defect levels. Expected quality loss models could be explored in order to underscore the importance of preventing underestimation of process fallout levels. It is important to note that in many industrial applications, the losses at two different specification limits are often not the same. In addition, most loss functions assume that a product will be reworked or scrapped if the product quality characteristic falls outside specification limits; however, it is a common practice in many industries to replace a defective item rather than spending resources to repair it. Therefore, one could compare quality loss functions of various processes in order to specify minimum expected quality loss conditions for processes where the product can be reworked and processes where the product cannot be reworked, as the mean and standard deviation of the process vary over time. Another possible extension of this work could apply to multivariate distributions. Multivariate distributions could be used to extend the concepts explored in this paper to multiple, simultaneous process variables of interest. This is important because most statistical process control methods track only a small number of process variables and examine them one at a time. These approaches may be inadequate for most modern process industries, since they ignore the realization that computers collect data continually on hundreds or thousands of process variables being updated continuously. Also, these variables are often not independent of each other, since usually only a limited number of underlying principles govern a process at any given time.

CHAPTER THREE

DEVELOPMENT OF STATISTICAL CONVOLUTIONS OF TRUNCATED NORMAL AND TRUNCATED SKEW NORMAL DISTRIBUTIONS WITH APPLICATIONS

This chapter has been published in the Journal of Statistical Theory and Practice and should be cited as:

Krenek, R., Cha J., Cho, B.R. and J. L. Sharp (2017) ‘Development of statistical convolutions of truncated normal and truncated skew normal distributions with applications’, Journal of Statistical Theory and Practice, Vol. 11,No. 1, pp.1-25.

Additionally, this was a joint work with Jinho Cha and can be found in Chapter Five of his dissertation:

Cha, Jinho, "Re-Establishing the Theoretical Foundations of a Truncated Normal Distribution: Standardization Statistical Inference, and Convolution" (2015).All Dissertations. Paper 1793. http://tigerprints.clemson.edu/cgi/viewcontent.cgi?article=2794&context=all_dissertations

3.1. Introduction

Several crucial contributions to the literature on convolutions are offered in this manuscript that have not been explored previously. Convolutions are analogous to the sum of random variables and are critical concepts in multistage production processes, statistical tolerance analysis, and gap analysis. More specifically, the focus of this paper is on the convolutions resulting from double and triple truncations associated with symmetric and asymmetric normal and skew normal distributions under three types of quality characteristics, which are the nominal-the-best type (*N*-type), smaller-the-better type (*S*-type), and larger-the-better type (*L*-type). It is known that the distributions of *S*- and *L*-type quality characteristics are typically negatively and positively skewed, respectively, while the distribution of *N*-type quality characteristics are approximately symmetric around the mean. In this paper, the normal distribution for N-type characteristics and the skew normal distribution for *S*- and *L*-type characteristics are chosen. One of the reasons for choosing the skew normal distribution as an underlying distribution of *S*- and *L*-type quality characteristics is that the skew normal distribution generalizes the normal distribution by allowing for non-zero skewness.

The convolutions of the combinations of truncated normal and truncated skew normal random variables have not been fully explored in the literature. This is a critical issue because specification limits on a process are implemented externally in most manufacturing and service processes, which means that the product is typically reworked or scrapped if its performance does not fall in the specification limits. This means that the actual distribution after inspection becomes truncated. Figure 1 shows two twice truncated distributions for symmetric and asymmetric *N*-type characteristics in (a) and (b), a one-sided left truncated distribution at the lower specification limit (x_l) for an *L*-type characteristic in (c), and a one-sided right truncated distribution at the upper specification limit (x_u) for an *S*-type characteristic in (d). These distributions have been well established in the literature (Barr and Sherrill (1999), Kim and Takayama (2003), Jawitz (2004), Khasawneh *et al*. (2005a, 2005b) , Hong and Cho (2007), Shin and Cho (2009) , Makarov *et al*. (2009), Goethals and Cho (2011),Cha and Cho (2014), and Cha *et al*. (2014)). The shape of a truncated distribution $f_{X_T}(x)$ varies based on its specification limits. Notice that the truncated variance after truncation will no longer be the same as the original variance associated with the untruncated normal distribution $f_X(x)$. Similarly, unless symmetric two-sided truncations are used, a truncated mean will not be the same as the original mean of an untruncated normal distribution.

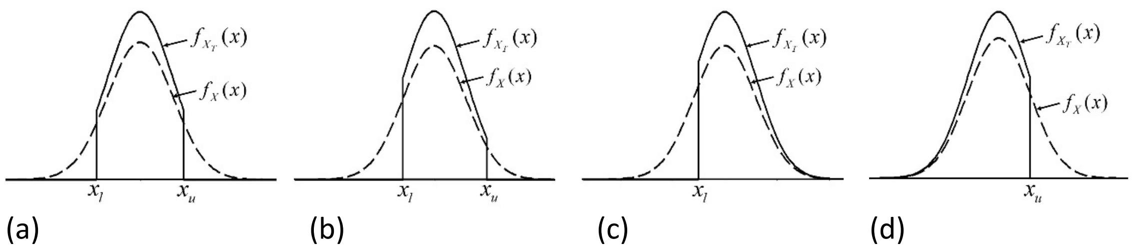

Figure 3.1. Different types of truncated distributions

A potential application of a truncated distribution can be found in a multistage production process, as shown in Figure 3.2, where only conforming products are passed on to the next stage. Examples of multistage processes are numerous. Typical systems of telecommunication, banking, and healthcare consist of multistage processes. A product part or service transferring from one stage to the next stage in a multistage process may introduce extra variation that does not occur in a single-stage process. An added advantage of screening inspection in a multistage process is the ability of reducing the extra variation by screening nonconforming items in each stage. The convolutions of the sum of truncated random variables help to estimate the mean and variance in each stage of a production process.

The convolutions of multiple truncations have practical importance in statistical tolerance design and gap analysis. In gap analysis, for example, tolerance stackups explain the engineering problem solving process of calculating the effects of the accumulated variation that is allowed by specified dimensions in part assembly. Usually, dimensions and tolerances are specified on engineering schematics. A problem arises, however, when arithmetic tolerance stackups are employed, since they use the worst-case maximum or minimum values of dimensions and tolerances to calculate clearance or interference between two features or parts. This results in errors because a non-skew normal distribution and the centering of the distribution on the tolerance interval midpoint are assumed.

By utilizing skew normal distributions and their convolutions, a much more accurate assessment of tolerance stackups can result in a lower product scrap rate, by accounting for asymmetric normal distributions, in addition to skewness. This would also allow for more accurate production forecasts, saving a company both time and money. Unfortunately, the mathematical framework of the convolutions associated with double and triple truncations have not been well established in the literature.

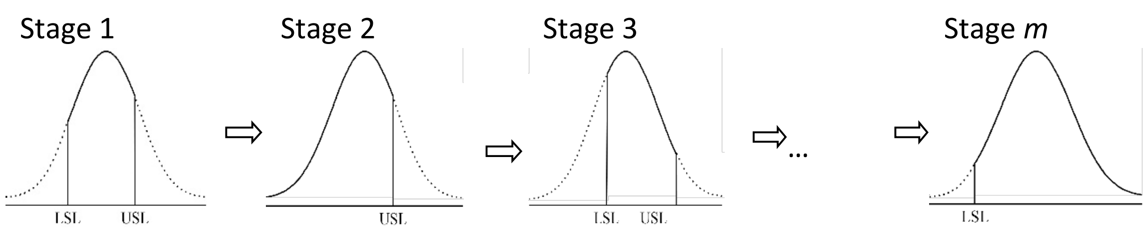

Figure 3.2: Screening inspections in multistage production process

In this paper, twenty-one cases of convolutions of truncated normal and truncated skew normal random variables are highlighted. The cases presented here represent a sample of all the possible types of convolutions of double truncations (i.e., the sum of all the possible combinations containing two truncated random variables with normal and skew normal probability distributions). Fifty-six cases of the convolutions of triple truncations (i.e., the sums of all the possible combinations containing three truncated random variables with normal and skew normal probability distributions) are then illustrated. Here the term double truncation refers to a probability distribution that has been pruned in two unique manufacturing steps; similarly, the term triple truncation refers to a probability distribution that has been pruned in three unique manufacturing steps. Numerical examples illustrate the application of convolutions of truncated normal random variables and truncated skew normal random variables to highlight the improved accuracy of tolerance analysis and gap analysis techniques.

3.2. Literature Review

Convolution is a mathematical way of combining two distributions to form a new distribution. In the middle of the 18th century, Euler (1748, 1750) , introduced the earliest convolution theorem, $\int_a^b g(x \pm u) f(u) du,$ based on Taylor series and Beta functions. Note that f and g are two real or complex-valued functions of real variables u and x. In the truncated environment, Francis (1946) first used convolution to obtain a density function of a sum of the truncated random variables, $h_S(s) = \int_{-\infty}^{\infty} g_{Y_T}(y) f_{X_T}(x) dx = \int_{-\infty}^{\infty} g_{Y_T}(s-x) f_{X_T}(x) dx,$ where $S = X_T + Y_T$ with X_T and Y_T being truncated random variables. To be more specific, Francis (1946) and Aggarwal and Guttman (1960) examined the probability density functions of the sums of singly and doubly truncated normal random variables and developed their cumulative probability tables under the assumption that the random variables were independently and identically distributed. Lipow *et al*. (1964) then investigated the density functions of the sums of a standard normal random variable and a left truncated normal random variable. Francis (1946), Aggarwal and Guttman (1960), and Lipow *et al*. (1964) studied the potential computational complexity associated with convolutions. Furthermore, Kratuengarn (1973) compared the means and variances of the sums of left truncated normal random variables numerically through the Laplace and Fourier transforms and evaluated the accuracy of those methods. Recently, Fletcher *et al.* (2010) examined an expression of the moments based on a truncated skew normal distribution. This method utilizes the double factorial and introduces the truncated skew-normal distribution as a truncation of a different type of skew normal distribution for multiple truncations all using moments of the truncated distributions. Tsai and Kuo (2012) applied the Monte Carlo method to obtain the densities of the sums of truncated normal random variables with 1,000,000 samples. However, most studies focused on identically truncated normal distributions. In this research, however, both identical and non-identical truncated normal distributions are explored and then extended to include a truncated skew normal distribution.

A skew normal distribution represents a parametric class of probability distributions, reflecting varying degrees of skewness, which includes the standard normal distribution as a special case. The skewness parameter makes it possible for probabilistic modeling of the data obtained from a skewed population. This fact makes these distributions useful in the study of the robustness and as priors in Bayesian analysis of data. Birnbaum (1949) first explored skew normal distributions while investigating educational testing using truncated normal random variables. Roberts (1966) was another early pioneer in skew normal distributions by studying correlation models of twins. The term, the skew normal distribution, was formally introduced by Azzalini (1985, 1986), who explored the distribution in depth. Gupta *et al.* (2004) defined a class of multivariate skew-normal models and studied its properties. Nadarajah and Kotz (2006) showed skewed distributions from different families of distributions, whereas Azzalini (2005) discussed the skew normal distribution and related multivariate families. Jamalizadeh, *et al.* (2008) and Kazemi *et al.* (2011) discussed generalizations of the skew normal distribution based on various families. Multivariate versions of the skew normal distribution have also been proposed by Azzalini and Valle (1996), Azzalini and Capitanio (1999), Arellano-Valle *et al.* (2002), Gupta and Chen (2004), and Vernic (2006). In many applications, the probability distribution function of some observed variables can be skewed and their values restricted to a fixed interval. This was demonstrated well in Fletcher *et al.* (2010).

As mentioned earlier, convolutions play an important role in statistical tolerance analysis. Most statistical tolerance analysis research, however, has focused on untruncated, non-skew normal distributions. (e.g., Gilson (1951), Mansoor (1963), Fortini (1967), Wade (1967), Evans (1975), Cox (1986), Greenwood and Chase (1987), Kirschling (1988), Bjorke (1989), Henzold (1995), and Nigam and Turner (1995) and Scholz (1995)). Many of these researchers in the 1980s and 1990s have chosen to focus on a beta distribution due to its ability to cover an actual range of distributions from normal to rectangular. In addition, it has a finite range and can cover asymmetrical cases. More recent research in the area has focused on applications to modern products such as computer hard drives by utilizing optimization models that minimize the tolerance deviations as discussed by Chattinnawat (2015). Structure and shape optimization models have also been explored by Das and Jones (2015) and Luo *et al*. (2014).

3.3. Review of Truncated Normal and Truncated Skew Normal Distributions

If a random variable Y is distributed with its location parameter μ, scale parameter σ, and shape parameter α then its probability density function is defined as

$$f_Y(y) = \frac{2}{\sigma}\cdot\frac{1}{\sqrt{2\pi}}e^{-\frac{1}{2}\left(\frac{y-\mu}{\sigma}\right)^2}\cdot\int_{-\infty}^{\alpha\frac{y-\mu}{\sigma}}\frac{1}{\sqrt{2\pi}}e^{-\frac{1}{2}t^2}dt \text{, where } -\infty < y < \infty.$$

It is noted that the probability density function of Y becomes a normal distribution when the shape parameter α is zero. When the skew normal distribution of Y is truncated with the lower and upper truncation points, y_l and y_u, the probability density function of the truncated skew normal (*TSN*) distribution is then expressed as

$$f_{Y_{TS}}(y) = \frac{f_Y(y)}{\int_{y_l}^{y_u} f_Y(y)dy} \text{ where } y_l < y < y_u.$$

or

$$f_{Y_{TS}}(y) = \frac{f_Y(y)}{\int_{y_l}^{y_u} f_Y(y)dy} I_{[y_l, y_u]}(y),$$

where the indicator function $I_{[y_l, y_u]}(y)$ is then defined as:

$$I_{[y_l, y_u]}(y) = \begin{cases} 1 & \text{if } y \in [y_l, y_u] \\ 0 & \text{otherwise} \end{cases}.$$

The truncated mean μ_{TS} and truncated variance σ_{TS}^2 of Y_{TS} are given by $\int_{y_l}^{y_u} y\cdot f_{Y_{TS}}(y)dy$ and $\int_{y_l}^{y_u} y^2\cdot f_{Y_{TS}}(y)dy - \left(\int_{y_l}^{y_u} y\cdot f_{Y_{TS}}(y)dy\right)^2$, respectively.

3.4. Development of the Convolutions of Truncated Normal and Truncated Skew Normal Random Variables on Double Truncations

The order of truncated random variables does not affect the probability density function of the sum of those random variables when using the convolution operator. The examples presented assume that the truncated normal and truncated skew normal random variables are independent, but not necessarily identically distributed. By using truncated normal and skew normal distributions, various cases of the sums on double truncations can be developed. As shown in Figure 3, four types of a truncated normal distribution and six types of a truncated skew normal distribution are categorized. In the notation of the truncated normal distribution, '*Sym*' and '*Asym*' denote symmetric and asymmetric, respectively, and *TN* stands for 'truncated normal.' Similarly, for the truncated skew normal distribution, '+' indicates a positive α value which means the untruncated original distribution is positively skewed. In contrast, '−' means that α is negative and the untruncated original distribution is negatively skewed. All computations for the mean and variance of symmetric and asymmetric truncated normal distributions were computed in Maple and R software packages. In particular, standard computational methods were used in the software using error function approximations where appropriate.

Truncated normal distributions Truncated skew normal distributions

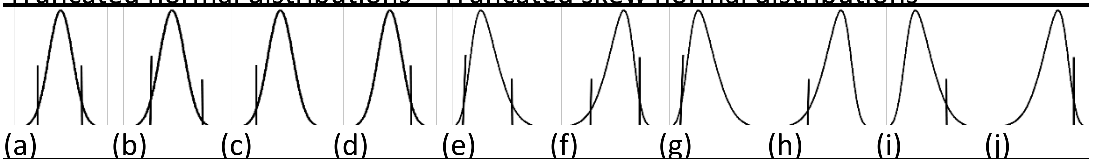

Notation

(a)	Sym $TN_{N-\text{type}}$	A symmetric doubly truncated normal distribution	(e)	$TSN^{+}_{N-\text{type}}$	A doubly truncated positive skew normal distribution
(b)	Asym $TN_{N-\text{type}}$	An asymmetric doubly truncated normal distribution	(f)	$TSN^{-}_{N-\text{type}}$	A doubly truncated negative skew normal distribution
(c)	$TN_{L-\text{type}}$	A left truncated normal distribution	(g)	$TSN^{+}_{L-\text{type}}$	A left truncated positive skew normal distribution
(d)	$TN_{S-\text{type}}$	A right truncated normal distribution	(h)	$TSN^{-}_{L-\text{type}}$	A left truncated negative skew normal distribution
			(i)	$TSN^{+}_{S-\text{type}}$	A right truncated positive skew normal distribution
			(j)	$TSN^{-}_{S-\text{type}}$	A right truncated negative skew normal distribution

Figure 3.3. Ten cases of truncated normal and truncated skew normal random variables

3.4.1 The Convolutions of Truncated Normal , and Truncated Skew Normal Random Variables on the Double Truncations

In order to develop the sums of two independent truncated normal random variables, the following two truncated normal random variables are considered: X_{T_1} and X_{T_2}, where there associated probability density functions are

$$f_{X_{T_1}}(x)=\frac{\frac{1}{\sigma_1\sqrt{2\pi}}\exp^{-\frac{1}{2}\left(\frac{x-\mu_1}{\sigma_1}\right)^2}}{\int_{x_{l_1}}^{x_{u_1}}\frac{1}{\sigma_1\sqrt{2\pi}}\exp^{-\frac{1}{2}\left(\frac{h-\mu_1}{\sigma_1}\right)^2}dh}I_{[x_{l_1},x_{u_1}]}(x) \text{ and}$$

$$f_{X_{T_2}}(y)=\frac{\frac{1}{\sigma_2\sqrt{2\pi}}\exp^{-\frac{1}{2}\left(\frac{y-\mu_2}{\sigma_2}\right)^2}}{\int_{x_{l_2}}^{x_{u_2}}\frac{1}{\sigma_2\sqrt{2\pi}}\exp^{-\frac{1}{2}\left(\frac{p-\mu_2}{\sigma_2}\right)^2}dp}I_{[x_{l_2},x_{u_2}]}(y)\text{, respectively.}$$

Let $Z_2 = X_{T_1} + X_{T_2}$. Based on the convolution operator, the probability density function of the sum of the above two truncated normal random variables is:

$$f_{Z_2}(z) = \int_{-\infty}^{\infty} f_{X_{T_2}}(z-x) f_{X_{T_1}}(x)dx$$
$$= \int_{-\infty}^{\infty} \frac{\frac{1}{\sigma_2\sqrt{2\pi}} \exp^{-\frac{1}{2}\left(\frac{z-x-\mu_2}{\sigma_2}\right)^2}}{\int_{x_{l_2}}^{x_{u_2}} \frac{1}{\sigma_2\sqrt{2\pi}} \exp^{-\frac{1}{2}\left(\frac{p-\mu_2}{\sigma_2}\right)^2} dp} \frac{\frac{1}{\sigma_1\sqrt{2\pi}} \exp^{-\frac{1}{2}\left(\frac{x-\mu_1}{\sigma_1}\right)^2}}{\int_{x_{l_1}}^{x_{u_1}} \frac{1}{\sigma_1\sqrt{2\pi}} \exp^{-\frac{1}{2}\left(\frac{h-\mu_1}{\sigma_1}\right)^2} dh} I_{[z-x_{u_2}, z-x_{l_2}]}(x) I_{[x_{l_1}, x_{u_1}]}(x)dx.$$

Note that $I_{[x_{l_2}, x_{u_2}]}(z-x)$ can be expressed as $I_{[z-x_{u_2}, z-x_{l_2}]}(x)$ since $z = x + y$. Ten cases of the sums of two truncated normal random variables are illustrated in Figure A.1 of the Appendix. The distributions, means and variances of the sums of truncated normal random variables are also shown in Table A.1 of the Appendix, where $E(Z_2)$ is equal to the sum of $E\left(X_{T_1}\right) = \mu_{T_1}$ and $E\left(X_{T_2}\right) = \mu_{T_2}$, and $Var(Z_2)$ is equal to the sum of $Var\left(X_{T_1}\right) = \sigma_{T_1}^2$ and $Var\left(X_{T_2}\right) = \sigma_{T_2}^2$. In Figure 4, μ_1=μ_2=8 and σ_1=σ_2=2. In addition, the lower and upper truncation points are considered according to different types of a truncation as shown in Appendix A, Table A.1.

The convolutions of the sums of two independent truncated skew normal random variables, Y_{TS_1} and Y_{TS_2}, are developed in the same way as the convolution of truncated normal random variables above:

$$f_{Y_{TS_1}}(x) = \frac{\frac{2}{\sigma_1}\frac{1}{\sqrt{2\pi}} e^{-\frac{1}{2}\left(\frac{y-\mu_1}{\sigma_1}\right)^2} \int_{-\infty}^{\alpha_1\frac{y-\mu_1}{\sigma_1}} \frac{1}{\sqrt{2\pi}} e^{-\frac{1}{2}t^2} dt}{\int_{y_{l_1}}^{y_{u_1}} \frac{2}{\sigma_1}\frac{1}{\sqrt{2\pi}} e^{-\frac{1}{2}\left(\frac{h-\mu_1}{\sigma_1}\right)^2} \left(\int_{-\infty}^{\alpha_1\frac{h-\mu_1}{\sigma_1}} \frac{1}{\sqrt{2\pi}} e^{-\frac{1}{2}t^2} dt\right) dh} I_{[y_l, y_{u_1}]}(x) \text{ and}$$

$$f_{Y_{TS_2}}(y)=\frac{\frac{2}{\sigma_2}\frac{1}{\sqrt{2\pi}}e^{-\frac{1}{2}\left(\frac{y-\mu_2}{\sigma_2}\right)^2}\int_{-\infty}^{\alpha_2\frac{y-\mu_2}{\sigma_2}}\frac{1}{\sqrt{2\pi}}e^{-\frac{1}{2}t^2}dt}{\int_{y_{l_2}}^{y_{u_2}}\frac{2}{\sigma_2}\frac{1}{\sqrt{2\pi}}e^{-\frac{1}{2}\left(\frac{p-\mu_2}{\sigma_2}\right)^2}\left(\int_{-\infty}^{\alpha_2\frac{p-\mu_2}{\sigma_2}}\frac{1}{\sqrt{2\pi}}e^{-\frac{1}{2}t^2}dt\right)dp}I_{[y_{l_2},y_{u_2}]}(y)\text{, respectively.}$$

Letting $Z_2 = Y_{TS_1}+Y_{TS_2}$, the probability density function of the sum of the two truncated skew normal random variables is obtained as:

$$f_{Z_2}(z)=\int_{-\infty}^{\infty}f_{Y_{TS_2}}(z-x)f_{Y_{TS_1}}(x)dx$$

$$=\int_{-\infty}^{\infty}\frac{\frac{2}{\sigma_2}\frac{1}{\sqrt{2\pi}}e^{-\frac{1}{2}\left(\frac{z-x-\mu_2}{\sigma_2}\right)^2}\int_{-\infty}^{\alpha_2\frac{z-x-\mu_2}{\sigma_2}}\frac{1}{\sqrt{2\pi}}e^{-\frac{1}{2}t^2}dt}{\int_{y_{l_2}}^{y_{u_2}}\frac{2}{\sigma_2}\frac{1}{\sqrt{2\pi}}e^{-\frac{1}{2}\left(\frac{p-\mu_2}{\sigma_2}\right)^2}\left(\int_{-\infty}^{\alpha_2\frac{p-\mu_2}{\sigma_2}}\frac{1}{\sqrt{2\pi}}e^{-\frac{1}{2}t^2}dt\right)dp}\cdot$$

$$\frac{\frac{2}{\sigma_1}\frac{1}{\sqrt{2\pi}}e^{-\frac{1}{2}\left(\frac{x-\mu_1}{\sigma_1}\right)^2}\int_{-\infty}^{\alpha_1\frac{x-\mu_1}{\sigma_1}}\frac{1}{\sqrt{2\pi}}e^{-\frac{1}{2}t^2}dt}{\int_{y_{l_1}}^{y_{u_1}}\frac{2}{\sigma_1}\frac{1}{\sqrt{2\pi}}e^{-\frac{1}{2}\left(\frac{h-\mu_1}{\sigma_1}\right)^2}\left(\int_{-\infty}^{\alpha_1\frac{h-\mu_1}{\sigma_1}}\frac{1}{\sqrt{2\pi}}e^{-\frac{1}{2}t^2}dt\right)dh}I_{[z-y_{u_2},z-y_{l_2}]}(x)\,I_{[y_{l_1},y_{u_1}]}(x)dx.$$

This can be extended to the convolution of truncated normal and truncated skew normal random variables as well from the following expression:

$$f_{X_{T_1}}(x)=\frac{\frac{1}{\sigma_1\sqrt{2\pi}}\exp^{-\frac{1}{2}\left(\frac{x-\mu_1}{\sigma_1}\right)^2}}{\int_{x_{l_1}}^{x_{u_1}}\frac{1}{\sigma_1\sqrt{2\pi}}\exp^{-\frac{1}{2}\left(\frac{p-\mu_1}{\sigma_1}\right)^2}dp}I_{[x_{l_1},x_{u_1}]}(x)\text{ and}$$

$$f_{Y_{TS_2}}(y)=\frac{\frac{2}{\sigma_2}\frac{1}{\sqrt{2\pi}}e^{-\frac{1}{2}\left(\frac{y-\mu_2}{\sigma_2}\right)^2}\int_{-\infty}^{\alpha_2\frac{y-\mu_2}{\sigma_2}}\frac{1}{\sqrt{2\pi}}e^{-\frac{1}{2}t^2}dt}{\int_{y_{l_2}}^{y_{u_2}}\frac{2}{\sigma_2}\frac{1}{\sqrt{2\pi}}e^{-\frac{1}{2}\left(\frac{p-\mu_2}{\sigma_2}\right)^2}\left(\int_{-\infty}^{\alpha_2\frac{p-\mu_2}{\sigma_2}}\frac{1}{\sqrt{2\pi}}e^{-\frac{1}{2}t^2}dt\right)dp}I_{[y_{l_2},y_{u_2}]}(y)\text{, respectively.}$$

Equating $Z_2 = X_{T_1}+Y_{TS_2}$,

$$f_{Z_2}(z)=\int_{-\infty}^{\infty}f_{Y_{TS_2}}(z-x)f_{X_{T_1}}(x)dx$$

$$=\int_{-\infty}^{\infty}\frac{\frac{2}{\sigma_2}\frac{1}{\sqrt{2\pi}}e^{-\frac{1}{2}\left(\frac{z-x-\mu_2}{\sigma_2}\right)^2}\int_{-\infty}^{\alpha_2\frac{z-x-\mu_2}{\sigma_2}}\frac{1}{\sqrt{2\pi}}e^{-\frac{1}{2}t^2}dt}{\int_{y_{l_2}}^{y_{u_2}}\frac{2}{\sigma_2}\frac{1}{\sqrt{2\pi}}e^{-\frac{1}{2}\left(\frac{p-\mu_2}{\sigma_2}\right)^2}\left(\int_{-\infty}^{\alpha_2\frac{p-\mu_2}{\sigma_2}}\frac{1}{\sqrt{2\pi}}e^{-\frac{1}{2}t^2}dt\right)dp}\frac{\frac{1}{\sigma_1\sqrt{2\pi}}\exp^{-\frac{1}{2}\left(\frac{x-\mu_1}{\sigma_1}\right)^2}}{\int_{x_{l_1}}^{x_{u_1}}\frac{1}{\sigma_1\sqrt{2\pi}}\exp^{-\frac{1}{2}\left(\frac{h-u_1}{\sigma_1}\right)^2}dh}\cdot$$

$$I_{[z-y_{u_2},z-y_{l_2}]}(x)I_{[x_{l_1},x_{u_1}]}(x)dx.$$

Similarly, $I_{[y_{l_2},y_{u_2}]}(z-x)$ can be written as $I_{[z-y_{u_2},z-y_{l_2}]}(x)$ since $z = x + y$.

Twenty-one cases of the sums of two truncated skew normal random variables are listed in Figure A.2 of the Appendix. It is assumed that the parameters, μ_1 and μ_2 are 8, and the parameters, σ_1 and σ_2 are 4. In addition, the shape parameter α discussed in Section 3, and the lower and upper truncation points are utilized in six different types of truncations as shown in Table A.2 of the Appendix.

3.5. Development of the Convolutions of the Combinations of Truncated Normal and Truncated Skew Normal Random Variables on Triple Truncations

In this section, the convolutions of the sums of independent truncated normal and truncated skew normal random variables on triple truncations are developed. First, the sums of three truncated normal random variables are discussed in Section 3.5.1. Second, the sums of three truncated skew normal random variables are then examined in Section 3.5.2. Finally, in Section 3.5.3, the sums of the combinations of truncated normal and truncated skew normal random variables on triple truncations are examined.

3.5.1 The Convolutions of Three Truncated Normal Random Variables

The probability density function of X_{T_3} is defined as:

$$f_{X_{T_3}}(k)=\frac{\frac{1}{\sigma_3\sqrt{2\pi}}\exp^{-\frac{1}{2}\left(\frac{k-\mu_3}{\sigma_3}\right)^2}}{\int_{x_{l_3}}^{x_{u_3}}\frac{1}{\sigma_3\sqrt{2\pi}}\exp^{-\frac{1}{2}\left(\frac{v-\mu_3}{\sigma_3}\right)^2}dv}I_{[x_{l_3},x_{u_3}]}(k).$$

Denoting $Z_3 = Z_2 + X_{T_3}$ where $Z_2 = X_{T_1} + X_{T_2}$, the probability density function of Z_3 is then given by

$$f_{Z_3}(s)=\int_{-\infty}^{\infty}\int_{-\infty}^{\infty}\frac{\frac{1}{\sigma_3\sqrt{2\pi}}\exp^{-\frac{1}{2}\left(\frac{s-z-\mu_3}{\sigma_3}\right)^2}}{\int_{x_{l_3}}^{x_{u_3}}\frac{1}{\sigma_3\sqrt{2\pi}}\exp^{-\frac{1}{2}\left(\frac{v-\mu_3}{\sigma_3}\right)^2}dv}\frac{\frac{1}{\sigma_2\sqrt{2\pi}}\exp^{-\frac{1}{2}\left(\frac{z-x-\mu_2}{\sigma_2}\right)^2}}{\int_{x_{l_2}}^{x_{u_2}}\frac{1}{\sigma_2\sqrt{2\pi}}\exp^{-\frac{1}{2}\left(\frac{p-\mu_2}{\sigma_2}\right)^2}dp}.$$
$$\frac{\frac{1}{\sigma_1\sqrt{2\pi}}\exp^{-\frac{1}{2}\left(\frac{x-\mu_1}{\sigma_1}\right)^2}}{\int_{x_{l_1}}^{x_{u_1}}\frac{1}{\sigma_1\sqrt{2\pi}}\exp^{-\frac{1}{2}\left(\frac{h-\mu_1}{\sigma_1}\right)^2}dh}I_{[x_{l_1},x_{u_1}]}(x)\,I_{[z-x_{u_2},z-x_{l_2}]}(x)\,I_{[s-x_{u_3},s-x_{l_3}]}(z)dxdz.$$

It is noted that $I_{[x_{l_3},x_{u_3}]}(s-z)$ can be written as $I_{[s-x_{u_3},s-x_{l_3}]}(z)$. This derivation is shown in the Appendix.

3.5.2 The Convolutions of Three Truncated Skew Normal Random Variables

The probability density function of Y_{TS_3} is defined as:

$$f_{Y_{TS_3}}(k)=\frac{\frac{2}{\sigma_3}\frac{1}{\sqrt{2\pi}}e^{-\frac{1}{2}\left(\frac{k-\mu_3}{\sigma_3}\right)^2}\int_{-\infty}^{\alpha_3\frac{k-\mu_3}{\sigma_3}}\frac{1}{\sqrt{2\pi}}e^{-\frac{1}{2}(t)^2}dt}{\int_{y_{l_3}}^{y_{u_3}}\frac{2}{\sigma_3}\frac{1}{\sqrt{2\pi}}e^{-\frac{1}{2}\left(\frac{v-\mu_3}{\sigma_3}\right)^2}\left(\int_{-\infty}^{\alpha_3\frac{v-\mu_3}{\sigma_3}}\frac{1}{\sqrt{2\pi}}e^{-\frac{1}{2}(t)^2}dt\right)dv}I_{[y_{l_3},y_{u_3}]}(k).$$

By denoting $Z_{TS_3} = Z_{TS_2} + Y_{TS_3}$ where $Z_{TS_2} = Y_{TS_1} + Y_{TS_2}$, the probability density function of Z_{TS_3} is obtained as:

$$f_{Z_{TS_3}}(s)=\int_{-\infty}^{\infty}\int_{-\infty}^{\infty}\frac{\frac{2}{\sigma_3}\frac{1}{\sqrt{2\pi}}e^{-\frac{1}{2}\left(\frac{s-z-\mu_3}{\sigma_3}\right)^2}\int_{-\infty}^{\alpha_3\frac{s-z-\mu_3}{\sigma_3}}\frac{1}{\sqrt{2\pi}}e^{-\frac{1}{2}t^2}dt}{\int_{y_{l_3}}^{y_{u_3}}\frac{2}{\sigma_3}\frac{1}{\sqrt{2\pi}}e^{-\frac{1}{2}\left(\frac{v-\mu_3}{\sigma_3}\right)^2}\left(\int_{-\infty}^{\alpha_3\frac{v-\mu_3}{\sigma_3}}\frac{1}{\sqrt{2\pi}}e^{-\frac{1}{2}t^2}dt\right)dv}\cdot$$

$$\frac{\frac{2}{\sigma_2}\frac{1}{\sqrt{2\pi}}e^{-\frac{1}{2}\left(\frac{z-x-\mu_2}{\sigma_2}\right)^2}\int_{-\infty}^{\alpha_2\frac{z-x-\mu_2}{\sigma_2}}\frac{1}{\sqrt{2\pi}}e^{-\frac{1}{2}t^2}dt}{\int_{y_{l_2}}^{y_{u_2}}\frac{2}{\sigma_2}\frac{1}{\sqrt{2\pi}}e^{-\frac{1}{2}\left(\frac{p-\mu_2}{\sigma_2}\right)^2}\left(\int_{-\infty}^{\alpha_2\frac{p-\mu_2}{\sigma_2}}\frac{1}{\sqrt{2\pi}}e^{-\frac{1}{2}t^2}dt\right)dp}\cdot$$

$$\frac{\frac{2}{\sigma_1}\frac{1}{\sqrt{2\pi}}e^{-\frac{1}{2}\left(\frac{x-\mu_1}{\sigma_1}\right)^2}\int_{-\infty}^{\alpha_1\frac{x-\mu_1}{\sigma_1}}\frac{1}{\sqrt{2\pi}}e^{-\frac{1}{2}t^2}dt}{\int_{y_{l_1}}^{y_{u_1}}\frac{2}{\sigma_1}\frac{1}{\sqrt{2\pi}}e^{-\frac{1}{2}\left(\frac{h-\mu_1}{\sigma_1}\right)^2}\left(\int_{-\infty}^{\alpha_1\frac{h-\mu_1}{\sigma_1}}\frac{1}{\sqrt{2\pi}}e^{-\frac{1}{2}t^2}dt\right)dh}I_{[x_{l_1},x_{u_1}]}(x)I_{[z-y_{u_2},z-y_{l_2}]}(x)I_{[s-y_{u_3},s-y_{l_3}]}(z)dxdz.$$

Since $s = z + k$, $I_{[y_{l_3},y_{u_3}]}(s-z)$ can be written as $I_{[s-y_{u_3},s-y_{l_3}]}(z)$. The details of this derivation are shown in the Appendix.

3.5.3 The Convolutions of the Combinations of the Truncated Normal and Truncated Skew Normal Random Variables on Triple Truncations

Figure 4 illustrates an example of the sum of truncated normal and truncated skew normal random variables on triple truncations. The mean and variance of $X_{T_1}+X_{T_2}+X_{T_3}$ are the sums of means and variances of X_{T_1}, X_{T_2} and X_{T_3} since X_{T_1}, X_{T_2} and X_{T_3} are independent of each other.

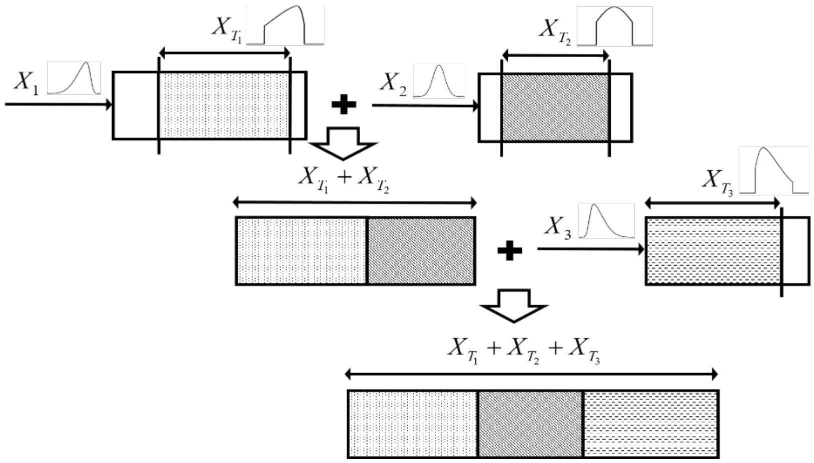

Figure 3.4. Illustration of a sum of truncated normal and truncated skew normal random variables on triple convolution

In this section, we have two subsections. First, the sums of two truncated normal random variables and one truncated skew normal random variable are examined in Section 3.5.3.1. Second, the sums of one truncated normal random variable and two truncated skew normal random variables are investigated in Section 3.5.3.2.

3.5.3.1 Sums of Two Truncated Normal Random Variables and One Truncated Skew Normal Random Variable

Let $Z_2 = X_{T_1} + X_{T_2}$ and $Z_3 = Z_2 + Y_{TS_3}$. Therefore, the probability density function of Z_3 is:

$$f_{Z_3}(s)=\int_{-\infty}^{\infty}\int_{-\infty}^{\infty}\frac{\frac{2}{\sigma_3}\frac{1}{\sqrt{2\pi}}e^{-\frac{1}{2}\left(\frac{s-z-\mu_3}{\sigma_3}\right)^2}\int_{-\infty}^{\alpha_3\frac{s-z-\mu_3}{\sigma_3}}\frac{1}{\sqrt{2\pi}}e^{-\frac{1}{2}t^2}dt}{\int_{y_{l_3}}^{y_{u_3}}\frac{2}{\sigma_3}\frac{1}{\sqrt{2\pi}}e^{-\frac{1}{2}\left(\frac{v-\mu_3}{\sigma_3}\right)^2}\left(\int_{-\infty}^{\alpha_3\frac{v-\mu_3}{\sigma_3}}\frac{1}{\sqrt{2\pi}}e^{-\frac{1}{2}t^2}dt\right)dv}\frac{\frac{1}{\sigma_2\sqrt{2\pi}}\exp^{-\frac{1}{2}\left(\frac{z-x-\mu_2}{\sigma_2}\right)^2}}{\int_{x_{l_2}}^{x_{u_2}}\frac{1}{\sigma_2\sqrt{2\pi}}\exp^{-\frac{1}{2}\left(\frac{s-\mu_2}{\sigma_2}\right)^2}ds}.$$

$$\frac{\frac{1}{\sigma_1\sqrt{2\pi}}\exp^{-\frac{1}{2}\left(\frac{x-\mu_1}{\sigma_1}\right)^2}}{\int_{x_{l_1}}^{x_{u_1}}\frac{1}{\sigma_1\sqrt{2\pi}}\exp^{-\frac{1}{2}\left(\frac{h-\mu_1}{\sigma_1}\right)^2}dh} I_{[x_{l_1},x_{u_1}]}(x)\, I_{[z-x_{u_2},z-x_{l_2}]}(x)\, I_{[s-y_{u_3},s-y_{l_3}]}(z)dxdz.$$

The details of this derivation are shown in the Appendix.

3.5.3.2 Sums of One truncated Normal Random Variable and Two Truncated Skew Normal Random Variables

When $Z_2 = Y_{TS_1} + Y_{TS_2}$ and then $Z_3 = Y_{TS_1} + Y_{TS_2} + X_{T_3} = Z_2 + X_{T_3}$. Therefore, the probability density function of Z_3 is expressed as

$$f_{Z_3}(s) = \int_{-\infty}^{\infty}\int_{-\infty}^{\infty} \frac{\frac{1}{\sigma_3\sqrt{2\pi}}\exp^{-\frac{1}{2}\left(\frac{s-z-\mu_3}{\sigma_3}\right)^2}}{\int_{x_{l_3}}^{x_{u_3}}\frac{1}{\sigma_3\sqrt{2\pi}}\exp^{-\frac{1}{2}\left(\frac{v-\mu_3}{\sigma_3}\right)^2}dv} \cdot \frac{\frac{2}{\sigma_2}\frac{1}{\sqrt{2\pi}}e^{-\frac{1}{2}\left(\frac{z-x-\mu_2}{\sigma_2}\right)^2}\int_{-\infty}^{\alpha_2\frac{z-x-\mu_2}{\sigma_2}}\frac{1}{\sqrt{2\pi}}e^{-\frac{1}{2}t^2}dt}{\int_{y_{l_2}}^{y_{u_2}}\frac{2}{\sigma_2}\frac{1}{\sqrt{2\pi}}e^{-\frac{1}{2}\left(\frac{p-\mu_2}{\sigma_2}\right)^2}\left(\int_{-\infty}^{\alpha_2\frac{p-\mu_2}{\sigma_2}}\frac{1}{\sqrt{2\pi}}e^{-\frac{1}{2}t^2}dt\right)dp} \cdot$$

$$\frac{\frac{2}{\sigma_1}\frac{1}{\sqrt{2\pi}}e^{-\frac{1}{2}\left(\frac{x-\mu_1}{\sigma_1}\right)^2}\int_{-\infty}^{\alpha_1\frac{x-\mu_1}{\sigma_1}}\frac{1}{\sqrt{2\pi}}e^{-\frac{1}{2}t^2}dt}{\int_{y_{l_1}}^{y_{u_1}}\frac{2}{\sigma_1}\frac{1}{\sqrt{2\pi}}e^{-\frac{1}{2}\left(\frac{h-\mu_1}{\sigma_1}\right)^2}\left(\int_{-\infty}^{\alpha_1\frac{h-\mu_1}{\sigma_1}}\frac{1}{\sqrt{2\pi}}e^{-\frac{1}{2}t^2}dt\right)dh} \cdot I_{[y_{l_1},y_{u_1}]}(x) I_{[z-y_{u_2},z-y_{l_2}]}(x) I_{[s-z-x_{u_3},s-z-x_{l_3}]}(z)dxdz.$$

The details are relegated to the Appendix.

3.6. Numerical Examples

Results of the convolutions developed in this paper are applied to two key application areas: statistical tolerance analysis and gap analysis. In Section 6.1, an example of the sum of one truncated normal and two truncated skew normal random variables is provided (see Section 3.5.3.2).

3.6.1 Application to Statistical Tolerance Analysis

In a typical assembly design, such as the one shown in Figure 3.5, the width of component 1 is a normal random variable X_1 and the width of component 2 is a positively skew normal random variable Y_2. Similarly, the width of component 3 is a negatively skewed normal random variable Y_3. Suppose that the parameters, μ_1, μ_2 and μ_3 of X_2, Y_2 and Y_3 are 10, 8, and 16, and the parameters, σ_1, σ_2 and σ_3 of X_1, Y_2 and X_3 are 3, 4, and 4, respectively. In this example, the random variable X_1 is doubly truncated at the lower and upper truncation points, 7 and 13, respectively. The random variable Y_2 is left truncated at 7, and the random variable Y_3 is right truncated at 17. Since Y_2 and Y_3 are negatively and positively skewed, the shape parameters of Y_2 and Y_3 are 3 and -3, respectively.

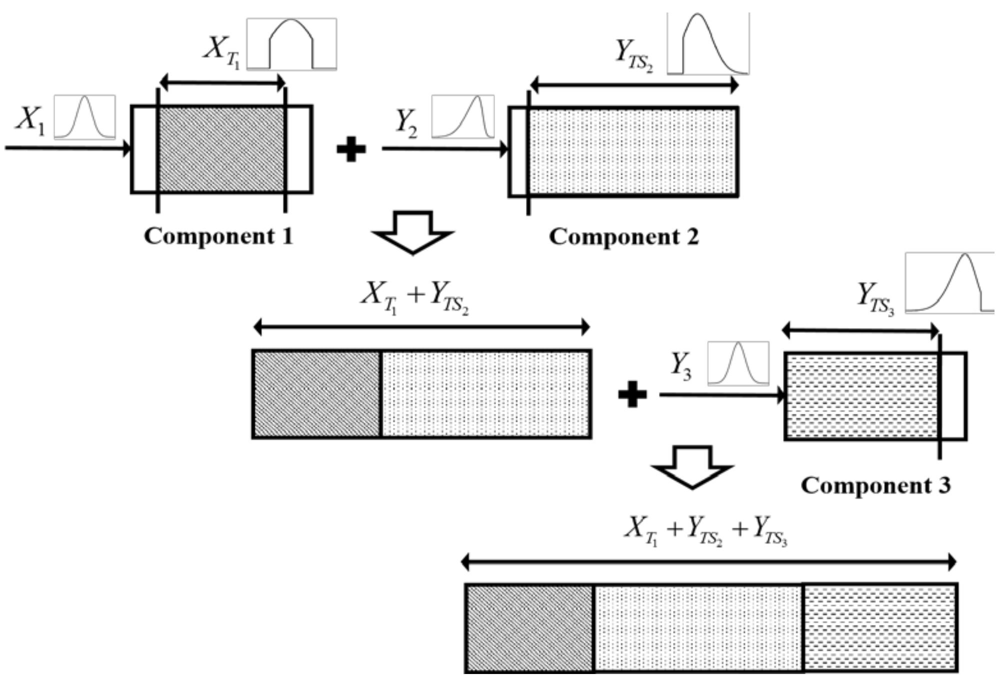

Figure 3.5. Assembly design of statistical tolerance design for three truncated components

Let $Z_2 = X_{T_1} + Y_{TS_2}$. Referring to equations in Section 3.4.3, the probability density function of the sum of the two truncated normal random variables X_{T_1} and Y_{TS_2} are expressed as

$$f_{Z_2}(z) = \int_{-\infty}^{\infty} f_{Y_{TS_2}}(y) f_{X_{T_1}}(x)dx$$

$$= \int_{-\infty}^{\infty} \frac{\frac{2}{4}\frac{1}{\sqrt{2\pi}} e^{-\frac{1}{2}\left(\frac{z-x-8}{4}\right)^2} \int_{-\infty}^{3\frac{z-x-8}{4}} \frac{1}{\sqrt{2\pi}} e^{-\frac{1}{2}t^2} dt}{\int_7^{\infty} \frac{2}{4}\frac{1}{\sqrt{2\pi}} e^{-\frac{1}{2}\left(\frac{p-8}{4}\right)^2} \left(\int_{-\infty}^{3\frac{p-8}{4}} \frac{1}{\sqrt{2\pi}} e^{-\frac{1}{2}t^2} dt\right) dp} \frac{\frac{1}{2\sqrt{2\pi}} \exp^{-\frac{1}{2}\left(\frac{x-10}{3}\right)^2}}{\int_7^{13} \frac{1}{2\sqrt{2\pi}} \exp^{-\frac{1}{2}\left(\frac{h-10}{3}\right)^2} dh} I_{[-\infty, z-7]}(x) I_{[7,13]}(x)dx.$$

Furthermore, the mean and variance of Z_2 are obtained as 21.18 and 7.63, respectively. Now let Z_3 be $X_{T_1} + Y_{TS_2} + X_{TS_3}$. Based on the equations in Section 3.5.3.2, the probability density function of Z_3 is then obtained as

$$f_{Z_3}(s) = \int_{-\infty}^{\infty} f_{X_{T_3}}(s-z) f_{Z_2}(z)dz$$

$$= \int_{-\infty}^{\infty}\int_{-\infty}^{\infty} \frac{\frac{2}{4}\frac{1}{\sqrt{2\pi}} e^{-\frac{1}{2}\left(\frac{z-x-16}{4}\right)^2} \int_{-\infty}^{-3\frac{z-x-16}{4}} \frac{1}{\sqrt{2\pi}} e^{-\frac{1}{2}t^2} dt}{\int_{-\infty}^{17} \frac{2}{4}\frac{1}{\sqrt{2\pi}} e^{-\frac{1}{2}\left(\frac{p-16}{4}\right)^2} \left(\int_{-\infty}^{-3\frac{p-16}{4}} \frac{1}{\sqrt{2\pi}} e^{-\frac{1}{2}t^2} dt\right) dp} \cdot$$

$$\frac{\frac{2}{4}\frac{1}{\sqrt{2\pi}} e^{-\frac{1}{2}\left(\frac{z-x-8}{4}\right)^2} \int_{-\infty}^{3\frac{z-x-8}{4}} \frac{1}{\sqrt{2\pi}} e^{-\frac{1}{2}t^2} dt}{\int_7^{\infty} \frac{2}{4}\frac{1}{\sqrt{2\pi}} e^{-\frac{1}{2}\left(\frac{p-8}{4}\right)^2} \left(\int_{-\infty}^{3\frac{p-8}{4}} \frac{1}{\sqrt{2\pi}} e^{-\frac{1}{2}t^2} dt\right) dp} \frac{\frac{1}{2\sqrt{2\pi}} \exp^{-\frac{1}{2}\left(\frac{x-10}{3}\right)^2}}{\int_7^{13} \frac{1}{2\sqrt{2\pi}} \exp^{-\frac{1}{2}\left(\frac{h-10}{3}\right)^2} dh} \cdot$$

$$I_{[s-z-17,\infty]}(z) I_{[-\infty, z-7]}(x) I_{[7,13]}(x)\, dxdz.$$

Finally, the mean and variance of Z_3 are obtained as 34.00 and 15.25, respectively. Figure 6 shows the shapes of X_{T_1}, Y_{TS_2}, Z_2, Y_{ST_3}, and Z_3.

X_{T_1}	Y_{TS_2}	$Z_2 = X_{T_1} + Y_{TS_2}$	X_{TS_3}	$Z_3 = X_{T_1} + Y_{TS_2} + X_{T}$
$Sym\ TN_{N-\text{type}}$	$TN_{S-\text{type}}$			
$\mu_{T_1} = 10.00,\ \sigma^2_{T_1} = 2.62$	$\mu_{T_2} = 11.18,\ \sigma^2_{T_2} = 6.32$	$\mu_{Z_2} = 21.18,\ \sigma^2_{Z_2} = 8.94$	$\mu_{T_3} = 12.82,\ \sigma^2_{T_3} = 6.32$	$\mu_{Z_3} = 34.00,\ \sigma^2_{Z_3} = 15.25$

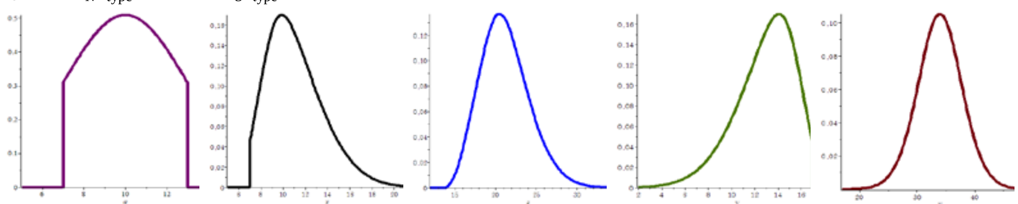

Figure 3.6. The statistical tolerance analysis example

This numerical example offers an insight as to how convolutions can be used in practice to more accurately convey the distribution properties such as skewness, mean, and variance of an overall assembly design. Consistent with the various plots shown in Appendix, Figure 3.7 indicates that the convolutions of the combinations of truncated random variables tend toward normal distributions as a new random variable is added, thereby decreasing the skewness, since the resultant distributions become less skewed. This would allow practitioners to more accurately predict statistical tolerances and have more intricate understanding of the initial engineering design, ultimately leading to a better understanding of the costs involved with the manufacturing processes, allowing for more accurate production forecasts to be made.

3.6.2 Application to Gap Analysis

Define a gap as $G = X_A - X_{C1i} - X_{C2j} - X_{C3k}$ for $i = 1, 2, 3$, $j = 1, 2$, and $k = 1, 2, 3$, where X_A, X_{C1i}, X_{C2j} and X_{C3k} are the dimensions of an assembly and a respective dimension of components. Assuming that the truncated mean of X_A is 41, nine different distributions of assembly components are illustrated in Table 3.1, and the means and variances of G are also shown in Table 3.2.

Table 3.1. Gap analysis data set 1

	Type	α	μ	σ	LTP	UTP	Truncated mean	Truncated variance
X_{C11}	$Sym\ TN_{N-\text{type}}$	0	15	2	13.5	16.5	15.0000	0.6953
X_{C12}	$TN_{L-\text{type}}$	0	15	2	13.5	∞	15.7788	2.2254
X_{C13}	$TN_{S-\text{type}}$	0	15	2	-∞	16.5	14.2212	2.2254
X_{C21}	$TSN^{+}_{L-\text{type}}$	5	10	1.5	10.2	∞	11.3533	0.7478
X_{C22}	$TSN^{+}_{S-\text{type}}$	5	10	1.5	-∞	12.0	10.8336	0.3514
X_{C31}	$Sym\ TN_{N-\text{type}}$	0	12	3	11.0	13.0	12.0000	0.3284
X_{C32}	$TN_{L-\text{type}}$	0	12	3	11.0	∞	13.7955	3.9808
X_{C33}	$TN_{S-\text{type}}$	0	12	3	-∞	13.0	10.2045	3.9808
X_{A}	$Sym\ TN_{N-\text{type}}$	0	41	1	40.5	41.5	41.0000	0.0806

Table 3.2. Mean and variance of gap for data set 1

	X_{C1}	X_{C2}	X_{C3}	X_{A}	μ_G	σ_G^2
1	X_{C11}	X_{C21}	X_{C31}	X_{A}	2.6467	1.8522
2	X_{C11}	X_{C21}	X_{C32}	X_{A}	0.8512	5.5046
3	X_{C11}	X_{C21}	X_{C33}	X_{A}	4.4422	5.5046
4	X_{C11}	X_{C22}	X_{C31}	X_{A}	3.1664	1.4558
5	X_{C11}	X_{C22}	X_{C32}	X_{A}	1.3709	5.1082
6	X_{C11}	X_{C22}	X_{C33}	X_{A}	4.9618	5.1082
7	X_{C12}	X_{C21}	X_{C31}	X_{A}	1.8679	3.3822
8	X_{C12}	X_{C21}	X_{C32}	X_{A}	0.0725	7.0346
9	X_{C12}	X_{C21}	X_{C33}	X_{A}	3.6634	7.0346
10	X_{C12}	X_{C22}	X_{C31}	X_{A}	2.3876	2.9858
11	X_{C12}	X_{C22}	X_{C32}	X_{A}	0.5921	6.6382
12	X_{C12}	X_{C22}	X_{C33}	X_{A}	4.1831	6.6382

13	X_{C13}	X_{C21}	X_{C31}	X_A	3.4255	3.3822
14	X_{C13}	X_{C21}	X_{C32}	X_A	1.6300	7.0346
15	X_{C13}	X_{C21}	X_{C33}	X_A	5.2209	7.0346
16	X_{C13}	X_{C22}	X_{C31}	X_A	3.9451	2.9858
17	X_{C13}	X_{C22}	X_{C32}	X_A	2.1497	6.6382
18	X_{C13}	X_{C22}	X_{C33}	X_A	5.7406	6.6382

Note that dimensional interference occurs when the gap becomes negative (i.e., $X_A < X_{C1} + X_{C2} + X_{C3}$) which often results in assembled products being scrapped or reworked. The convolutions developed in this paper could be an effective tool to help predict the dimensional interference. Now assuming that the truncated mean of X_A is 39, nine different distributions of assembly components are illustrated in Table 3.3, and the means and variances of G are shown in Table 3.4. In this particular example, there are six cases where the mean of gap is negative, creating the extreme dimensional interference highlighting the importance of using truncated normal and skew normal distributions in gap analysis.

Table 3.3. Gap analysis data set 2

	Type	α	μ	σ	LTP	UTP	Truncated mean	Truncated variance
X_{C11}	$Sym\ TN_{N-\text{type}}$	0	15	2	13.5	16.5	15.0000	0.6953
X_{C12}	$TN_{L-\text{type}}$	0	15	2	13.5	∞	15.7788	2.2254
X_{C13}	$TN_{S-\text{type}}$	0	15	2	-∞	16.5	14.2212	2.2254
X_{C21}	$TSN^{+}_{L-\text{type}}$	5	10	1.5	10.2	∞	11.3533	0.7478
X_{C22}	$TSN^{+}_{S-\text{type}}$	5	10	1.5	-∞	12.0	10.8336	0.3514
X_{C31}	$Sym\ TN_{N-\text{type}}$	0	12	3	11.0	13.0	12.0000	0.3284
X_{C32}	$TN_{L-\text{type}}$	0	12	3	11.0	∞	13.7955	3.9808
X_{C33}	$TN_{S-\text{type}}$	0	12	3	-∞	13.0	10.2045	3.9808

X_A	$Sym\ TN_{N-\text{type}}$	0	39	1	38.5	39.5	39.0000	0.0806

Table 3.4. Mean and variance of gap for data set 2

	X_{C1}	X_{C2}	X_{C3}	X_A	μ_G	σ_G^2
1	X_{C11}	X_{C21}	X_{C31}	X_A	0.6467	1.8522
2	X_{C11}	X_{C21}	X_{C32}	X_A	-2.8512	5.5046
3	X_{C11}	X_{C21}	X_{C33}	X_A	2.4422	5.5046
4	X_{C11}	X_{C22}	X_{C31}	X_A	1.1664	1.4558
5	X_{C11}	X_{C22}	X_{C32}	X_A	-1.3709	5.1082
6	X_{C11}	X_{C22}	X_{C33}	X_A	2.9618	5.1082
7	X_{C12}	X_{C21}	X_{C31}	X_A	-1.8679	3.3822
8	X_{C12}	X_{C21}	X_{C32}	X_A	-2.0725	7.0346
9	X_{C12}	X_{C21}	X_{C33}	X_A	1.6634	7.0346
10	X_{C12}	X_{C22}	X_{C31}	X_A	0.3876	2.9858
11	X_{C12}	X_{C22}	X_{C32}	X_A	-2.5921	6.6382
12	X_{C12}	X_{C22}	X_{C33}	X_A	2.1831	6.6382
13	X_{C13}	X_{C21}	X_{C31}	X_A	1.4255	3.3822
14	X_{C13}	X_{C21}	X_{C32}	X_A	-1.6300	7.0346
15	X_{C13}	X_{C21}	X_{C33}	X_A	3.2209	7.0346
16	X_{C13}	X_{C22}	X_{C31}	X_A	1.9451	2.9858
17	X_{C13}	X_{C22}	X_{C32}	X_A	0.1497	6.6382
18	X_{C13}	X_{C22}	X_{C33}	X_A	3.7406	6.6382

3.7. Conclusions

This paper has presented the theoretical foundations of convolutions of truncated normal and skew normal distributions based on double and triple truncations. Convolutions of truncated normal and truncated skew normal random variables were highlighted. The cases presented in this paper illustrate the possible types of convolutions of double truncations. This includes the sum of all the possible combinations containing two truncated random variables with normal and skew normal probability distributions. Numerical examples illustrate the application of convolutions of truncated normal random variables and truncated skew normal random variables to highlight the improved accuracy of tolerance analysis and gap analysis techniques. New findings have the potential to impact a wide range of many other engineering and science problems such as those found in statistical tolerance analysis, more specifically, tolerance stack analysis methods. By utilizing skew normal distributions in tolerance stack analysis methods this allows the tolerance interval to be covered more precisely, allowing for a more accurate understanding of the variation in the gap. Due to algorithmic and hardware constraints, the authors believe that it may not be possible to obtain closed-form convolutions on more than three truncated normal and truncated skew normal random variables at this time. This merits further investigation into algorithms involved in more than three sums of truncated normal random variables and would be a good topic for further research. New algorithmic procedures might allow the convolutions of more than three truncated normal random variables to be obtained with reasonable computational times. From a practical perspective, this would allow statistical tolerance models to be applied at every step of a manufacturing process that has hundreds or thousands of manufacturing steps, instead of at two or three manufacturing steps at a time. This could result in substantially increased savings for a company and an extremely accurate production forecast in terms of identifying the number of components that need to be scrapped or reworked.

CHAPTER FOUR

ZIPPING AND RE-ZIPPING METHODS TO IMPROVE THE PRECISION AND ACCURACY OF MANUFACTURING PROCESSES

This chapter has been published in the International Journal of Experimental Design and Process Optimisation and was a joint work with Jinho Cha. This work should be cited as:

Krenek, R., Cha, J. and Cho, B.R. (2015) 'Zipping and re-zipping methods to improve the precision and accuracy of manufacturing processes', Int. J. Experimental Design and Process Optimisation, Vol. 4, Nos. 3/4, pp.256–289

4.1. Introduction and Literature Review

Understanding truncated random variables and their roles in screening inspection is paramount to the modern industry, as this type of inspection arises in many engineering applications. First, final products are often subjected to screening, and only conforming products are distributed to the customer, while the rejected products, which do not meet the specification requirements, are scrapped or reworked. This screening inspection of the products results in a truncated distribution which represents the conforming products delivered to the customer, as shown in Figure 4.1. This concept has been well advanced in the literature. See for example, Barr and Sherrill (1999), Kim and Takayama (2003), Jawitz (2004), Khasawneh *et al*. (2005a, 2005b), Makarov *et al*. (2009), Cha and Cho (2014), Cha *et al*. (2014). Second, another potential application of screening inspection can be found in a multistage assembly production process, as shown in Figure 4.2, where only conforming items are passed on to the next stage. Examples of multistage processes are numerous. Typical systems of telecommunication, banking, and healthcare consist of multistage processes. It is noted that a product part or service transferring from one stage to the next stage in a multistage process may introduce extra variations that do not occur in a generic single-stage process. An added advantage of screening inspection in a multistage process is the ability of reducing the extra variations by screening noncomforming items in each stage. This can lead to a greater understanding of production costs and a greater understanding of the scrap and reuse of wasted raw materials.

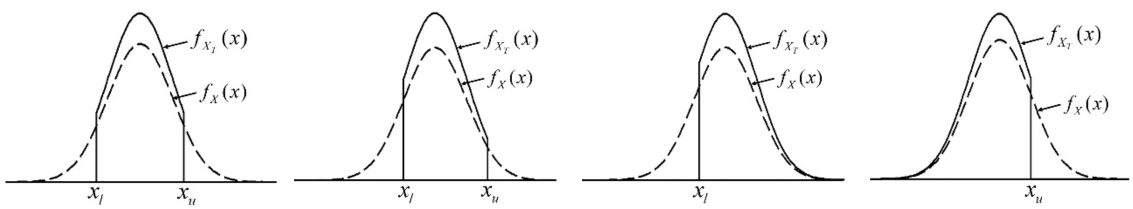

Figure 4.1. Four different types of a truncated normal distribution

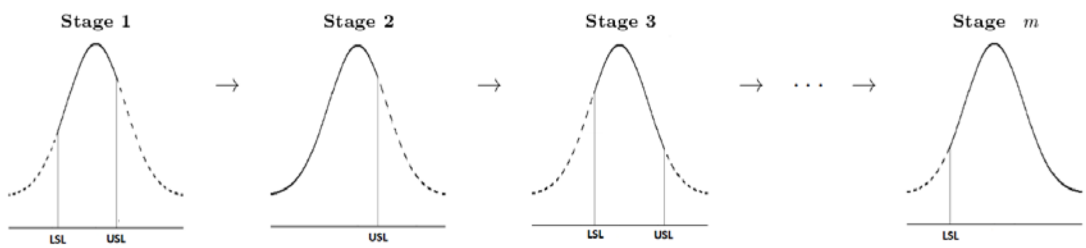

Figure 4.2: Process steps in multi-iterative manufacturing process

Lou (2015) notes that with increasingly competitive global markets, it is becoming more important than ever to be abreast on modern manufacturing techniques such as sustainable development and green manufacturing strategies. Unfortunately, complex modern multistage manufacturing processes are not easy to understand or explain in a straight foreword manner due to industrial globalization along with new technologies as paired with a strong customer oriented paradigm as noted in Ngaile, Wang, & Gau (2015).

This means that it is more important than ever to exploit every possible advantage in order to better understand and improve manufacturing processes.

It is important to note that a multistage assembly process sometimes requires the sum of truncated process distributions, also known as the convolution of process distributions. These convolutions of multiple truncations have practical importance in statistical tolerance design, gap analysis, and other quality engineering areas.

Convolution is a mathematical way of combining two distributions to form a new distribution. In the middle of the 18th century, Euler (1748, 1750) , introduced the earliest convolution theorem, $\int_a^b g(x \pm u) f(u) du,$ based on Taylor series and Beta functions. Note that f and g are two real or complex-valued functions of real variables u and x. In the truncated environment, Francis (1946) first used convolution to obtain a density function of a sum of the truncated random variables, $h_S(s) = \int_{-\infty}^{\infty} g_{Y_T}(y) f_{X_T}(x) dx = \int_{-\infty}^{\infty} g_{Y_T}(s-x) f_{X_T}(x) dx,$ where $S = X_T + Y_T$ with X_T and Y_T being truncated random variables. To be more specific, Francis (1946) and Aggarwal and Guttman (1960) examined the probability density functions of the sums of singly and doubly truncated normal random variables and developed their cumulative probability tables under the assumption that the random variables were independently and identically distributed. Lipow *et al*. (1964) then investigated the density functions of the sums of a standard normal random variable and a left truncated normal random variable. Francis (1946), Aggarwal and Guttman (1960), and Lipow *et al*. (1964) studied the potential computational complexity associated with convolutions. Furthermore, Kratuengarn (1973) compared the means and variances of the sums of left truncated normal random variables numerically through the Laplace and Fourier transforms and evaluated the accuracy of those methods. Recently, Fletcher *et al.* (2010) examined an expression of the moments based on a truncated skew normal distribution. Tsai and Kuo (2012) applied the Monte Carlo method to obtain the densities of the sums of truncated normal random variables with 1,000,000 samples. However, most studies focused on identically truncated normal distributions.

In this manuscript, the term double truncation refers to a random variable that has been pruned in two unique steps; similarly the term triple truncation refers to a random variable that has been pruned in three unique steps. The terms ‘zipping’ and ‘re-zipping’ refer to the truncation of a convolution performed on a distribution or multiple distributions.

4.2. Truncation Assembly

4.2.1 Double Truncation in a Two Stage Process

When a normal random variable X is first truncated, we can obtain a truncated normal random variable X_{T_1} as shown in Figure 4.3. If an additional truncation occurs to enhance quality, another truncated normal random variable X_{T_2} is given. The domain of the truncated normal random variable X_{T_2} is determined by the maximum (minimum) value of the lower (upper) truncation points of X_{T_1} and X_{T_2} .

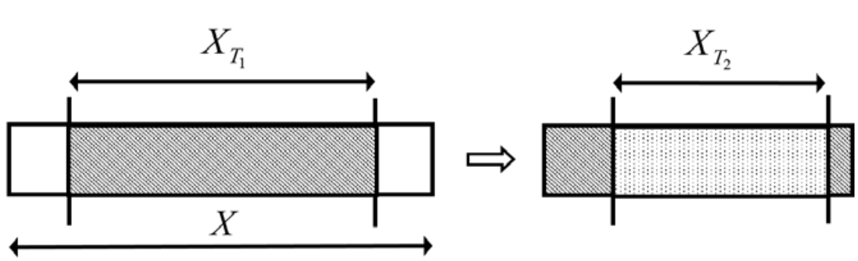

Figure 4.3. Diagram of double truncation in two stage process

The probability density function of X_{T_1} 1 is obtained as $f_{X_{T_1}}(x) = \dfrac{f_X(x)}{\int_{x_{l_1}}^{x_{u_1}} f_X(x)dx} \cdot I_{[x_{l_1}, x_{u_1}]}(x)$

and the probability density function of X_{T_2} is expressed as

$g_{X_{T_2}}(x) = \dfrac{f_{X_T}(x)}{\int_{x_{l_2}}^{x_{u_2}} f_{X_T}(x)dx} \cdot I_{[x_{l_2}, x_{u_2}]}(x)$.

In the two-stage process, cases are classified into sixteen as shown in Figure 4.4. In each stage, a symmetric truncated normal distribution is produced when the distance between the lower truncation point and untruncated original mean is equal to the distance between the untruncated original mean and upper truncation point.

Ca	Stage 1	Stage 2	**Ca**	Stage 1	Stage 2
1	Sym $TN_{N-\text{type}}$ 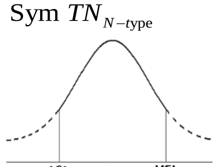	Sym $TN_{N-\text{type}}$ 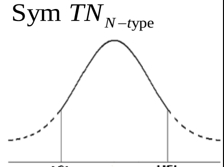	2	Sym $TN_{N-\text{type}}$ 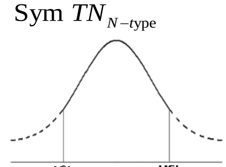	Asym $TN_{N-\text{type}}$ 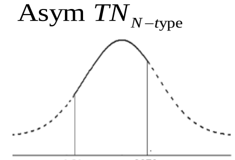
3	Sym $TN_{N-\text{type}}$ 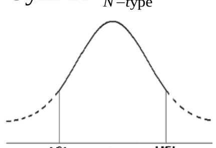	$TN_{L-\text{type}}$ 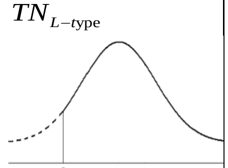	4	Sym $TN_{N-\text{type}}$ 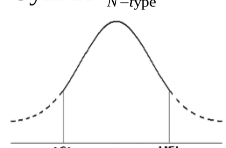	$TN_{S-\text{type}}$ 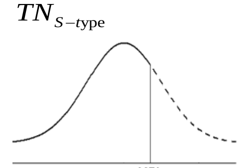
5	Asym $TN_{N-\text{type}}$ 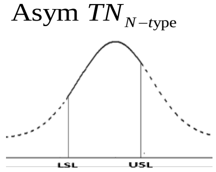	Sym $TN_{N-\text{type}}$ 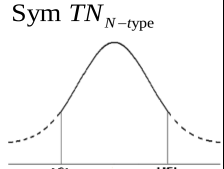	6	Asym $TN_{N-\text{type}}$ 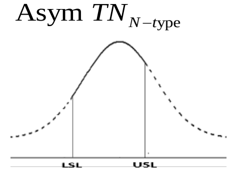	Asym $TN_{N-\text{type}}$ 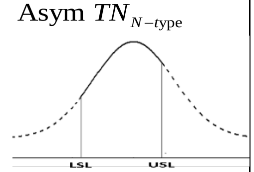
7	Asym $TN_{N-\text{type}}$ 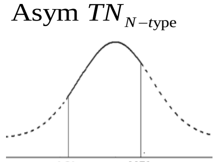	$TN_{L-\text{type}}$ 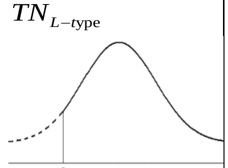	8	Asym $TN_{N-\text{type}}$ 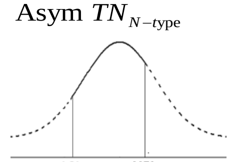	$TN_{S-\text{type}}$ 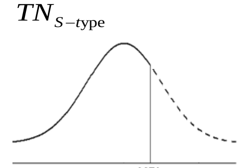
	$TN_{L-\text{type}}$	Sym $TN_{N-\text{type}}$		$TN_{L-\text{type}}$	Asym $TN_{N-\text{type}}$

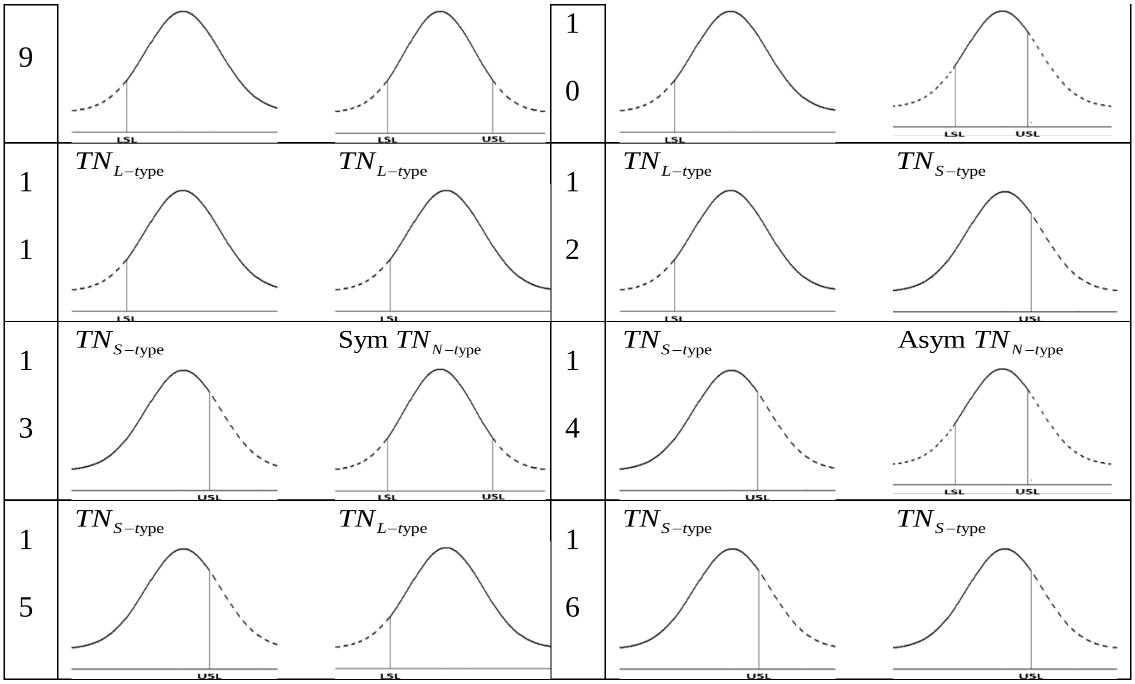

Figure 4.4. Sixteen cases in two-stage process

Now we examine the shape of the truncated normal distributions in each stage. First, we suppose that the mean μ and variance σ^2 of X are 4 and 1, respectively. Second, the lower truncation points (LTPs) and upper truncation points (UTPs) in the sixteen cases are shown in Table 4.1.

Table 4.1. The lower and upper truncation points in two-stage process

Case #	Stage 1 (LTP, UTP)	Stage 2 (LTP, UTP)	Case #	Stage 1 (LTP, UTP)	Stage 2 (LTP, UTP)	Case #	Stage 1 (LTP, UTP)	Stage 2 (LTP, UTP)	Case #	Stage 1 (LTP, UTP)	Stage 2 (LTP, UTP)
1	(2.5, 5.5)	(3, 5)	2	(2.5, 5.5)	(3, 4.5)	3	(2.5, 5.5)	(3, ∞)	4	(2.5, 5.5)	(-∞, 5)
5	(3, 6)	(3.5, 4.5)	6	(3, 6)	(3.5, 5.5)	7	(3, 6)	(3.5, ∞)	8	(3, 6)	(-∞, 5)
9	(2.5, ∞)	(3.5, 4.5)	10	(2.5, ∞)	(3.5, 5.5)	11	(2.5, ∞)	(3.7, ∞)	12	(2.5, ∞)	(-∞, 5)
13	(-∞, 5.5)	(3.5, 4.5)	14	(-∞, 5.5)	(3, 4.5)	15	(-∞, 5.5)	(3.5, ∞)	16	(-∞, 5.5)	(-∞, 5)

Shown in Figure 4.5 are the shapes of truncated normal distributions, truncated means and truncated variances in the two-stage process. The values of the truncated means where truncated normal distributions are symmetric, are equal to the value of the untruncated original mean. The values of the truncated variance decreases in each case as a truncation occurs. In the plot of Stage 2 of Case 3, the value of the upper truncation point is finite as 5.5 even though the upper truncation point in Stage 2 of Case 3 shown in Table 4.1 is infinite. This result shows that the domain of X_{T_2} is determined based on the maximum lower truncation point and minimum upper truncation point. In Cases 5, 9 and 13, the probability density functions of X_{T_2} are expressed as $g_{X_{T_2}}(x) = 1.042\exp^{-\frac{1}{2}(x-4)^2} \cdot I_{[3.5,5.5]}(x)$. Notice that the maximum lower truncation points of X_{T_2} are 3.5 and the minimum upper truncation points of X_{T_2} are 4.5.

Case #	**Stage 1** X_{T_1}	**Stage 2** X_{T_2}	**Case #**	**Stage 1** X_{T_1}	**Stage 2** X_{T_2}
1	Sym $TN_{N-\text{type}}$ 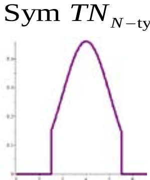 $\mu_{T_1}=4.00,$ $\sigma^2_{T_1}=0.55$	Sym $TN_{N-\text{type}}$ 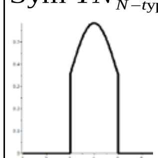 $\mu_{T_2}=4.00$ $\sigma^2_{T_2}=0.29$	**2**	Sym $TN_{N-\text{type}}$ 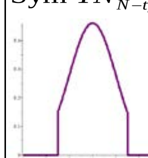 $\mu_{T_1}=4.00,$ $\sigma^2_{T_1}=0.55$	Asym $TN_{N-\text{type}}$ 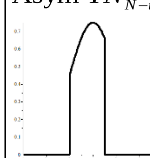 $\mu_{T_2}=3.79,$ $\sigma^2_{T_2}=0.17$
3	Sym $TN_{N-\text{type}}$ 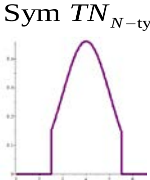 $\mu_{T_1}=4.00,$ $\sigma^2_{T_1}=0.55$	$TN_{L-\text{type}}$ 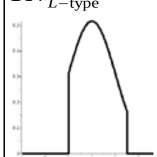 $\mu_{T_2}=4.15$ $\sigma^2_{T_2}=0.42$	**4**	Sym $TN_{N-\text{type}}$ 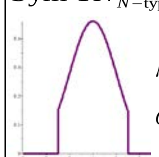 $\mu_{T_1}=4.00,$ $\sigma^2_{T_1}=0.55$	$TN_{S-\text{type}}$ 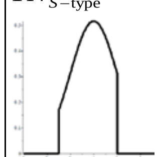 $\mu_{T_2}=3.85$ $\sigma^2_{T_2}=0.42$
5	Asym $TN_{N-\text{type}}$	Sym $TN_{N-\text{type}}$	**6**	Asym $TN_{N-\text{type}}$	Asym $TN_{N-\text{type}}$

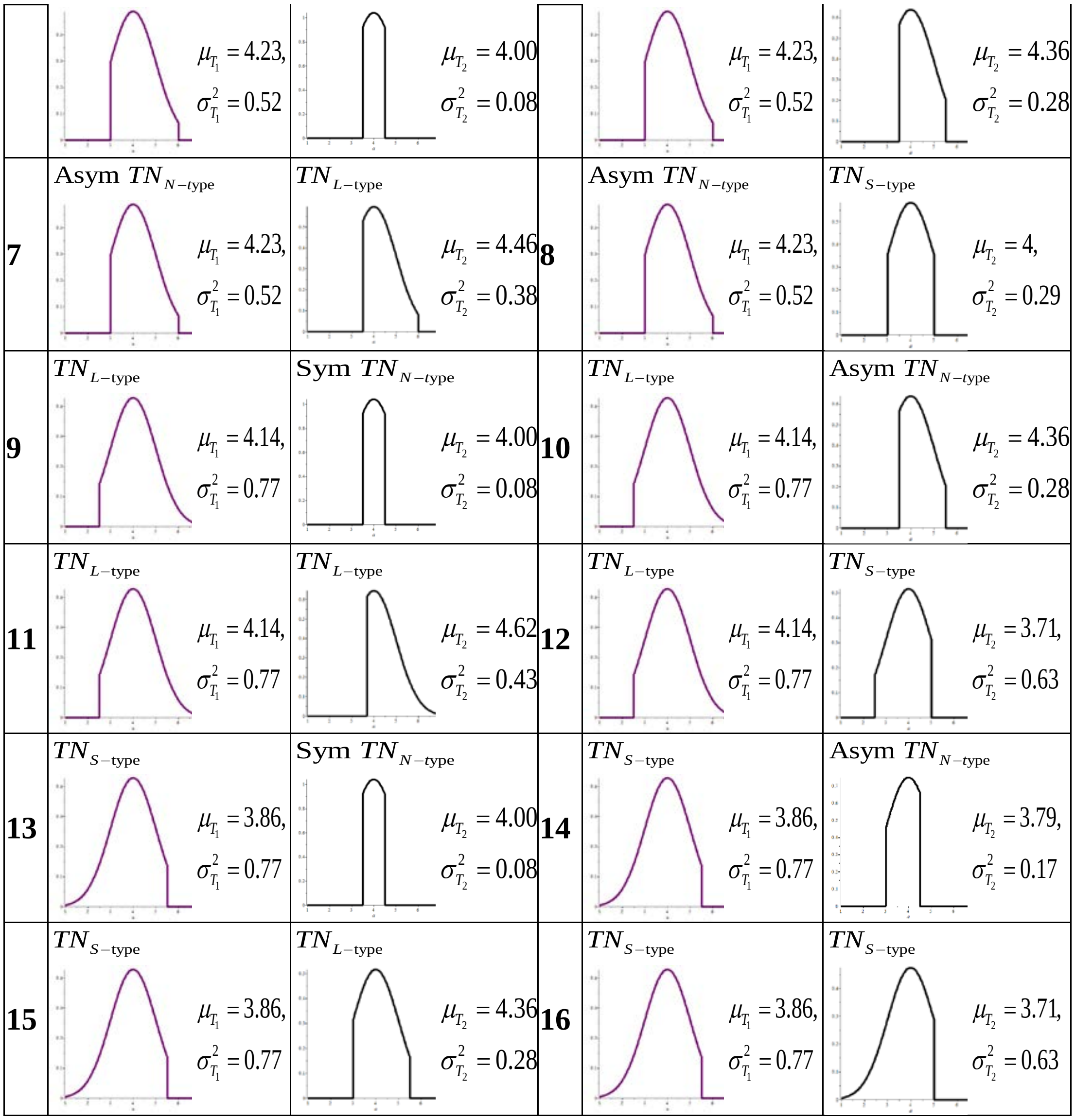

Figure 4.5. The properties of sixteen cases in two-stage process

4.2.2 Triple Truncation in a Three Stage Process

Based on the results of Section 2.1, a stage is added by truncating the random variable X_{T_2} for triple truncation. The probability density function of X_{T_3} in Stage 3 is expressed as $h_{X_{T_3}}(x) = \dfrac{g_{X_{T_2}}(x)}{\int_{x_{l_3}}^{x_{u_3}} g_{X_{T_2}}(x)dx} \cdot \quad I_{[x_{l_3}, x_{u_3}]}(x)$. Figure 6 shows that diagram of the triple truncation in three-stage process.

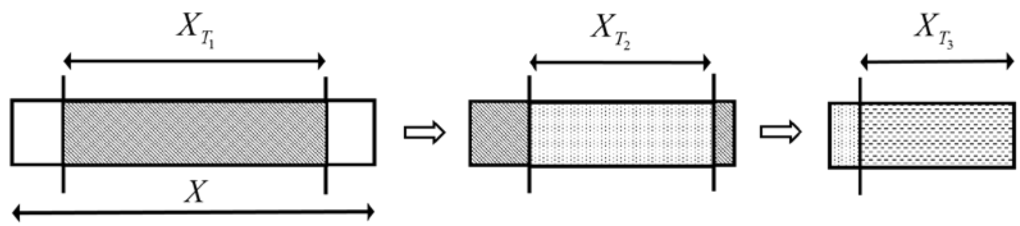

Figure 4.6. Diagram of triple truncation process

Since there are also four types of a truncation in Stage 3, sixty four cases need to be considered as shown in Table 4.2. In each stage, a symmetric truncated normal distribution is produced when the distance between the lower truncation point and untruncated original mean is equal to the distance between the untruncated original mean and upper truncation point.

Table 4.2. Sixty four cases in three-stage process

Case #	Stage 1	Stage 2	Stage 3	Case #	Stage 1	Stage 2	Stage 3
1	Sym $TN_{N-\text{type}}$	Sym $TN_{N-\text{type}}$	Sym $TN_{N-\text{type}}$	2	Sym $TN_{N-\text{type}}$	Sym $TN_{N-\text{type}}$	Asym $TN_{N-\text{type}}$
3	Sym $TN_{N-\text{type}}$	Sym $TN_{N-\text{type}}$	$TN_{L-\text{type}}$	4	Sym $TN_{N-\text{type}}$	Sym $TN_{N-\text{type}}$	$TN_{S-\text{type}}$
5	Sym $TN_{N-\text{type}}$	Asym $TN_{N-\text{type}}$	Sym $TN_{N-\text{type}}$	6	Sym $TN_{N-\text{type}}$	Asym $TN_{N-\text{type}}$	Asym $TN_{N-\text{type}}$
7	Sym $TN_{N-\text{type}}$	Asym $TN_{N-\text{type}}$	$TN_{L-\text{type}}$	8	Sym $TN_{N-\text{type}}$	Asym $TN_{N-\text{type}}$	$TN_{S-\text{type}}$
9	Sym $TN_{N-\text{type}}$	$TN_{L-\text{type}}$	Sym $TN_{N-\text{type}}$	10	Sym $TN_{N-\text{type}}$	$TN_{L-\text{type}}$	Asym $TN_{N-\text{type}}$
11	Sym $TN_{N-\text{type}}$	$TN_{L-\text{type}}$	$TN_{L-\text{type}}$	12	Sym $TN_{N-\text{type}}$	$TN_{L-\text{type}}$	$TN_{S-\text{type}}$

13	Sym $TN_{N-\text{type}}$	$TN_{S-\text{type}}$	Sym $TN_{N-\text{type}}$	**14**	Sym $TN_{N-\text{type}}$	$TN_{S-\text{type}}$	Asym $TN_{N-\text{type}}$
15	Sym $TN_{N-\text{type}}$	$TN_{S-\text{type}}$	$TN_{L-\text{type}}$	**16**	Sym $TN_{N-\text{type}}$	$TN_{S-\text{type}}$	$TN_{S-\text{type}}$
17	Asym $TN_{N-\text{type}}$	Sym $TN_{N-\text{type}}$	Sym $TN_{N-\text{type}}$	**18**	Asym $TN_{N-\text{type}}$	Sym $TN_{N-\text{type}}$	Sym $TN_{N-\text{type}}$
19	Asym $TN_{N-\text{type}}$	Sym $TN_{N-\text{type}}$	$TN_{L-\text{type}}$	**20**	Asym $TN_{N-\text{type}}$	Sym $TN_{N-\text{type}}$	$TN_{L-\text{type}}$
21	Asym $TN_{N-\text{type}}$	Asym $TN_{N-\text{type}}$	Sym $TN_{N-\text{type}}$	**22**	Asym $TN_{N-\text{type}}$	Asym $TN_{N-\text{type}}$	Asym $TN_{N-\text{type}}$
23	Asym $TN_{N-\text{type}}$	Asym $TN_{N-\text{type}}$	$TN_{L-\text{type}}$	**24**	Asym $TN_{N-\text{type}}$	Asym $TN_{N-\text{type}}$	$TN_{S-\text{type}}$
25	Asym $TN_{N-\text{type}}$	$TN_{L-\text{type}}$	Sym $TN_{N-\text{type}}$	**26**	Asym $TN_{N-\text{type}}$	$TN_{L-\text{type}}$	Asym $TN_{N-\text{type}}$
27	Asym $TN_{N-\text{type}}$	$TN_{L-\text{type}}$	$TN_{L-\text{type}}$	**28**	Asym $TN_{N-\text{type}}$	$TN_{L-\text{type}}$	$TN_{S-\text{type}}$
29	Asym $TN_{N-\text{type}}$	$TN_{S-\text{type}}$	Sym $TN_{N-\text{type}}$	**30**	Asym $TN_{N-\text{type}}$	$TN_{S-\text{type}}$	Asym $TN_{N-\text{type}}$
31	Asym $TN_{N-\text{type}}$	$TN_{S-\text{type}}$	$TN_{L-\text{type}}$	**32**	Asym $TN_{N-\text{type}}$	$TN_{S-\text{type}}$	$TN_{S-\text{type}}$
33	$TN_{L-\text{type}}$	Sym $TN_{N-\text{type}}$	Sym $TN_{N-\text{type}}$	**34**	$TN_{L-\text{type}}$	Sym $TN_{N-\text{type}}$	Sym $TN_{N-\text{type}}$
35	$TN_{L-\text{type}}$	Sym $TN_{N-\text{type}}$	$TN_{L-\text{type}}$	**36**	$TN_{L-\text{type}}$	Sym $TN_{N-\text{type}}$	$TN_{L-\text{type}}$
37	$TN_{L-\text{type}}$	Asym $TN_{N-\text{type}}$	Sym $TN_{N-\text{type}}$	**38**	$TN_{L-\text{type}}$	Asym $TN_{N-\text{type}}$	Sym $TN_{N-\text{type}}$
39	$TN_{L-\text{type}}$	Asym $TN_{N-\text{type}}$	$TN_{L-\text{type}}$	**40**	$TN_{L-\text{type}}$	Asym $TN_{N-\text{type}}$	$TN_{L-\text{type}}$
41	$TN_{L-\text{type}}$	$TN_{L-\text{type}}$	Sym $TN_{N-\text{type}}$	**42**	$TN_{L-\text{type}}$	$TN_{L-\text{type}}$	Sym $TN_{N-\text{type}}$
43	$TN_{L-\text{type}}$	$TN_{L-\text{type}}$	$TN_{L-\text{type}}$	**44**	$TN_{L-\text{type}}$	$TN_{L-\text{type}}$	$TN_{L-\text{type}}$
45	$TN_{L-\text{type}}$	$TN_{S-\text{type}}$	Sym $TN_{N-\text{type}}$	**46**	$TN_{L-\text{type}}$	$TN_{S-\text{type}}$	Sym $TN_{N-\text{type}}$
47	$TN_{L-\text{type}}$	$TN_{S-\text{type}}$	$TN_{L-\text{type}}$	**48**	$TN_{L-\text{type}}$	$TN_{S-\text{type}}$	$TN_{L-\text{type}}$
49	$TN_{S-\text{type}}$	Sym $TN_{N-\text{type}}$	Sym $TN_{N-\text{type}}$	**50**	$TN_{S-\text{type}}$	Sym $TN_{N-\text{type}}$	Asym $TN_{N-\text{type}}$
51	$TN_{S-\text{type}}$	Sym $TN_{N-\text{type}}$	$TN_{L-\text{type}}$	**52**	$TN_{S-\text{type}}$	Sym $TN_{N-\text{type}}$	$TN_{S-\text{type}}$
53	$TN_{S-\text{type}}$	Asym $TN_{N-\text{type}}$	Sym $TN_{N-\text{type}}$	**54**	$TN_{S-\text{type}}$	Asym $TN_{N-\text{type}}$	Asym $TN_{N-\text{type}}$
55	$TN_{S-\text{type}}$	Asym $TN_{N-\text{type}}$	$TN_{L-\text{type}}$	**56**	$TN_{S-\text{type}}$	Asym $TN_{N-\text{type}}$	$TN_{S-\text{type}}$
57	$TN_{S-\text{type}}$	$TN_{L-\text{type}}$	Sym $TN_{N-\text{type}}$	**58**	$TN_{S-\text{type}}$	$TN_{L-\text{type}}$	Asym $TN_{N-\text{type}}$
59	$TN_{S-\text{type}}$	$TN_{L-\text{type}}$	$TN_{L-\text{type}}$	**60**	$TN_{S-\text{type}}$	$TN_{L-\text{type}}$	$TN_{S-\text{type}}$
61	$TN_{S-\text{type}}$	$TN_{S-\text{type}}$	Sym $TN_{N-\text{type}}$	**62**	$TN_{S-\text{type}}$	$TN_{S-\text{type}}$	Asym $TN_{N-\text{type}}$
63	$TN_{S-\text{type}}$	$TN_{S-\text{type}}$	$TN_{L-\text{type}}$	**64**	$TN_{S-\text{type}}$	$TN_{S-\text{type}}$	$TN_{S-\text{type}}$

Among the sixty four cases, we select sixteen cases in order to investigate how the shapes of truncated normal distributions, truncated means and truncated variances change as shown in Table 4.3. A• and B• indicate the lower and upper truncation points, respectively.

Table 4.3. Lower and upper truncation points under sixteen cases among sixty four cases in three stage process

Case #	Stage 1 (A1,B1)	Stage 2 (A2,B2)	Stage 3 (A3,B3)	Case #	Stage 1 (A1,B1)	Stage 2 (A2,B2)	Stage 3 (A3,B3)	Case #	Stage 1 (A1,B1)	Stage 2 (A2,B2)	Stage 3 (A3,B3)	Case #	Stage 1 (A1,B1)	Stage 2 (A2,B2)	Stage 3 (A3,B3)
1	(2,6)	(3,5)	(3.5,4.5)	5	(2,6)	(2.5,5)	(3.5,4.5)	9	(2,6)	(2.5,∞)	(3.5,4.5)	13	(2,6)	(-∞,5)	(3.5,4.5)
17	(1,5)	(3.3,4.7)	(3.5,4.5)	21	(1,5)	(2,4.7)	(3.5,4.5)	25	(1,5)	(2,∞)	(3.5,4.5)	29	(1,5)	(-∞,5)	(3.5,4.5)
33	(2, ∞)	(2.5,5.5)	(3.5,4.5)	37	(2, ∞)	(2.5,6)	(3.5,4.5)	41	(2, ∞)	(3,∞)	(3.5,4.5)	45	(2, ∞)	(-∞,5)	(3.5,4.5)

49	**(-∞,6)**	**(2.3,5.7)**	**(3.5,4.5)**	**53**	**(-∞,6)**	**(2,5.5)**	**(3.5,4.5)**	**57**	**(-∞,6)**	**(2.3,∞)**	**(3.5,4.5)**	**61**	**(-∞,6)**	**(-∞,5)**	**(3.5,4.5)**

In the three-stage process, the shapes of truncated normal distributions, truncated means and truncated variances are illustrated in Figure 4.7. The probability density functions of X_{T_3} are expressed as $h_{X_{T_3}}(x) = 1.042\exp^{-\frac{1}{2}(x-4)^2} \cdot I_{[3.5,5.5]}(x)$ since the lower and upper truncation points are 3.5 and 5.5, respectively.

Cas	**Stage 1**	**Stage 2**	**Stage 3**	**Cas**	**Stage 1**	**Stage 2**	**Stage 3**
1	Sym TN 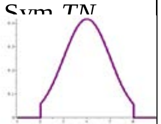 $\mu_{T_1}=4.00,\ \sigma^2_{T_1}=0.7$	Sym TN 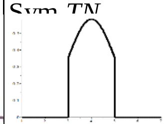 $\mu_{T_2}=4.00,\ \sigma^2_{T_2}=0.29$	Sym TN 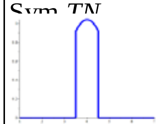 $\mu_{T_3}=4.00,\ \sigma^2_{T_3}=0.08$	**5**	Sym TN 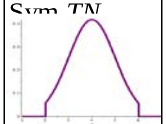 $\mu_{T_1}=4.00,\ \sigma^2_{T_1}=0.7$	Asym TN 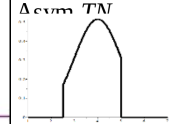 $\mu_{T_2}=3.85,\ \sigma^2_{T_2}=0.42$	Sym TN 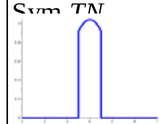 $\mu_{T_3}=4.00,\ \sigma^2_{T_3}=0.08$
9	Sym $TN_{N-\text{type}}$ 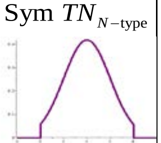 $\mu_{T_1}=4.00,\ \sigma^2_{T_1}=0.7$	$TN_{L-\text{type}}$ 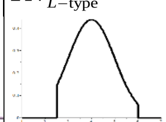 $\mu_{T_2}=4.08,\ \sigma^2_{T_2}=0.66$	Sym $TN_{N-\text{type}}$ 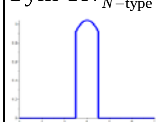 $\mu_{T_3}=4.00,\ \sigma^2_{T_3}=0.08$	**13**	Sym $TN_{N-\text{type}}$ 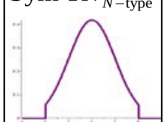 $\mu_{T_1}=4.00,\ \sigma^2_{T_1}=0.7$	$TN_{S-\text{type}}$ 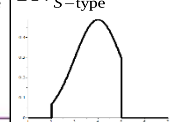 $\mu_{T_2}=3.77,\ \sigma^2_{T_2}=0.52$	Sym $TN_{N-\text{type}}$ 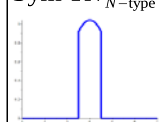 $\mu_{T_3}=4.00,\ \sigma^2_{T_3}=0.08$
17	Asym $TN_{N-\text{type}}$ 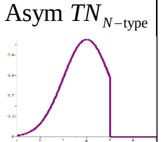 $\mu_{T_1}=3.72,\ \sigma^2_{T_1}=0.6$	Sym $TN_{N-\text{type}}$ 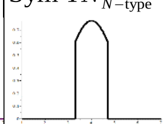 $\mu_{T_2}=4.00,\ \sigma^2_{T_2}=0.15$	Sym $TN_{N-\text{type}}$ 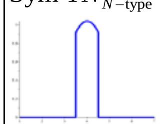 $\mu_{T_3}=4.00,\ \sigma^2_{T_3}=0.08$	**21**	Asym $TN_{N-\text{type}}$ 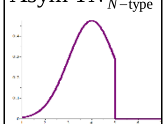 $\mu_{T_1}=3.72,\ \sigma^2_{T_1}=0.6$	Asym $TN_{N-\text{type}}$ 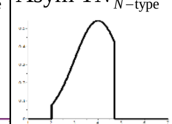 $\mu_{T_2}=3.65,\ \sigma^2_{T_2}=0.43$	Sym $TN_{N-\text{type}}$ 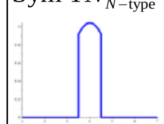 $\mu_{T_3}=4.00,\ \sigma^2_{T_3}=0.08$
25	Asym $TN_{N-\text{type}}$ 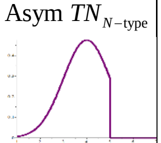 $\mu_{T_1}=3.72,\ \sigma^2_{T_1}=0.6$	$TN_{L-\text{type}}$ 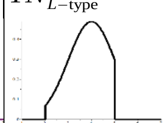 $\mu_{T_2}=3.77,\ \sigma^2_{T_2}=0.52$	Sym $TN_{N-\text{type}}$ 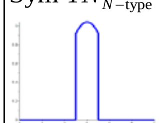 $\mu_{T_3}=4.00,\ \sigma^2_{T_3}=0.08$	**29**	Asym $TN_{N-\text{type}}$ 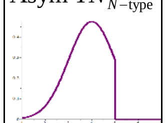 $\mu_{T_1}=3.72,\ \sigma^2_{T_1}=0.6$	$TN_{S-\text{type}}$ 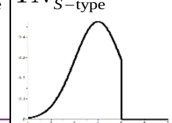 $\mu_{T_1}=3.72,\ \sigma^2_{T_1}=0.62$	Sym $TN_{N-\text{type}}$ 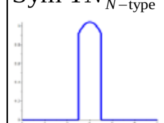 $\mu_{T_3}=4.00,\ \sigma^2_{T_3}=0.08$
33	$TN_{L-\text{type}}$ 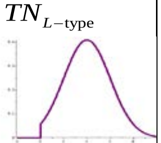 $\mu_{T_1}=4.06,\ \sigma^2_{T_1}=0.8$	Sym $TN_{N-\text{type}}$ 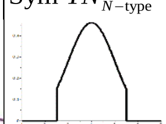 $\mu_{T_2}=4.00,\ \sigma^2_{T_2}=0.55$	Sym $TN_{N-\text{type}}$ 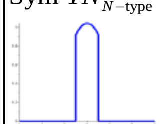 $\mu_{T_3}=4.00,\ \sigma^2_{T_3}=0.08$	**37**	$TN_{L-\text{type}}$ 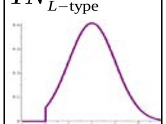 $\mu_{T_1}=4.06,\ \sigma^2_{T_1}=0.8$	Asym $TN_{N-\text{type}}$ 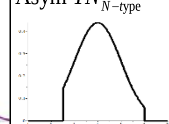 $\mu_{T_2}=4.08,\ \sigma^2_{T_2}=0.66$	Sym $TN_{N-\text{type}}$ 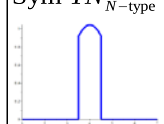 $\mu_{T_3}=4.00,\ \sigma^2_{T_3}=0.08$
41	$TN_{L-\text{type}}$	$TN_{L-\text{type}}$	Sym $TN_{N-\text{type}}$	**45**	$TN_{L-\text{type}}$	$TN_{S-\text{type}}$	Sym $TN_{N-\text{type}}$

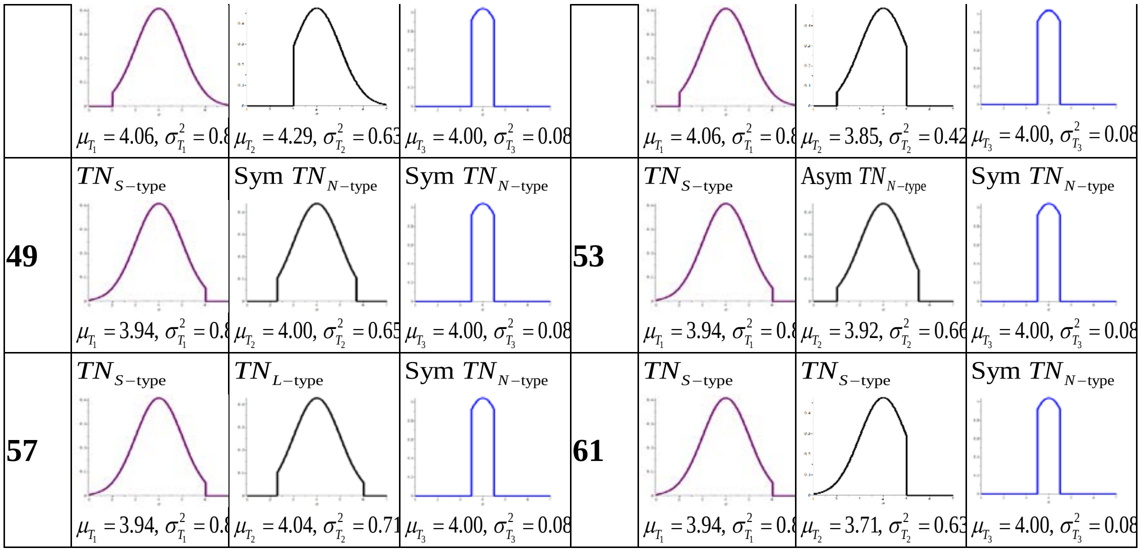

Figure 4.7. The properties of sixteen cases in three-stage process

4.3. Formal Definition of Convolution

As previously discussed, convolution is a mathematical way combining two distributions. Given the following general form

$$h(z) = g(y) * f(x) = \int_a^b g(z-x) \cdot f(x)dx,$$

the functions $f(x)$ and $g(y)$ are said to be convoluted into $h(z)$ with x having a domain restricted to be between a and b. the convolution concept was first used to obtain a density function of the sums of truncated random variables:

$$h_Z(z) = \int_{-\infty}^{\infty} g_{Y_T}(y) f_{X_T}(x)dx = \int_{-\infty}^{\infty} g_{Y_T}(z-x) f_{X_T}(x)dx$$

Note that $Z = X_T + Y_T$ where X_T and Y_T are truncated random variables. If a random variable X is normally distributed with mean μ and variance σ^2, its probability density function is defined as

$$f_X(x) = \frac{1}{\sqrt{2\pi\sigma^2}} \exp^{-\frac{1}{2}\left(\frac{x-\mu}{\sigma}\right)^2} \text{ where } -\infty < x < \infty. \quad (1)$$

When the distribution of X is truncated with the lower and upper truncation points, x_l and x_u, the probability density function of the truncated normal distribution can then be expressed as follows

$$f_{X_T}(x) = \frac{f_X(x)}{\int_{x_l}^{x_u} f_X(x)dx} \text{ where } x_l < x < x_u. \quad (2)$$

By using an indication function, the probability density function of $f_{X_T}(x)$ is also written as

$$f_{X_T}(x) = \frac{f_X(x)}{\int_{x_l}^{x_u} f_X(x)dx} I_{[x_l, x_u]}(x), \quad (3)$$

where the indicator function $I_{[x_l, x_u]}(x)$ is defined as

$$I_{[x_l, x_u]}(x) = \begin{cases} 1 & \text{if } x \in [x_l, x_u] \\ 0 & \text{otherwise} \end{cases}. \quad (4)$$

The truncated mean μ_T and truncated variance σ_T^2 of X_T are given by $\int_{x_l}^{x_u} x\, f_{X_T}(x)dx$ and $\int_{x_l}^{x_u} x^2 f_{X_T}(x)dx - \left(\int_{x_l}^{x_u} x\, f_{X_T}(x)dx\right)^2$, respectively.

The shapes of a truncated distribution vary based on its truncation point(s), and mean and variance of the untruncated original distribution. It is noticed that a truncated variance after implementing a single truncation will be no longer the same as the original variance associated with the untruncated normal distribution $f_X(x)$. Similarly, unless symmetric truncations are used, a truncated mean is not the same as the original mean of an untruncated normal distribution. Finally, properties of S- and L- types of quality characteristics can be described from the above notation. Specifically, eliminating the lower specification limit, while retaining a finite upper specification limit for x_u results in an S-type quality characteristic. Eliminating the upper specification limit x_u, while retaining a finite lower specification limit for x_l results in an L-type quality characteristic.

Figure 4.8 illustrates the plots of the distribution of the sum of two truncated normal random variables from an assembly process. Plots (a) and (b) show the distributions of two independently, identically distributed symmetric two times truncated normal random variables, respectively. The distribution of the sum of the truncated normal random variables which is obtained by convolution is shown in plot (c). Note that its probability density function $h_Z(z)$ is different from the density of a traditional normal distribution.

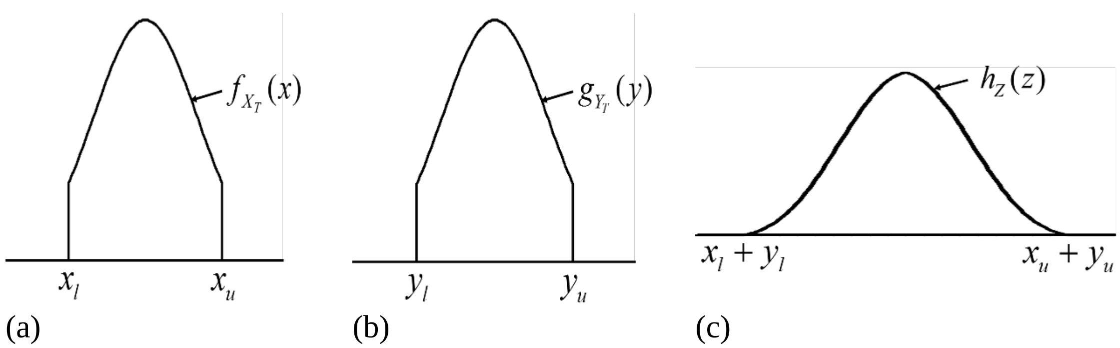

Figure 4.8. Plots of the sum of two truncated normal random variables from an assembly process

4.4. Numerical Examples

4.4.1 Zipping Under the Sum of Two Truncated Normal Random Variables

Zipping from circular and rectangular types can be considered as shown in Figure 9.

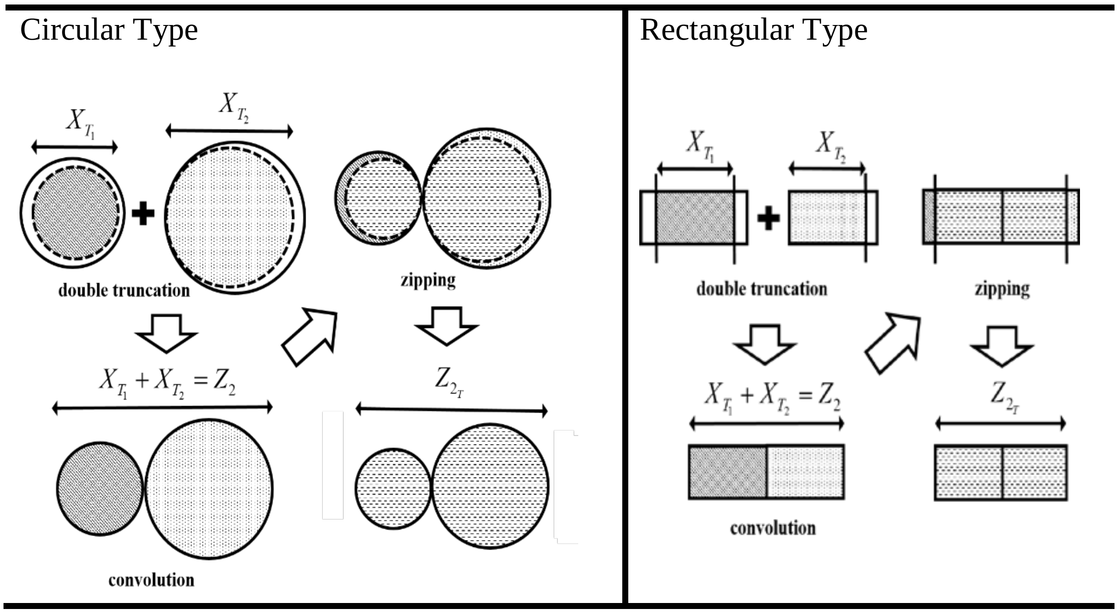

Figure 4.9. Two types of truncation of the sum of two truncated normal random variables

In this section, numerical examples of zipping based on the sums of convolutions of two truncated normal distributions are illuminated. The probability density function of the sum of two truncated normal random variables, X_{T_1} and X_{T_2} is first obtained. The random variable Z_2 is then truncated. Parameters of two truncated normal random variables are shown in Table 4.4. For numerical examples, assume that the means, μ_1 and μ_2, are 12 and 7, and the standard deviations, σ_1 and σ_2 are 1.2 and 0.8, respectively. The lower and upper truncation points of X_{T_1} and X_{T_2} are also assumed as shown in Table 4.

Table 4.4. Parameters of two truncated normal random variables

	μ	σ	LTP	UTP
X_{T_1}	12	1.2	10	14
X_{T_2}	7	0.8	-∞	10

By letting Z_2 be $X_{T_1}+X_{T_2}$, the probability density function of the sum of the above two truncated normal random variables is expressed as

$$f_{Z_2}(z)=\int_{-\infty}^{\infty} f_{X_{T_2}}(y) f_{X_{T_1}}(x)dx$$

$$=\int_{-\infty}^{\infty}\frac{\frac{1}{0.8\sqrt{2\pi}}\exp^{-\frac{1}{2}\left(\frac{y-7}{0.8}\right)^2}}{\int_{-\infty}^{10}\frac{1}{0.8\sqrt{2\pi}}\exp^{-\frac{1}{2}\left(\frac{s-7}{0.8}\right)^2}ds}\frac{\frac{1}{1.2\sqrt{2\pi}}\exp^{-\frac{1}{2}\left(\frac{x-12}{1.2}\right)^2}}{\int_{10}^{14}\frac{1}{1.2\sqrt{2\pi}}\exp^{-\frac{1}{2}\left(\frac{h-12}{1.2}\right)^2}dh} I_{[-\infty,10]}(y)\, I_{[10,14]}(x)\,dx.$$

Mean and standard deviation (variance) of Z_2 are also obtained as 18.9997 and 1.2455 (1.5512), respectively. Next, the distribution of Z_2 with the lower and upper truncation points, 17 and 21, is zipped. The probability of density function of Z_{2_T} is then obtained as

$$f_{Z_{2_T}}(z)=\frac{f_{Z_2}(z)}{\int_{17}^{21} f_{Z_2}(z)dz} I_{[17,21]}(z)$$

$$=\frac{\int_{-\infty}^{\infty}\frac{\frac{1}{0.8\sqrt{2\pi}}\exp^{-\frac{1}{2}\left(\frac{y-7}{0.8}\right)^2}}{\int_{-\infty}^{10}\frac{1}{0.8\sqrt{2\pi}}\exp^{-\frac{1}{2}\left(\frac{s-7}{0.8}\right)^2}ds}\frac{\frac{1}{1.2\sqrt{2\pi}}\exp^{-\frac{1}{2}\left(\frac{x-12}{1.2}\right)^2}}{\int_{10}^{14}\frac{1}{1.2\sqrt{2\pi}}\exp^{-\frac{1}{2}\left(\frac{h-12}{1.2}\right)^2}dh} I_{[10,14]}(x) I_{[-\infty,10]}(y)\, I_{[17,21]}(z)dx}{\int_{17}^{21}\int_{-\infty}^{\infty}\frac{\frac{1}{0.8\sqrt{2\pi}}\exp^{-\frac{1}{2}\left(\frac{y-7}{0.8}\right)^2}}{\int_{-\infty}^{10}\frac{1}{0.8\sqrt{2\pi}}\exp^{-\frac{1}{2}\left(\frac{s-7}{0.8}\right)^2}ds}\frac{\frac{1}{1.2\sqrt{2\pi}}\exp^{-\frac{1}{2}\left(\frac{x-12}{1.2}\right)^2}}{\int_{10}^{14}\frac{1}{1.2\sqrt{2\pi}}\exp^{-\frac{1}{2}\left(\frac{h-12}{1.2}\right)^2}dh} I_{[-\infty,10]}(y)\, I_{[10,14]}(x)\,dxdz}.$$

The mean, variance and distribution, of Z_2 and Z_{2_T} are shown in Figure 4.10.

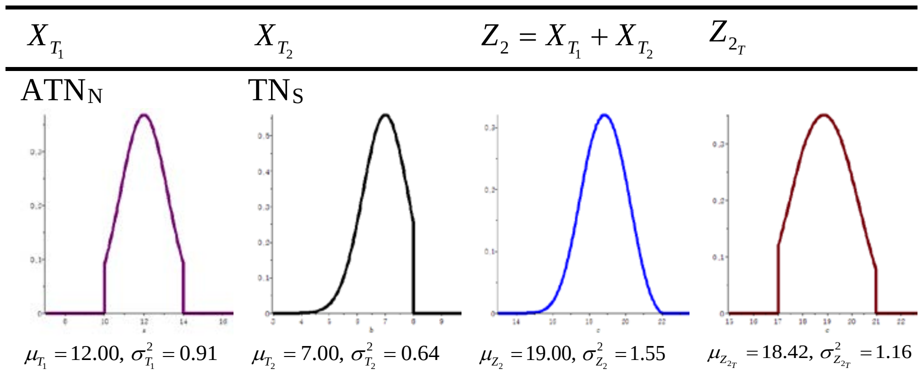

Figure 4.10. Zipping based on the sum of two truncated normal random variables

When considering sums of truncated normal random variables which are independent and identically distributed, the mean of the sum of the truncated normal random variables is equal to the sum of the means of each individual truncated normal random variable. Similarly, the variance of the sum of the truncated normal random variables is equal to the sum of the variances of each individual truncated normal random variable. The variance of Z_{2_T} is always smaller than the variance of Z_2, and the truncation points cause the mean of Z_{2_T} to be larger than the mean of Z_2.

4.4.2 Re-zipping Under the Sum of Three Truncated Normal Random Variables

Re-zipping from rectangular type can be considered as shown in Figure 4.11.

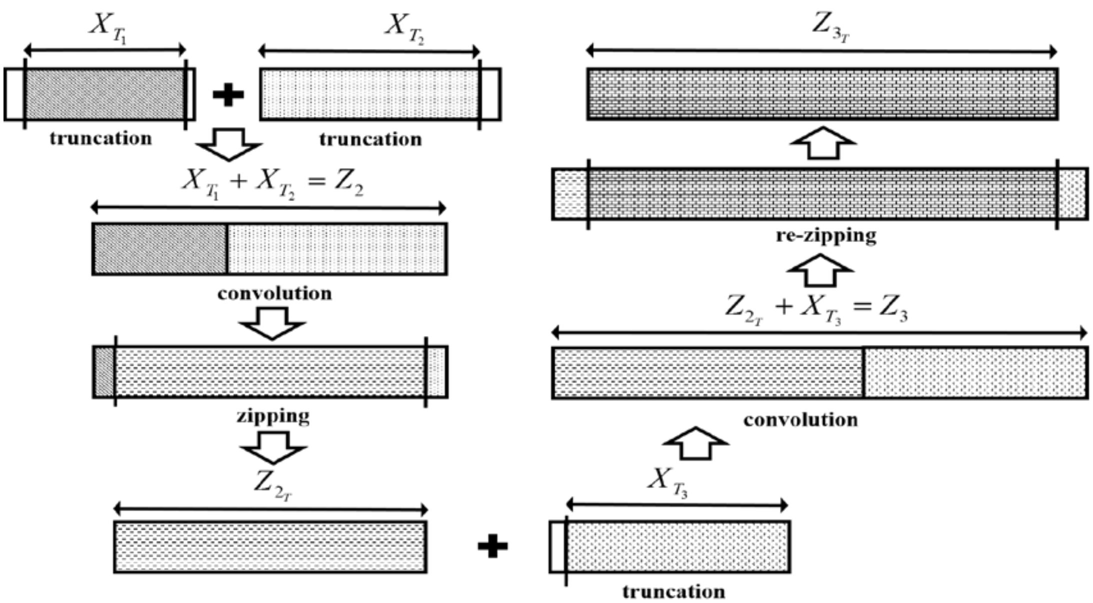

Figure 4.11. Re-zipping based on the sum of three truncated normal random variables

In this section, we assume that X_{T_1}, X_{T_2}, and X_{T_3} are independent and identically distributed. For numerical examples, consider the means, μ_1, μ_2, and μ_3 are 10, and the standard deviations, σ_1, σ_2, and σ_3 are 2. The lower and upper truncation points of X_{T_1} and X_{T_2} are also assumed as $-\infty$ and 14, respectively. By referring Section 5.1, the probability density function of Z_2 is obtained as

$$f_{Z_2}(z) = \int_{-\infty}^{\infty} f_{X_{T_2}}(y) f_{X_{T_1}}(x) dx$$

$$= \int_{-\infty}^{\infty} \frac{\frac{1}{2\sqrt{2\pi}} \exp^{-\frac{1}{2}\left(\frac{y-10}{2}\right)^2}}{\int_{-\infty}^{14} \frac{1}{2\sqrt{2\pi}} \exp^{-\frac{1}{2}\left(\frac{s-10}{2}\right)^2} ds} \frac{\frac{1}{2\sqrt{2\pi}} \exp^{-\frac{1}{2}\left(\frac{x-10}{2}\right)^2}}{\int_{-\infty}^{14} \frac{1}{2\sqrt{2\pi}} \exp^{-\frac{1}{2}\left(\frac{h-10}{2}\right)^2} dh} I_{[-\infty,14]}(y) I_{[-\infty,14]}(x) dx$$

and then the probability density function of Z_{2_T}

$$f_{Z_{2_T}}(z) = \frac{f_{Z_2}(z)}{\int_{-\infty}^{24} f_{Z_2}(z)dz} I_{[-\infty,14]}(z)$$

$$= \frac{\int_{-\infty}^{\infty} \frac{\frac{1}{2\sqrt{2\pi}} \exp^{-\frac{1}{2}\left(\frac{y-10}{2}\right)^2}}{\int_{-\infty}^{14} \frac{1}{2\sqrt{2\pi}} \exp^{-\frac{1}{2}\left(\frac{s-10}{2}\right)^2} ds} \frac{\frac{1}{2\sqrt{2\pi}} \exp^{-\frac{1}{2}\left(\frac{x-10}{2}\right)^2}}{\int_{-\infty}^{14} \frac{1}{2\sqrt{2\pi}} \exp^{-\frac{1}{2}\left(\frac{h-10}{2}\right)^2} dh} I_{[-\infty,14]}(y) I_{[-\infty,14]}(x) dx \cdot I_{[-\infty,14]}(z)}{\int_{-\infty}^{24}\int_{-\infty}^{\infty} \frac{\frac{1}{2\sqrt{2\pi}} \exp^{-\frac{1}{2}\left(\frac{y-10}{2}\right)^2}}{\int_{-\infty}^{14} \frac{1}{2\sqrt{2\pi}} \exp^{-\frac{1}{2}\left(\frac{s-10}{2}\right)^2} ds} \frac{\frac{1}{2\sqrt{2\pi}} \exp^{-\frac{1}{2}\left(\frac{x-10}{2}\right)^2}}{\int_{-\infty}^{14} \frac{1}{2\sqrt{2\pi}} \exp^{-\frac{1}{2}\left(\frac{h-10}{2}\right)^2} dh} I_{[-\infty,14]}(y) I_{[-\infty,14]}(x) dxdz}$$

with the lower and upper truncation points, $-\infty$ and 24, Based on the above probability density functions, the means, variances and distributions as shown in Figure 4.12. By letting $Z_3 = Z_{2_T} + X_{T_3}$, the probability density function of Z_3 is given by

$$f_{Z_3}(k) = \int_{-\infty}^{\infty} f_{X_{T_3}}(m) f_{Z_{2_T}}(z)dz = \int_{-\infty}^{\infty} \frac{\frac{1}{2\sqrt{2\pi}} \exp^{-\frac{1}{2}\left(\frac{m-10}{2}\right)^2}}{\int_{-\infty}^{14} \frac{1}{2\sqrt{2\pi}} \exp^{-\frac{1}{2}\left(\frac{t-10}{2}\right)^2} dt} f_{Z_{2_T}}(z)dz.$$

Mean and standard deviation (variance) of Z_3 are obtained as 29.3835 and 3.0751 (9.4564), respectively. Then, the distribution of Z_3 is re-zipped with the lower and upper truncation points, $-\infty$ and 34. The probability of density function of Z_{3_T} is then expressed as

$$f_{Z_{3_T}}(k) = \frac{f_{Z_3}(k)}{\int_{-\infty}^{34} f_{Z_3}(k)dk} I_{[-\infty,34]}(k).$$

The mean, variance and distribution of Z_{3_T} are also shown in Figure 4.12.

X_{T_1}	X_{T_2}	$Z_2 = X_{T_1} + X_{T_2}$	Z_{2_T}
ATN_N	TN_S		
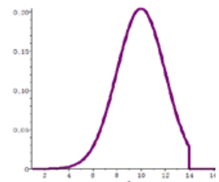	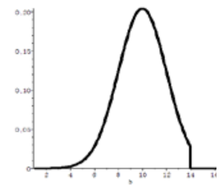	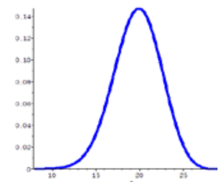	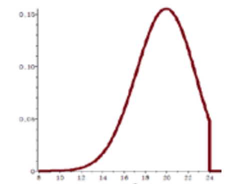
$\mu_{T_1} = 9.89,\ \sigma_{T_1}^2 = 3.55$	$\mu_{T_2} = 9.89,\ \sigma_{T_2}^2 = 3.55$	$\mu_{Z_2} = 19.78,\ \sigma_{Z_2}^2 = 7.09$	$\mu_{Z_{2_T}} = 19.49,\ \sigma_{Z_{2_T}}^2 = 5.91$
	X_{T_3}	$Z_3 = Z_{2_T} + X_{T_3}$	Z_{3_T}
	TN_L		
	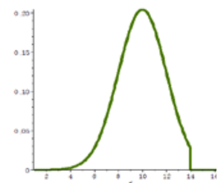	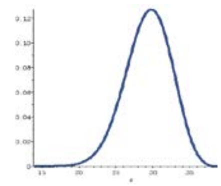	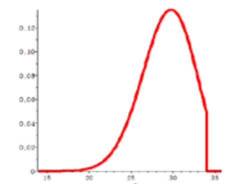
	$\mu_{T_3} = 9.89,\ \sigma_{T_3}^2 = 3.55$	$\mu_{Z_3} = 29.38,\ \sigma_{Z_3}^2 = 9.46$	$\mu_{Z_{3_T}} = 29.03,\ \sigma_{Z_{3_T}}^2 = 7.91$

Figure 4.12. Re-zipping based on the sum of three truncated normal random variables

Note that the mean and variance of Z_2 is equal to the sum of the means and variances of the truncated normal random variables, X_{T_1} and X_{T_2}, respectively, while the mean and variance of Z_3 is equal to the sum of the means and variances of the truncated normal random variables, Z_{2_T} and X_{T_3}, respectively. Furthermore, the variance of Z_{3_T} is always smaller than the variance of Z_3, and the truncation points cause the mean of Z_{3_T} to be smaller than the mean of Z_3.

4.5. Conclusion and Future Study

The mathematical foundations of various truncated normal distributions and the convolutions of these distributions were explored in order to offer insight into methods used to meticulously account for material use. Furthermore, understanding the mean and standard deviations of production processes using a truncated normal distribution could lead to an enhanced understanding of a modern production process that could help identify key bottlenecks and resource usage on the manufacturing floor.

Areas for future study include examining expected quality loss functions as a result of the process output in order to establish key relationships among interdependent process steps. This could lead to a multivariate approach for zipping and truncations. This leads to another related topic on computational efficiency. Key issues to be addressed include finding efficient algorithms for multivariate convolutions in assembly processes that have dependent variables. These algorithms must be explored thoroughly enough to see if they can converge in at least polynomial time.

CHAPTER FIVE

DEVELOPING A TWO-STAGE STOCHASTIC PROGRAMMING MODEL IN TOLERANCE OPTIMIZATION USING A GUARD BAND APPROACH

5.1 Introduction

Uncertainty is difficult to account for and can arise in several different ways in a manufacturing setting. If one plans to sell a final product, the price not only depends on the quality of the final product, but also a competing firm's planned product selling price. In this situation uncertainty can arise from a lack of knowledge. Uncertainty can also arise from the complexity of the process as demand also depends on economic factors, customer preferences, and ultimately a company's and competitor's actions. Inputs in a production process may also be uncertain due to difficulty to measure a certain quantity. All processes that we try to model also have inherent statistical randomness in them as well. This type of uncertainty is called irreducible uncertainty. One may be able to reduce the effect of the random variation on the model for the situation, or reduce the model's sensitivity to variation, but it will always be there. In other situations one deals with reducible uncertainties. These reducible uncertainties can be dealt with by collecting more accurate data or using more accurate measuring tools. The purpose of this paper is to propose a model that accounts for irreducible uncertainties, while reducing uncertainties that are able to be reduced through a better manufacturing process.

Parts cannot be manufactured to exact nominal dimensions due to variation in materials, machines and the people that control the manufacturing process. As a result, the specification limits and their associated tolerances can have a vast impact on the quality, performance and cost of the finished product. This has created a large research interest in obtaining optimal tolerances and specification limits in order to not only reduce manufacturing costs, but also to minimize the expected quality loss of a product. The expected quality loss of a product includes not only scrap and rework costs, but also incorporates costs as a part or product deviates from a nominal value. Furthermore, unnecessarily tight tolerances may result in a complicated and costly manufacturing process, while low tolerances mean a lower manufacturing cost, but weaker product performance.

One of the key difficulties of any process is defining the specification limits and tolerances precisely in a given production process. This may not always be possible, however, since the production process may not be sophisticated or accurate enough to manufacture a product within the specification limits. Consider the situation where the probability that a product's specifications fall outside the tolerance limits cannot be calculated because the production process is not stable. In this situation, one could guarantee that the product is within the specification limit or outside the specification limits within a certain threshold value. This would allow practitioners to have the maximum amount of control over setting specifications and tolerances of their product, within their inherently unstable process. This could be done by integrating stochastic chance-constrained and tolerance optimization models.

Finding optimal tolerances has previously been looked at through a deterministic lens however, for complex processes this may not always be possible and one may need to account for ambiguous production criteria. Chance-constrained stochastic programming is an approach for modeling problems that have uncertain parameters. This is opposed to deterministic programming approaches that have known parameters and are usually tractable; however, most deterministic approaches often do not accurately account for real world variables and parameters which are often uncertain at the time of making a decision. Subject pioneers Charnes and Cooper define chance-constrained programming as the process of selecting certain random variables as functions of random variables in order to maximize a functional of random variables subject to constraints that must be maintained at prescribed levels of certainty represented by a probabilistic value (Charnes and Cooper, 1959). They illustrate this idea by comparing the deterministic and chance-constrained forms of an inventory model involving oil tankage facilities supplied by a refinery, where expected profit is maximized subject to specified probability constraints where a certain minimum inventory must be maintained with a certain probability and inventory must not exceed a certain maximum with a certain specified probability. Other prominent examples of chance-constrained programming include situations in which decisions are made repeatedly within a similar set of circumstances and the objective is to formulate a solution that will perform well on average, such as designing truck routes for package carriers, whose customers have random demand for packages. Chance-constrained programming can also be applied to situations in which a one-time decision must be made such as the initial investments in a financial portfolio with varying interest rates (Li, 1995), activity analysis and technology planning with production horizon uncertainties (Thore, 1987), capital budgeting (Huang, 2007), dietary planning with stochastic costs over multiple time periods, and material composition selection with stochastic costs dictated by market terms.

5.2 Previous Works

5.2.1 Tolerance Optimization

Initially, only manufacturing cost was considered in objective functions when minimizing the cost for setting tolerances, while ignoring expected quality loss. A large amount of research has been carried out on optimal tolerance allocation using cost-vs-tolerance functions. Several of these functions have been proposed including linear tolerance functions, various reciprocal of tolerance functions, exponential functions, and others. A wide array of solution techniques have been employed with these functions including the Lagrange multiplier method, linear programming, nonlinear programming, the branch and bound method, and combinatorial techniques (Chase et al., 1990). Polynomial time solution algorithms and corresponding hybrids models were introduced by Dong et al. to solve the models listed above (Dong et al., 1994).(Singh et al., 2004) Introduced a genetic algorithm and compared its performance to exact algorithms which conduct an exhaustive search of the solution space. More recently, quality loss functions have received the attention of researchers. These researchers combine quality loss functions and manufacturing costs. They use particle swarm and genetic algorithms to solve these models (Sivakumar et al., 2011; Geetha et al., 2013). Cheng and Maghsoodloo considered the effects of shifting components' means and variances on quality loss. It was found that by shifting a component's variance the optimal allowance, tolerance costs and quality loss of each component will be affected (Chang and Maghsoodloo, 1995). Wu et al. considered asymmetric quality loss functions (Wu et al., 1998). Other numerical methods used to minimize expected quality loss include neural learning algorithms (Chen, 2001), continuous ants colony algorithms (Prabhaharan et al., 2005), game theoretic (Lu et al., 2012), and fuzzy quality loss approaches (Cao et al., 2009).

Despite numerical methods being widely used, the Karush-Kuhn-Tucker conditions and Lagrange multiplier methods are usually the first choice in solving a tolerance optimization problem since it can yield a closed-form solution (Singh et al., 2009). If closed-form solutions can be found, then optimal tolerances can be calculated fast and accurately.

It is important to note that the performance of a product and its quality characteristics depend greatly on the variation of component parts produced. In order to reduce the effect of variation on component parts and reduce errors, several techniques are often used in tolerance optimization to reduce errors. One of these techniques is selective assembly, which involves matching of low-precision components to help achieve an overall final assembly of high precision, while at the same time being cost effective. Here, components of mating pairs are measured and grouped into several different bins or classes as they are created. The final product is then assembled by selecting components in certain bins to meet the required specifications as precisely as possible. This approach is often less expensive than designing tolerances with tighter specifications. Techniques for improving quality have been widely investigated in the literature. See for example (Mease et al., 2004; Pugh, 1992, 1986). One industry that is greatly affected by dimensional part variation is the automotive industry, since there are several quality issues that arise from similar variations in the assembly process (Ceglarek and Shi, 1995).

Another important technique to reduce errors in complex assemblies includes adaptive manufacturing. Adaptive manufacturing involves manipulation of manufacturing parameters in order to build suitable components for assembly. Business enterprises often have to deal with the manufacturing of assemblies with quality requirements close to technological limits. These enterprises include advanced production systems, such as semiconductor manufacturing, automotive manufacturing, and aerospace manufacturing. In the context of selective assembly and in particular, additive manufacturing, new measurement technologies and advanced information technology systems, such as cyber-physical systems, give the ability to use quality control data generated in real time, in order to control the production process adaptively (Lanza et al., 2015).

5.2.2 Chance-Constrained Optimization

Charnes and Cooper established deterministic equivalents of chance constraints by relaxing the form of the stochastic programming constraints and incorporating three different classes of objective functions which include finding the maximum expected value, the minimum variance and the maximum probability of various objective functions and established these to be convex (Charnes and Cooper, 1963). Miller and Wagner introduced joint chance constraints by modeling multivariate events. One model that was studied was when the right-hand side constants of the linear constraints were random. Another model included when the coefficients of the variables were described by a multinomial distribution. They showed that under certain restrictions both models can be viewed as a deterministic nonlinear programming problem. They also explored whether these models can be considered concave or convex under various conditions (Miller and Wagner, 1965).

The main difficulty of working with the chance-constrained programming models comes from the need for the optimal decisions to be made before the observation of certain random parameters takes place; therefore, it is difficult to make any decision, since this could result in violating constraints caused by random effects. Sometimes, however, these constraint violations can be compensated for in further stages of decision making in which a penalty is assigned to constraint violations, as long as the costs for not satisfying the constraints are known. This leads to what is known as multistage stochastic programming (Birge and Louveaux, 1997). Several applications, however, do not lend themselves to having any constraint violations. For example, there are situations where the safety levels of water that must be maintained in a water tower in case of emergency. In this case it would be better to guarantee feasibility of constraints as a high probability, since there is always the case where an unexpected extreme event can occur. Another issue with chance-constrained programming stems from the fact that the probability distribution underlying the already probabilistic problem is not known with absolute certainty (Erdogan, 2006).

More recent research has yielded results on the convex approximations of chance constraints. This work is needed as chance-constrained programs are not necessarily convex. Nemirovski and Shapiro (Nemirovski and Shapiro, 2006), for example, created a tractable method of solving these particular chance-constrained models by constructing a general class of convex conservative approximations of the corresponding chance constrained problem.

5.3 Problem Statement

A guard band is defined as the amount by which minimum product tolerance specifications are increased to ensure that, even with measurement uncertainty, the product will be within the tolerances within a specified level of confidence. In the case of tolerance optimization, an added guard band serves two distinct purposes. The first is to ensure a high quality product by accounting for uncertainty in the manufacturing process and the second is to differentiate between the quality of finished products through product binning, such as in semiconductor device fabrication.

Care must be taken when applying guard banding to tolerance optimization as a quality loss of a product may occur both symmetrically and asymmetrically. The target value of the critical-to-quality (CTQ) characteristic must also be taken into consideration when determining optimal tolerances. As the CTQ value deviates from the target, the loss in product performance may either be symmetric or asymmetric depending on the nature of the CTQ under study.

Tolerance optimization refers to setting specification limits or tolerances in a manufacturing process in order to minimize the total cost of the process. Initially, only the manufacturing cost was considered in objective functions when minimizing the cost for setting tolerances, while ignoring expected quality loss. In the proposed two-stage model, the goal is to minimize the total expected quality loss when the production process is not well defined or stable enough to be able to obtain the exact probability that the product falls outside of specification limits. In both situations the probability cannot be estimated precisely. By utilizing stochastic programming, one can guarantee that the product is within specification limits with a certain probability. By further incorporating a guard band approach, a safeguard can be incorporated into the model further reducing the possibility for error. In the model we assume that error-free inspection of the products occur.

We propose a two-stage optimization model. The random variables include the dimension of the product produced due to manufacturing process, as well as, uncertainty as well as uncertain market conditions. The first stage decision variables are the selling prices that depend on the quality of the product produced. Then, in the second stage, the recourse variables are specification limits, as well as, the inner guard bands that are used to differentiate between higher and lower quality products. This allows the practitioner to maximize profits when taking into account both an uncertain manufacturing process as well as uncertain market conditions.

The overarching goal of this paper is to optimize a system's performance by using models which account for uncertainties in problem parameters. The specific model developed achieves tolerance optimization via the use of chance-constrained programming. In this paper we assume that the distribution of the production process is either normal, or truncated normal since they are often used in the literature to model tolerance optimization problems. The normal distribution and the truncated normal distribution also help make constraints relatively manageable. This helps improve tractability in these difficult types of tolerance optimization problems. We expect that, the models proposed in this research can benefit manufacturers utilizing complex processes by allowing practitioners to modify the algorithms and techniques illustrated in this paper.

Schematically, the model is summarized in Figure 5.1 below:

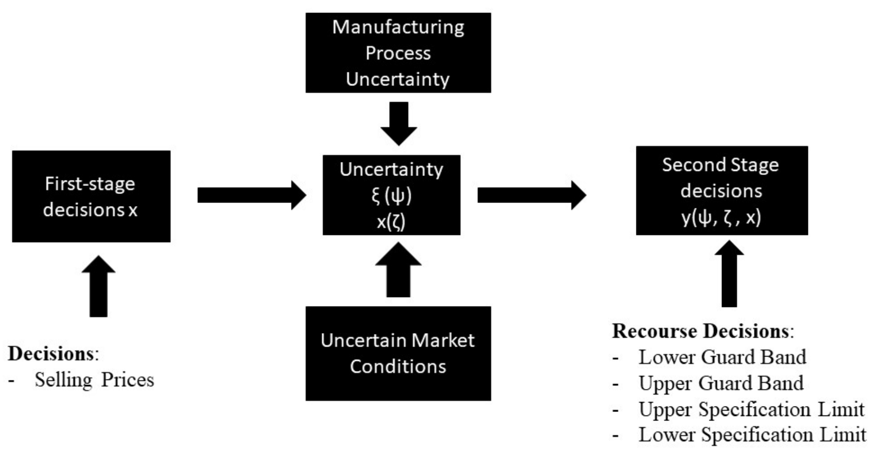

Figure 5.1: Proposed Stochastic Model Stages

5.4 Development of the Two-Stage Stochastic Programming Model

In this section a chance-constrained non-linear programming model is developed in order to analyze the effect of guard banding and tolerance optimization in order to maximize the profitability of a company with an imprecise manufacturing process subject to uncertain market demand. The model is presented in the next two subsections.

5.4.1 Abbreviations and Notation

Sets

- $K = \{A, B, C\}$ is the set of products
- S is the set of scenarios generated

Parameters

- α is the maximum allowable violation of the lower specification limit
- β is the maximum allowable violation of the upper specification limit
- γ is the maximum allowable violation of the upper guard band
- δ is the maximum allowable violation of the lower guard band
- Δ is the maximum process precision
- q is the unit production cost
- l is the cost of quality loss when the product specification is greater than the UGB
- e is the cost of quality loss when the product specification is less than the LGB
- f is the cost of quality loss when the product specification is greater than the USL
- k is the cost of quality loss when the product specification is less than the LSL

- τ is the target value
- κ_i is the mean demand for product i
- η_i is the price elasticity for product i
- η_{ij} is the price elasticity for product i to changes in the price of product j

Random problem parameters

- $\tilde{\xi}_i$ is a characteristic of product i from stage 1 that follows $N(\mu_1, \sigma_1)$
- $\tilde{\psi}_i$ s a characteristic of product i from stage 2 that follows $N(\mu_2, \sigma_2)$
- $D_i(x_i, \tilde{\zeta_i})$ is demand for product i, which is a function of market conditions $\tilde{\zeta}_i$ and price x_i
- $\Xi = \{\zeta, \xi, \psi\}$ is the set of random market conditions, quality of product produced in stage 1, and quality of product produced in stage 2, respectively
- $K = \{A, B, C\}$ is the set of products

Decision Variables

- x_i is price of product $i \in K$
- y_i is the process specific guard band, $y_1 = LGB, y_2 = UGB$
- z_i is the process specific specification limits, $z_1 = LSL, z_2 = USL$

5.4.2 Initial Model Formulation

$$\min \sum_{i=1}^{k} L_i(\mathbf{y}) + \sum_{i=1}^{k} L_i(\mathbf{z}) - \mathbf{E}[h(\mathbf{x}, \xi, \psi)] \tag{1a}$$

Subject to,

$$x_i \geq q_i \qquad \forall i \in K \tag{1b}$$
$$y_2 \leq z_2 - \Delta \tag{1c}$$
$$z_1 \leq y_1 - \Delta \tag{1d}$$
$$\tau \leq y_2 - \Delta \tag{1e}$$
$$y_1, y_2, z_1, z_2 \geq 0 \tag{1f}$$

where the recourse function $h(\mathbf{x}, \xi, \psi)$ for a given value of the first-stage decisions $\mathbf{x}$ and realization ζ of random variables $\tilde{\zeta}$ is given by:

$$h(\mathbf{x}, \xi, \psi) = \min_{\mathbf{y},\mathbf{z}} [\pi(\mathbf{x}, \xi, \psi)] \tag{2a}$$

Subject to

$$D_i\left(x_i, \tilde{\zeta}\right) = \kappa_i(\tilde{\xi}) - \eta_i x_i + \sum_{j=1, i \neq j}^{|K|} \eta_{ij} x_j \qquad \forall i \in K \tag{2b}$$
$$P(\xi_i \leq z_1) \leq \alpha \qquad \forall i \in K \tag{2c}$$
$$P(\xi_i \geq z_2) \leq \beta \qquad \forall i \in K \tag{2d}$$
$$P(\psi_i \leq y_1) \leq \delta \qquad \forall i \in K \tag{2e}$$
$$P(\psi_i \geq y_2) \leq \gamma \qquad \forall i \in K \tag{2f}$$
$$\tag{2g}$$

where, $\pi(\mathbf{x}, \xi) = \sum_{i=1}^{|K|} D_i(x_i, \tilde{\xi})(x_i - q_i)$.

5.4.3 The First Stage of the Stochastic Programming Model

In modeling the first stage of the tolerance optimization model, the random variables include the dimension of the product produced, with two of the decision variables being the selling prices with the objective being to minimize the expected quality loss.

In terms of finding a selling price based upon uncertain market demand, assume that the product produced is separated into three groups or bins according to the truncated distribution ψ in order to be sold on the market. The three classification bins defined by $A = (LSL, LGB)$, $B = (LGB, UGB)$, and $C = (UGB, USL)$ each represent a separate level of quality of the product produced that can be sent to market. In the first stage the objective is to maximize profit based upon market demand by setting appropriate selling prices. We must then decide how many products with specifications A, B and C to produce during the production process based on the truncated normal distribution ψ and separate demands for A, B, and C. For example, it is possible to meet demand for products with specification B and reduce the amount of products with specifications A and C. If we decide to produce more product to meet the demand for products with specifications A and C, we would then be left with a surplus of product with specification B. The question is how to minimize quality loss in the second stage based on both the uncertainties in demand for the product, which is based on the uncertain production process by setting the guard band values appropriately.

Assume that the demand for products with specifications A, B, and C are dependent on one another based on the selling prices. Then one can maximize the profit per unit based on the selling prices. The expected profit part of the objective function can be written as:

$$\pi\left(\mathbf{x},\xi\right)=\sum_{i=1}^{|K|}D_i(x_i,\tilde{\xi})(x_i-q_i).\ (3)$$

in the final formulation.

5.4.4 The Second Stage of the Stochastic Programming Model

In the second stage of the model, the specification limits and guard bands must be introduced as recourse variables after the uncertain market demand as well as initial manufacturing process uncertainties are realized in order to separate the product into high quality or low quality versions to sell to consumers. A practical application of this is used in the semiconductor industry. Semiconductor manufacturing is an example of an imprecise process, with product yields as low as 30 percent. In this industry defects in manufacturing are not necessarily fatal, so that it may be possible to salvage part of a failed batch of integrated circuits by modifying performance characteristics. As an example, if one lowered the clock frequency of a CPU, and disabled critical parts that are defective, the part can be sold at a lower price, thereby fulfilling needs of lower end market segments. This practice is common on products such as CPUs, GPUs and RAM. A specific example of this occurs in using selective voltage binning in order to maximize the yield of high quality semiconductor products (Lichensteiger and Bickford, 2013). By using a guard banding type approach, we can separate a product into high quality levels and low quality levels to be sold at different prices based on market demand. The guard bands will be determined in the second stage after the specification limits are set.

For example, assume that $\xi\sim N\left(\mu,\sigma^2\right)$, where μ and σ are estimated process parameters from the production process and the distribution has a lower truncation point at zero, since the dimension of a part cannot be less than zero. In this case, $f(\xi) = \frac{1}{\sqrt{2\pi\sigma^2}}e^{-\frac{(\xi-\mu)^2}{2\sigma^2}}$,where $-\infty < \xi < \infty$ so that the probability density function of the truncated normal distribution at zero, $f_T(\xi)$, can be described as $f_T(\xi) = \frac{f(\xi)}{\int\limits_0^\infty f(\xi)d\xi}, where\, 0 < \xi < \infty$. Here, note that the truncated mean $\mu_T = \int\limits_0^\infty \xi f_T\left(\xi\right) d\xi$ and the truncated variance $\sigma_T^2 = \int\limits_0^\infty \xi^2 f_T\left(\xi\right) d\xi - \left(\int\limits_0^\infty \xi f_T\left(\xi\right) d\xi\right)^2$. Suppose a sample of n observations of ξ_i are taken, then in trying to minimize the expected quality loss, one can use sample average approximation to convert the above part of the objective function into:

$$\mathbf{E}\left(L(\mathbf{z}, \xi_i)\right) = \int_0^\infty f_T(\xi)L(\mathbf{z}, \xi)d\xi = \frac{1}{n}\sum_{i=1}^{n} L(\mathbf{z}, \xi_i) \tag{4}$$

Assume a piece-wise linear symmetric loss function, where the loss incurred at the target value is zero and the loss incurred at the upper and lower specification limits is \$$c$. In this case,

$$L(\mathbf{z}, \xi_i) = \left\{ \begin{matrix} \frac{c(\xi_i-\tau)}{(z_2-\tau)},\, where\, \tau < \xi_i \\ \frac{c(\xi_i-\tau)}{(z_1-\tau)},\, where\, _i < \tau \end{matrix} \right\}$$

(5)

Call the case where $\tau < \xi_i$ case 1 and where $\xi_i < \tau$ case 2. This symmetric loss function looks like:

$$\left[\frac{1}{a}\sum_{\forall \xi_i > \tau} \frac{c\left(\xi_i - \tau\right)}{\left(USL - \tau\right)} + \frac{1}{b}\sum_{\forall \xi_i < \tau} \frac{c\left(\xi_i - \tau\right)}{\left(LSL - \tau\right)}\right] \tag{6}$$

where a is the number of case 1 scenarios and b is the number of case 2 scenarios so that $a + b = n$. Note that in $P(\xi_i \geq z_2) \leq \beta$, β is the maximum allowable probability of violating the upper specification limit and in $P(\xi_i \leq z_1) \leq \alpha$ where α is the maximum allowable probability of violating the lower specification limit. These constraints can be estimated once a sample of n observations of are taken as $z_2 \geq (1-\beta)^{th}$ percentile of the n observations and $z_1 \leq \alpha^{th}$ percentile of the n observations. Finally, in the specific case of the symmetric loss function, the constraint $\tau - z_1 = z_2 - \tau$ must be introduced to enforce symmetry.

Assume a piecewise linear asymmetric loss function, where the loss incurred at the target value is zero and the loss incurred at the upper and lower specification limits is \$$d$ and \$$e$, respectively. Then the deterministic equivalent of the asymmetric loss function becomes:

$$\left[\frac{1}{a}\sum_{\forall \xi_i > \tau} \frac{d(\xi_i - \tau)}{(z_2 - \tau)} + \frac{1}{b}\sum_{\forall \xi_i < \tau} \frac{e(\xi_i - \tau)}{(z_1 - \tau)}\right] \tag{7}$$

Similarly, in the second stage, one solves for the guard bands after the upper and lower specification limits are determined and market demand has been realized. Assume that the product here can be separated into high and low quality versions based on where the guard bands are set. Assume that the upper and lower specification limits are set and second sample of m data points need to be taken from the modified production process, where $\psi \sim N(\mu, \sigma^2)$, and is truncated at the specification limits. In this case, one can follow similar steps as outlined with ξ to minimize the expected quality loss, using sample average approximation to convert part of the objective function into

$$\mathbf{E}\left(L(\mathbf{y}, \psi_i)\right) = \int_{LSL}^{USL} f_T(\psi) L(\mathbf{y}, \psi) d\psi = \frac{1}{m}\sum_{i=1}^{m} L(\mathbf{y}, \psi_i)$$

(8)

Assume a new piecewise linear symmetric loss function, where the loss incurred at the target value is zero and the loss incurred at the upper and lower guard bands is \$$f$ in the new production process. In this case

$$L(\mathbf{y}, \psi_{\mathbf{i}}) = \begin{Bmatrix} \frac{f(\psi_i - \tau)}{(y_2 - \tau)}, \, where \, \tau < \psi_i \\ \frac{f(\psi_i - \tau)}{(y_1 - \tau)}, \, where \, \psi_i < \tau \end{Bmatrix}$$

(9)

Let the instance where $\tau < \psi_i$ be case 3 and where $\psi_i < \tau$ case 4. Under symmetric conditions, the loss function is expressed as

$$\left[\frac{1}{g} \sum_{\forall \, \psi_i > \tau} \frac{f\left(\psi_i - \tau\right)}{\left(y_2 - \tau\right)} + \frac{1}{h} \sum_{\forall \, \psi_i < \tau} \frac{f\left(\psi_i - \tau\right)}{\left(y_1 - \tau\right)} \right] \tag{10}$$

where g is the number of case 3 scenarios and h is the number of case 4 scenarios so that $g + h = m$. Note that in $P\left(\psi_i \geq y_2\right) \leq \gamma$, γ is the maximum allowable probability of violating the upper guard band and in $P\left(\psi_i \leq y_1\right) \leq \delta$, δ is the maximum allowable probability of violating the lower guard band. These constraints can be estimated once a sample of m observations of ψ are taken as $y_2 \geq \left(1 - \gamma\right)^{th}$ percentile of the m observations and $y_1 \leq \delta^{th}$ percentile of the m observations. Finally, in the specific case of the symmetric loss function, the constraint $\tau - y_1 = y_2 - \tau$ must be introduced to enforce the symmetry of the quality loss functions. Putting this altogether one has for the discrete approximation of the loss function between the guard bands of the second stage of symmetric stochastic programming model:

$$\left[\frac{1}{g}\sum_{\forall\psi_i>\tau}\frac{f\left(\psi_i-\tau\right)}{\left(y_2-\tau\right)}+\frac{1}{h}\sum_{\forall\psi_i<\tau}\frac{f\left(\psi_i-\tau\right)}{\left(y_1-\tau\right)}\right] \tag{11}$$

The asymmetric guard band loss function:

$$\left[\frac{1}{g}\sum_{\forall\psi_i>\tau}\frac{i\left(\psi_i-\tau\right)}{\left(y_2-\tau\right)}+\frac{1}{h}\sum_{\forall\psi_i<\tau}\frac{j\left(\psi_i-\tau\right)}{\left(y_1-\tau\right)}\right] \tag{12}$$

5.4.5 Final Model Formulation

$$\min\sum_{i=1}^{k}L_i(\mathbf{y})+\sum_{i=1}^{k}L_i(\mathbf{z})-\mathbf{E}[h(\mathbf{x},\xi,\psi)] \tag{13a}$$

subject to

$$x_i \geq q_i \qquad \forall i \in K \tag{13b}$$

$$y_2 \leq z_2-\Delta \tag{13c}$$

$$z_1 \leq y_1-\Delta \tag{13d}$$

$$\tau \leq y_2-\Delta \tag{13e}$$

$$L_i\left(\mathbf{y}\right)=\left[\sum_{s=1,\psi_{is}<\tau}^{S}\frac{l\left(\psi_{is}-\tau\right)}{\left(y_1-\tau\right)}+\sum_{s=1\psi_{is}>\tau}^{S}\frac{e\left(\psi_{is}-\tau\right)}{\left(y_2-\tau\right)}\right] \qquad \forall i \in K \tag{13f}$$

$$L_i\left(\mathbf{z}\right)=\left[\sum_{s=1,\psi_{i}<\tau}^{S}\frac{l\left(\psi_{is}-\tau\right)}{\left(z_1-\tau\right)}+\sum_{s=1,\psi_{is}>\tau}^{S}\frac{e\left(\psi_{is}-\tau\right)}{\left(z_2-\tau\right)}\right] \qquad \forall i \in K \tag{13g}$$

$$y_1,y_2,z_1,z_2 \geq 0 \tag{13h}$$

$$\tag{13i}$$

where, the recourse function $h(\mathbf{x}, \xi, \psi)$ for a given value of the first-stage decisions $\mathbf{x}$ and realization ζ of random variables $\tilde{\zeta}$ is given by:

$$h(\mathbf{x}, \xi, \psi) = \min_{\mathbf{y},\mathbf{z}} \left[\pi(\mathbf{x}, \xi, \psi)\right] \tag{14a}$$

subject to

$$\begin{aligned}
D_i\left(x_i, \tilde{\zeta}\right) = \kappa_i(\tilde{\xi}) - \eta_i x_i + \sum_{j=1, i\neq j}^{|K|} \eta_{ij} x_j & \qquad \forall i \in K & \text{(14b)}\\
z_1 - \xi_{is} \leq M * \nu_s & \qquad \forall s \in S & \text{(14c)}\\
\sum_{s=1}^{|S|} \nu_s \leq \alpha |S| & & \text{(14d)}\\
\xi_{is} - z_2 \leq M * w_s & \qquad \forall s \in S & \text{(14e)}\\
\sum_{s=1}^{|S|} w_s \leq \beta |S| & & \text{(14f)}\\
y_1 - \psi_{is} \leq M * v_s & \qquad \forall s \in S & \text{(14g)}\\
\sum_{s=1}^{|S|} v_s \leq \delta |S| & & \text{(14h)}\\
\psi_{is} - y_2 \leq M * u_s & \qquad \forall s \in S & \text{(14i)}\\
\sum_{s=1}^{|S|} u_s \leq \gamma |S| & & \text{(14j)}\\
\nu_s \in \{0, 1\} & \qquad \forall s \in S & \text{(14k)}\\
w_s \in \{0, 1\} & \qquad \forall s \in S & \text{(14l)}\\
v_s \in \{0, 1\} & \qquad \forall s \in S & \text{(14m)}\\
u_s \in \{0, 1\} & \qquad \forall s \in S & \text{(14n)}\\
& & \text{(14o)}
\end{aligned}$$

where, $\pi\left(\mathbf{x}, \xi\right) = \sum_{s=1}^{|S|} D_i(x_i, \xi_{is})(x_i - q_i)$

5.5 Solving the Two-Stage Stochastic Programming Model

5.5.1 Solving the Model

Solving the model first involves initializing appropriate constants for the model including setting appropriate maximum probabilities for constraint and guard-band violations within the stochastic model, as well as establishing an upper bound on the maximum possible precision of the manufacturing process. Creating realistic loss functions with appropriate quality loss coefficients at the specification limits and the guard-bands is also important and depends on the specific manufacturing process being modeled. The cost of running the manufacturing process to produce a product must also be considered. Generating a reasonable number of scenarios to run is also important.

The next step in solving the model involves generating truncated normal random variables for all the scenarios in order to reasonably simulate the outcomes of the production process and allow for a reasonable degree of accuracy in generating process outputs. Establishing deterministic equivalents of the stochastic model is also key to solving the model.

The final step in solving the model involves using interior point optimization methods that exploit first and second derivative information of the established deterministic equivalents, via numerical methods. This was done by using the commercial solver IPOPT (Interior Point OPTimizer), which is a software package for nonlinear optimization developed by Andreas Wächer for his PhD thesis in Chemical Engineering at Carnegie Mellon University (Wächer, 2002) . This is part of the COIN-OR (Computational Infrastructure for Operations Research) open source initiative which was initialized through the JuMP (Julia for Mathematical Optimization) modeling language.

The basic solution approach is outlined in Figure 5.2 below:

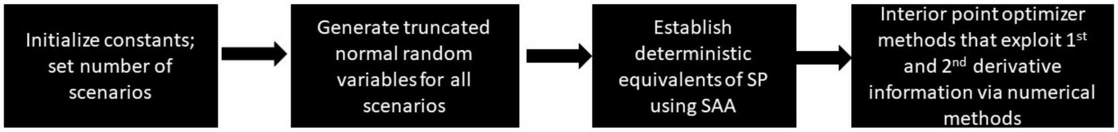

Figure 5.2: Solving the Proposed Two-Stage Stochastic Programming Model

5.6 Two-Stage Stochastic Programming Model Results

5.6.1 Scenario Generation

The number of optimal scenarios to run was determined by running 30 different seed values in order to account for different strings of random numbers. Ten to three hundred scenarios, which increased by increments of ten, of each of the 30 seed values for 900 total runs, were performed under the following initial conditions given in table 1 below.

It was determined that, under these conditions, by running a one-way ANOVA that the number of scenarios had no statistically significant effect at the alpha = 0.05 level on the objective function (P-value $\approx$ .924), the final upper specification limit value (P-value $\approx$ 1), or the upper guard band value (P-value $\approx$ 1). By contrast it was determined that the number of scenarios ran had a statistically significant effect on the values of the lower specification limit (P-value$\approx$0), the lower guard band (P-value $\approx$ 0), p_a (P-value = 0.005), p_b (P-value = 0.005), and p_c (P-value=0.005). Furthermore, Tukey's multiple comparison test was run on the statistically significant values in order to determine to within ten scenarios the optimal number of scenarios to run so that the optimization model could be used under a fixed number of scenarios. The results of Tukey's test showed that as long as at least 30 scenarios were run, model solutions would not be affected by the random numbers generated, so it is

Constants	
Constant	Value
α	0.1
β	0.1
γ	0.1
δ	0.1
Δ	0.05
q	100
μ_1	25
σ_1	2
μ_2	25
σ_2	2
l (UGB quality loss cost)	3
e(LGB quality loss cost)	1
f (USL quality loss cost)	5
k (LSL quality loss cost)	2
τ	25

Table 5.1: Table of constants used when determining the optimal number of scenarios

particularly robust.

Upon further analysis, once the scenarios were set at 30, under the same initial conditions in Table 1, individual constants were varied over the different values shown in Table 2, while holding all the other values fixed as shown in Table 1. None of these values were determined to be statistically significant, with the exception of the cost of production, q. A boxplot, ANOVA table, and the results of Tukey's test for five different production costs: \$50, \$100, \$200, \$300, \$325 are given in Tables 2 and 3 along with Figure 5. It should be noted that these costs values were chosen so that positive profits would result using the demand functions in (7) and that the selling prices were higher than the production costs, q. In particular, the following fixed demand functions based on market conditions were chosen:

$$D_A(p_A, p_B, p_C, \zeta_i) = \begin{Bmatrix} 10000 - 5(4p_A + p_B + p_C), \ \zeta_i = good \\ 5000 - 2(4p_A + p_B + p_C), \ \zeta_i = bad \end{Bmatrix} \tag{15}$$

$$D_B(p_A, p_B, p_C, \zeta_i) = \begin{Bmatrix} 10000 - 5(p_A + 2p_B + p_C), \ \zeta_i = good \\ 5000 - 2(p_A + 2p_B + p_C), \ \zeta_i = bad \end{Bmatrix} \tag{16}$$

$$D_C(p_A, p_B, p_C, \zeta_i) = \begin{Bmatrix} 10000 - 5(p_A + p_B + 4p_C), \ \zeta_i = good \\ 5000 - 2(p_A + p_B + 4p_C), \ \zeta_i = bad \end{Bmatrix} \tag{17}$$

Note that product b is of a higher quality than products a and c. This is reflected in the differences between equations (13), (14) and (15). For these demand functions, the probabilities of good and bad market conditions are $P(\zeta_i = good) = 0.3$ and $P(\zeta_i = bad) = 0.7$.

These results indicate that the production cost along with the mean and variance of the production process are the key components in determining the expected profit of the company given fixed demand functions for products a, b, and c. It can also be seen that the variance in profit decreases as production costs increase. This is due to the lower quality products a and c needing to be sold at a price at least equal to the production costs in order not to incur a loss when the products are sold. This then forces the higher quality product b to be sold at a lower cost in order to have a non-negative demand for products a and c under good market conditions. This means that the high production costs result in market conditions limiting the supplier's selling option. A boxplot of production cost vs. selling price illustrating this concept can be seen below. Given a fixed product demand equation, companies with different production processes will be looked at in the next section.

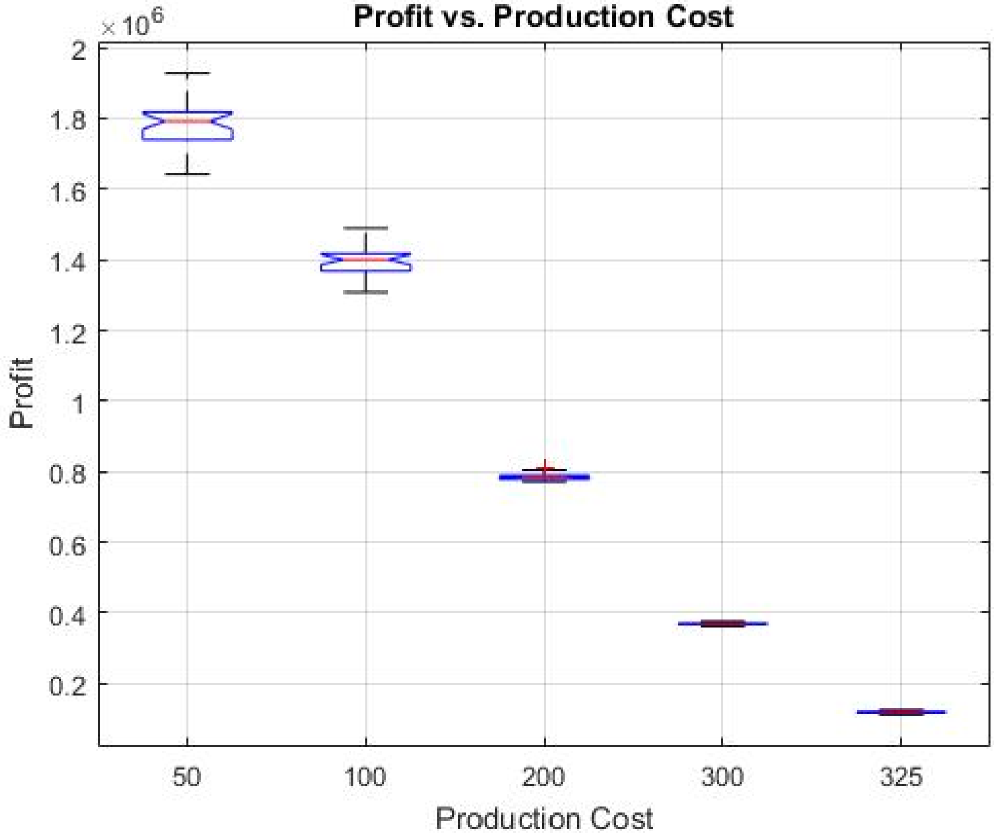

Figure 5.3: Boxplot of Production Costs

Analysis of Variance for Production Costs					
Source	Degrees of Freedom	Adjusted Sums of Squares	Adjusted Mean Squares	F	P-Value
q(cost)	4	$5.81*10^{13}$	$1.45*10^{13}$	14964.62	0.000
Error	145	$1.41*10^{11}$	$9.71*10^{8}$		
Total	149	$5.83*10^{13}$			

Table 5.2: Results of the ANOVA for the Production Costs q

Tukey Simultaneous Tests for Difference of Means					
Difference of Levels	Difference of Means	Standard Error of Difference	95 Percent Confidence Interval	T	P-Value
100-50	-389417	8046	(-411663, -367170)	-48.10	0.000
200-50	-1001250	8046	(-1023496, -979004)	-124.44	0.000
300-50	-1417510	8046	(-1439757, -1395264)	-176.17	0.000
325-50	-1667511	8046	(-1689758, -1645265)	-207.24	0.000
200-100	-611833	8046	(-634080, -589587)	-76.04	0.000
300-100	-1028094	8046	(-1050340, -1005847)	-127.77	0.000
325-100	-1278094	8046	(-1300341, -1255848)	-158.84	0.000
300-200	-416260	8046	(-438507, -394014)	-51.73	0.000
325-200	-666261	8046	(-688508, -644015)	-82.80	0.000
325-300	-250001	8046	(-272247, -227754)	-31.07	0.000

Table 5.3: Results of Tukey's Test for the Production Costs q

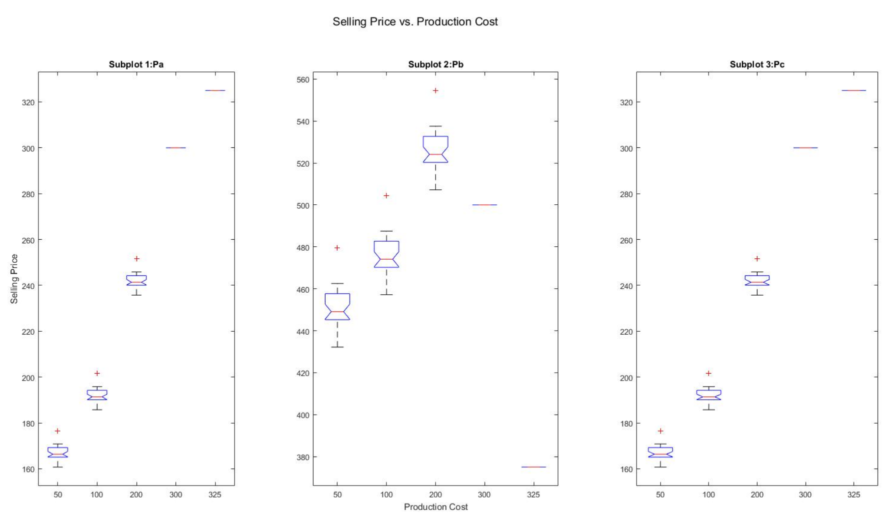

Figure 5.4: Boxplots Comparing Selling Prices to Production Costs

5.6.2 Scenario Analysis for Five Different Suppliers

When analyzing different processes from suppliers in a complex manufacturing setting, which often requires an extremely high degree of production planning, but is also imprecise, such as in semiconductor manufacturing, achieving low yields of high quality products is typical. In these types of situations, it is possible to salvage failed batches of integrated circuits by modifying performance characteristics of the product. In this way, parts manufactured may be binned into groups of high and low quality parts to be sold on the market. Consider an example where special CPUs are to be manufactured as close as possible to a 25nm lithography. Note that lithography here refers to the average space between the processor's logic gates (transistors). It is generally advantageous to produce processors with the smallest lithography possible, since more transistors can be placed on a CPU. As of 2017, 10 nm lithography is the manufacturing standard that most new commercial CPUs follow. Since manufacturers may all have different characteristics of their production processes, it would be advantageous to consider five different suppliers with the following characteristics given in table 4 below. Assume that the market demand for the products are given in equations (13)-(15) in the previous section, as well as the general loss functions defined in Section 3, with costs that vary according to Table 4.

It can be seen in the ANOVA table and the Tukey test below that all the suppliers were significantly different from each other. In particular, it should be noted that the suppliers with the same production costs, which were suppliers 1 and 4 as well as suppliers 2 and 5 had profits that were somewhat similar to each other. For example, supplier 5 posted higher profits than supplier 2 because supplier 5 had a mean that was less than the target value (the same as the mean for supplier 2 was greater than the target value), but there was a lower cost for violating the the lower guard band than the upper guard band. This was not the case for supplier 2, which had the same cost of \$150 for violating the guard bands. Looking at suppliers 1 and 4, the opposite seemed to be true. This is due to the tighter overall chance constraints placed on suppliers 1 and 4 in conjunction with the lower guard band costs being higher. Overall, as shown in the previous section, the production cost q, has the most significant impact on the overall profitability of the supplier.

Production Constants					
Constant	Supplier 1	Supplier 2	Supplier 3	Supplier 4	Supplier 5
α	0.05	0.1	0.05	0.05	0.1
β	0.05	0.1	0.05	0.05	0.1
γ	0.3	0.4	0.1	0.3	0.4
δ	0.3	0.4	0.1	0.3	0.4
Δ	0.05	0.05	0.05	0.05	0.05
q	250	230	325	250	230
μ_1	24.5	26	25	25.5	24
σ_1	.5	2	.25	.5	2
μ_2	24.5	26	25	25.5	24
σ_2	.5	2	.25	.5	2
l	200	150	250	190	165
e	200	150	250	210	135
f	250	230	325	250	230
k	250	230	325	250	230
τ	25	25	25	25	25

Table 5.4: Characteristics of Five Different Suppliers

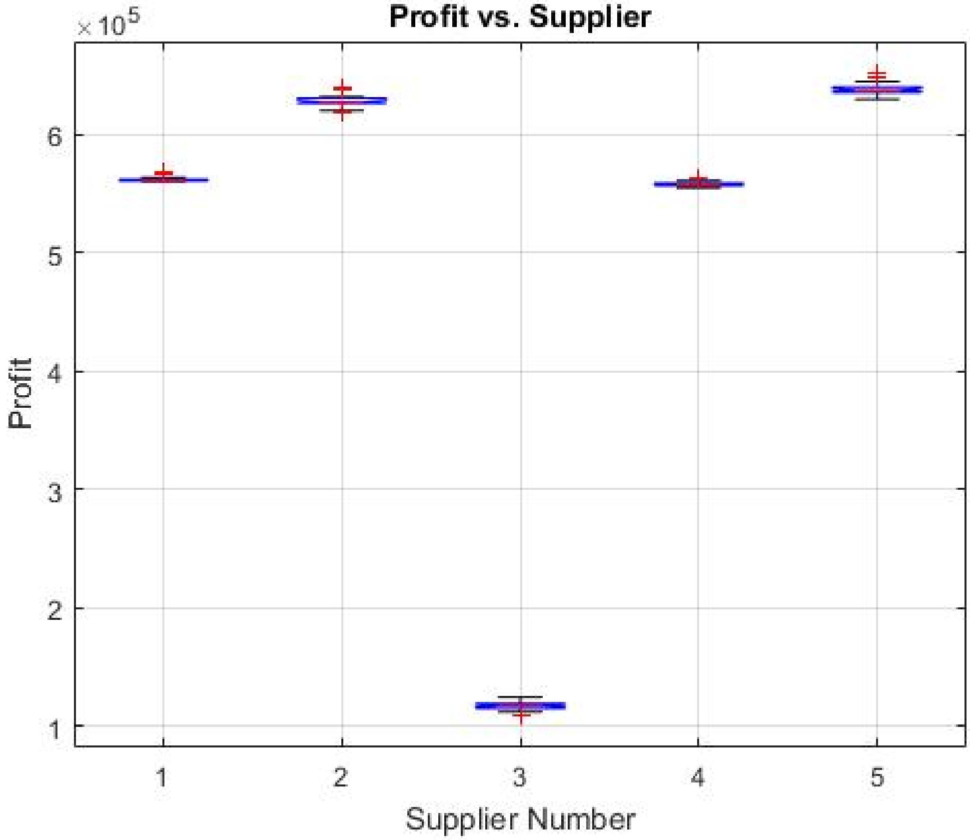

Figure 5.5: Boxplot of Supplier Profits

Analysis of Variance for Suppliers					
Source	Degrees of Freedom	Adjusted Sums of Squares	Adjusted Mean Squares	F-Value	P-Value
Supplier Number	4	$5.68*10^{12}$	$1.42*10^{12}$	112605.5	0.000
Error	145	$1.83*10^{9}$	$1.26*10^{7}$		
Total	149	$5.69*10^{12}$			

Table 5.5: Results of the ANOVA for the Suppliers

Tukey Simultaneous Tests for Difference of Means					
Difference of Levels	Difference of Means	Standard Error of Difference	95 Percent Confidence Interval	T-Value	P-Value
2-1	66062	917	(63526, 68598)	72.03	0.000
3-1	-445006	917	(-447541, -442470)	-485.20	0.000
4-1	-3810	917	(-6346, -1274)	-4.15	0.001
5-1	76294	917	(73758, 78830)	83.18	0.000
3-2	-511068	917	(-513604, -508532)	-557.23	0.000
4-2	-69872	917	(-72408, -67337)	-76.18	0.000
5-2	10232	917	(7696, 12768)	11.16	0.000
4-3	441195	917	(438660, 443731)	481.04	0.000
5-3	521300	917	(518764, 523836)	568.38	0.000
5-4	80104	917	(77569, 82640)	87.34	0.000

Table 5.6: Results of Tukey's test for the Suppliers

5.7 Conclusions and Future Work

A novel tolerance optimization model was presented that used stochastic programming to address issues involving uncertainty in both the manufacturing process as well as uncertain market demand. This was demonstrated through the utilization of the normal distribution and the truncated normal distribution through sensitivity analysis as well scenario analysis for five different suppliers. It was found that the suppliers with the lowest production costs had the highest profits. Furthermore, among suppliers with similar costs, that had off-target process means had higher profitability if their costs for violating the specification limits and guard bands were lower in the direction of the process mean shift. It is hoped practitioners in complex manufacturing industries that regularly utilize complex processes on a regular basis can benefit from and modify their production processes using the insights provided in this paper. By specifically utilizing the algorithms and techniques illustrated in this paper based upon both the market demand for their product in their particular industry as well as their own manufacturing processes it is hoped that practitioners can simultaneously improve both quality and profitability.

This work into tolerance optimization can be expanded upon by considering different stochastic elements resulting from the manufacturing process as well as considering different demand functions for the product. For example, considering the Weibull distribution in a tolerance optimization scheme would be beneficial, since Weibull distributions can be used to accurately account for failure rates of a product. In this sense, a time-to-failure component could be added as a third stage to the optimization, incorporating a post-manufacturing quality component. Another option could be to incorporate a multivariate process, such as the multivariate normal distribution to account for multiple critical-to-quality characteristics that may be correlated with each other. It would also be interesting to apply this model to uncertain processes in the service sector.

CHAPTER SIX

CONCLUSION AND FUTURE STUDIES

In accounting for uncertainty, the importance of understanding how process variability shifts over time is just as important as mean shifts over time. This result demonstrates the importance to practitioners that special care must be taken in understanding the root causes of change in not only their process means, but also the variability, if process fallout is to be minimized. It should be noted that processes can have the same process fallout over time but have vastly different process capability indices as the mean and standard deviation of the process shift over time. This further shows the critical need for practitioners to consider calculating process fallout in terms of DPMO by considering both the mean and variability shifts of their processes. Otherwise, their incorrect assumptions about their processes will lead to costly errors in manufacturing and service defects.

Further development of the theoretical foundations of convolutions of truncated normal and skew normal distributions based on double and triple truncations was needed in chapters 3 and 4 in order to enhance the understanding of production outputs. Numerical examples illustrated the application of convolutions of truncated normal random variables and truncated skew normal random variables to showcase the improved accuracy of tolerance analysis and gap analysis techniques. The findings have the potential to impact a wide range of many other engineering and science problems such as those found in statistical tolerance analysis, more specifically, tolerance stack analysis methods. From a practical perspective, this would allow statistical tolerance models to be applied at every step of a manufacturing process that has hundreds or thousands of manufacturing steps, instead of at two or three manufacturing steps at a time. This could result in substantially increased savings for a company and an extremely accurate production forecast in terms of identifying high quality components and the number of components that need to be scrapped or reworked.

Finally, a novel tolerance optimization model was developed that used stochastic programming to address issues involving uncertainty in both the manufacturing process and market demand. The methods created provide a framework to practitioners in complex manufacturing industries. By specifically utilizing the algorithms and techniques illustrated in chapter 5, it is hoped that practitioners can simultaneously improve both quality and profitability.

Future studies into accounting for uncertainties in process optimization initiatives can be undertaken by considering different stochastic elements resulting from the manufacturing process as well as considering different demand functions for the product. For example, considering the Weibull distribution in a process optimization scheme would be beneficial, since Weibull distributions can be used to accurately account for failure rates of a product. In this sense, a time-to-failure component could be incorporated into a post-manufacturing quality component. Another option could be to model a production process using a multivariate distribution, such as the multivariate normal distribution to account for multiple critical-to-quality characteristics that may be correlated with each other. The models developed here could also be used to enrich the understanding of processes within the service sector.

APPENDICES

Appendix A

Sample Convolution and Skewness Calculations

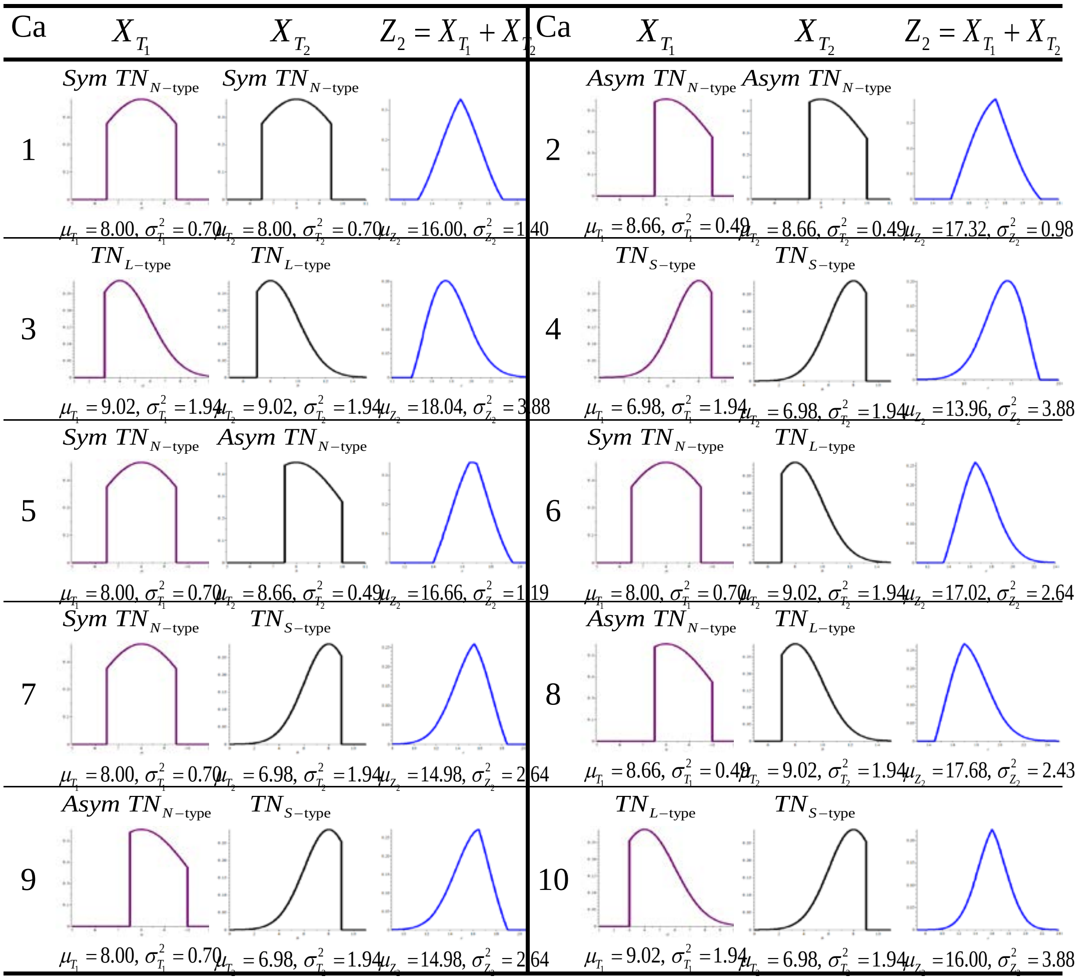

Figure A.1. Ten cases of sums of two truncated normal random variables

Table A.1. LTP and UTP of distributions used in Figure A.1.

Type	LTP	UTP	Type	LTP	UTP
Sym $TN_{N-\text{type}}$	6.5	9.5	Asym $TN_{N-\text{type}}$	7.5	10
$TN_{L-\text{type}}$	7	∞	$TN_{S-\text{type}}$	-∞	9

Table B.1. Skewness of distributions used in Figure A.1.

Case	X_{T_1}	X_{T_2}	$Z_2 = X_{T_1} + X_{T_2}$	Case	X_{T_1}	X_{T_2}	$Z_2 = X_{T_1} + X_{T_2}$
1	$Sym\ TN_{N-\text{ty}}$ 0.060	$Sym\ TN_{N-\text{type}}$ 0.060	0.060	2	$Asym\ TN_{N-}$ 0.064	$Asym\ TN_{N-\text{type}}$ 0.064	0.064
3	$TN_{L-\text{type}}$ 0.431	$TN_{L-\text{type}}$ 0.431	0.431	4	$TN_{S-\text{type}}$ -0.372	$TN_{S-\text{type}}$ -0.372	-0.372
5	$Sym\ TN_{N-\text{type}}$ 0.060	$Asym\ TN_{N-\text{type}}$ 0.064	0.207	6	$Sym\ TN_{N-\text{type}}$ 0.060	$TN_{L-\text{type}}$ 0.431	0.262
7	$Sym\ TN_{N-\text{type}}$ 0.060	$TN_{S-\text{type}}$ -0.372	-0.110	8	$Asym\ TN_{N-\text{type}}$ 0.064	$TN_{L-\text{type}}$ 0.431	0.182
9	$Asym\ TN_{N-\text{type}}$ 0.064	$TN_{S-\text{type}}$ -0.372	-0.373	10	$TN_{L-\text{type}}$ 0.431	$TN_{S-\text{type}}$ -0.372	-0.021

Case	X_{T_1}	X_{T_2}	$Z_2 = X_{T_1} + X_{T_2}$	Case	X_{T_1}	X_{T_2}	$Z_2 = X_{T_1} + X_{T_2}$
1	$TSN^{+}_{N-\text{type}}$ 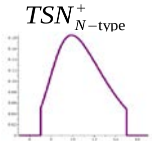 $\mu_{T_1} = 10.69,\ \sigma^2_{T_1} = 3.79$	$TSN^{+}_{N-\text{type}}$ 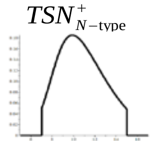 $\mu_{T_2} = 10.69,\ \sigma^2_{T_2} = 3.79$	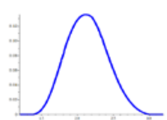 $\mu_{Z_2} = 21.38,\ \sigma^2_{Z_2} = 7.58$	2	$TSN^{-}_{N-\text{type}}$ 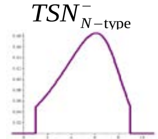 $\mu_{T_1} = 5.31,\ \sigma^2_{T_1} = 3.79$	$TSN^{-}_{N-\text{type}}$ 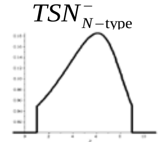 $\mu_{T_2} = 5.31,\ \sigma^2_{T_2} = 3.79$	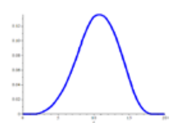 $\mu_{Z_2} = 10.62,\ \sigma^2_{Z_2} = 7.58$
3	$TSN^{+}_{L-\text{type}}$ 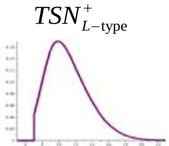 $\mu_{T_1} = 11.18,\ \sigma^2_{T_1} = 6.32$	$TSN^{+}_{L-\text{type}}$ 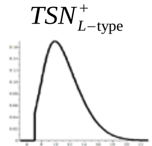 $\mu_{T_2} = 11.18,\ \sigma^2_{T_2} = 6.32$	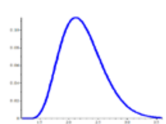 $\mu_{Z_2} = 22.36,\ \sigma^2_{Z_2} = 12.64$	4	$TSN^{-}_{L-\text{type}}$ 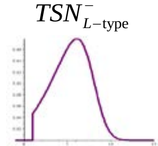 $\mu_{T_1} = 5.46,\ \sigma^2_{T_1} = 4.29$	$TSN^{-}_{L-\text{type}}$ 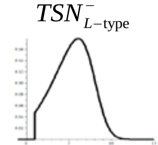 $\mu_{T_2} = 5.46,\ \sigma^2_{T_2} = 4.29$	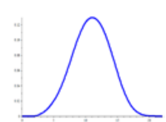 $\mu_{Z_2} = 10.92,\ \sigma^2_{Z_2} = 8.58$
5	$TSN^{+}_{S-\text{type}}$ 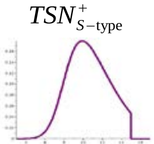 $\mu_{T_1} = 10.54,\ \sigma^2_{T_1} = 4.29$	$TSN^{+}_{S-\text{type}}$ 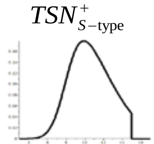 $\mu_{T_2} = 10.54,\ \sigma^2_{T_2} = 4.29$	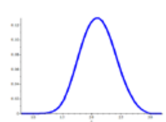 $\mu_{Z_2} = 21.08,\ \sigma^2_{Z_2} = 8.58$	6	$TSN^{-}_{S-\text{type}}$ 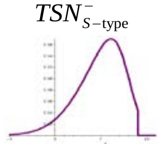 $\mu_{T_1} = 4.82,\ \sigma^2_{T_1} = 6.32$	$TSN^{-}_{S-\text{type}}$ 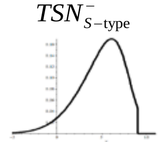 $\mu_{T_2} = 4.82,\ \sigma^2_{T_2} = 6.32$	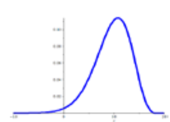 $\mu_{Z_2} = 9.64,\ \sigma^2_{Z_2} = 12.63$
7	$TSN^{+}_{N-\text{type}}$	$TSN^{-}_{N-\text{type}}$		8	$TSN^{+}_{N-\text{type}}$	$TSN^{+}_{L-\text{type}}$	

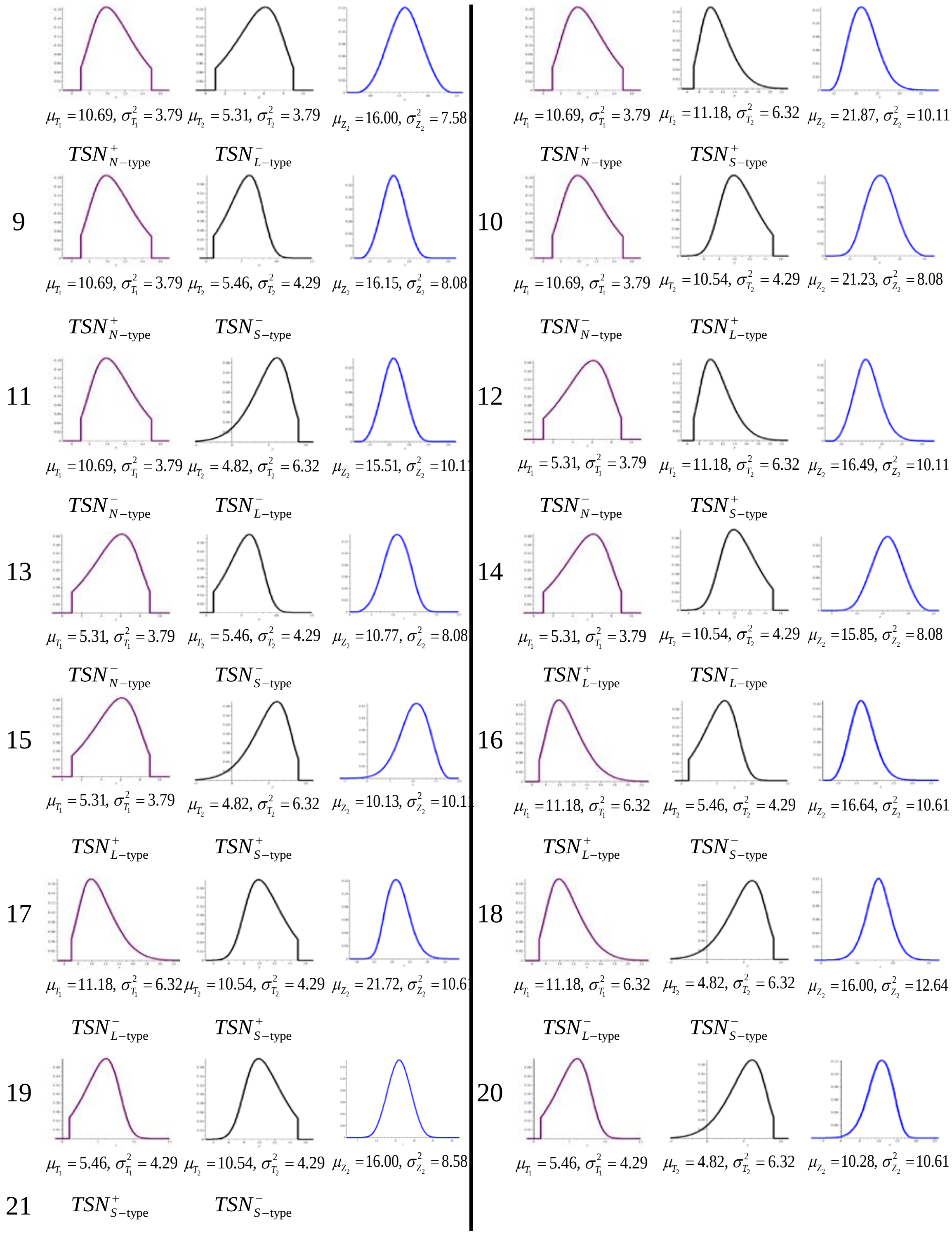

$\mu_{T_1}=10.69,\ \sigma^2_{T_1}=3.79$ $\mu_{T_2}=5.31,\ \sigma^2_{T_2}=3.79$ $\mu_{Z_2}=16.00,\ \sigma^2_{Z_2}=7.58$
$TSN^+_{N-\text{type}}$ $TSN^-_{L-\text{type}}$
9
$\mu_{T_1}=10.69,\ \sigma^2_{T_1}=3.79$ $\mu_{T_2}=5.46,\ \sigma^2_{T_2}=4.29$ $\mu_{Z_2}=16.15,\ \sigma^2_{Z_2}=8.08$
$TSN^+_{N-\text{type}}$ $TSN^-_{S-\text{type}}$
11
$\mu_{T_1}=10.69,\ \sigma^2_{T_1}=3.79$ $\mu_{T_2}=4.82,\ \sigma^2_{T_2}=6.32$ $\mu_{Z_2}=15.51,\ \sigma^2_{Z_2}=10.11$
$TSN^-_{N-\text{type}}$ $TSN^-_{L-\text{type}}$
13
$\mu_{T_1}=5.31,\ \sigma^2_{T_1}=3.79$ $\mu_{T_2}=5.46,\ \sigma^2_{T_2}=4.29$ $\mu_{Z_2}=10.77,\ \sigma^2_{Z_2}=8.08$
$TSN^-_{N-\text{type}}$ $TSN^-_{S-\text{type}}$
15
$\mu_{T_1}=5.31,\ \sigma^2_{T_1}=3.79$ $\mu_{T_2}=4.82,\ \sigma^2_{T_2}=6.32$ $\mu_{Z_2}=10.13,\ \sigma^2_{Z_2}=10.11$
$TSN^+_{L-\text{type}}$ $TSN^+_{S-\text{type}}$
17
$\mu_{T_1}=11.18,\ \sigma^2_{T_1}=6.32$ $\mu_{T_2}=10.54,\ \sigma^2_{T_2}=4.29$ $\mu_{Z_2}=21.72,\ \sigma^2_{Z_2}=10.61$
$TSN^-_{L-\text{type}}$ $TSN^+_{S-\text{type}}$
19
$\mu_{T_1}=5.46,\ \sigma^2_{T_1}=4.29$ $\mu_{T_2}=10.54,\ \sigma^2_{T_2}=4.29$ $\mu_{Z_2}=16.00,\ \sigma^2_{Z_2}=8.58$
21 $TSN^+_{S-\text{type}}$ $TSN^-_{S-\text{type}}$
$\mu_{T_1}=10.69,\ \sigma^2_{T_1}=3.79$ $\mu_{T_2}=11.18,\ \sigma^2_{T_2}=6.32$ $\mu_{Z_2}=21.87,\ \sigma^2_{Z_2}=10.11$
$TSN^+_{N-\text{type}}$ $TSN^+_{S-\text{type}}$
10
$\mu_{T_1}=10.69,\ \sigma^2_{T_1}=3.79$ $\mu_{T_2}=10.54,\ \sigma^2_{T_2}=4.29$ $\mu_{Z_2}=21.23,\ \sigma^2_{Z_2}=8.08$
$TSN^-_{N-\text{type}}$ $TSN^+_{L-\text{type}}$
12
$\mu_{T_1}=5.31,\ \sigma^2_{T_1}=3.79$ $\mu_{T_2}=11.18,\ \sigma^2_{T_2}=6.32$ $\mu_{Z_2}=16.49,\ \sigma^2_{Z_2}=10.11$
$TSN^-_{N-\text{type}}$ $TSN^+_{S-\text{type}}$
14
$\mu_{T_1}=5.31,\ \sigma^2_{T_1}=3.79$ $\mu_{T_2}=10.54,\ \sigma^2_{T_2}=4.29$ $\mu_{Z_2}=15.85,\ \sigma^2_{Z_2}=8.08$
$TSN^+_{L-\text{type}}$ $TSN^-_{L-\text{type}}$
16
$\mu_{T_1}=11.18,\ \sigma^2_{T_1}=6.32$ $\mu_{T_2}=5.46,\ \sigma^2_{T_2}=4.29$ $\mu_{Z_2}=16.64,\ \sigma^2_{Z_2}=10.61$
$TSN^+_{L-\text{type}}$ $TSN^-_{S-\text{type}}$
18
$\mu_{T_1}=11.18,\ \sigma^2_{T_1}=6.32$ $\mu_{T_2}=4.82,\ \sigma^2_{T_2}=6.32$ $\mu_{Z_2}=16.00,\ \sigma^2_{Z_2}=12.64$
$TSN^-_{L-\text{type}}$ $TSN^-_{S-\text{type}}$
20
$\mu_{T_1}=5.46,\ \sigma^2_{T_1}=4.29$ $\mu_{T_2}=4.82,\ \sigma^2_{T_2}=6.32$ $\mu_{Z_2}=10.28,\ \sigma^2_{Z_2}=10.61$

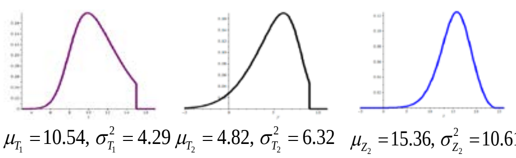

Figure A.2. Twenty-one Different cases of the sums of Truncated Skew Normal Random Variables

Table A.2. Shape parameter α and lower and upper truncation points of distributions used in Figure A.2

Type	α	LTP	UTP	Type	α	LTP	UTP
$TSN^{+}_{N-\text{type}}$	3	7	15	$TSN^{-}_{N-\text{type}}$	-3	1	9
$TSN^{+}_{L-\text{type}}$	3	7	∞	$TSN^{-}_{L-\text{type}}$	-3	1	∞
$TSN^{+}_{S-\text{type}}$	3	$-\infty$	15	$TSN^{-}_{S-\text{type}}$	-3	$-\infty$	9

Table B.2. Skewness of distributions used in Figure A.2

Cas	X_{T_1}	X_{T_2}	$Z_2 = X_{T_1} + X_{T_2}$	Cas	X_{T_1}	X_{T_2}	$Z_2 = X_{T_1} + X_{T_2}$
1	$TSN^{+}_{N-\text{type}}$ 0.322	$TSN^{+}_{N-\text{type}}$ 0.322	0.322	2	$TSN^{-}_{N-\text{type}}$ -0.317	$TSN^{-}_{N-\text{type}}$ -0.317	-0.317
3	$TSN^{+}_{L-\text{type}}$ 0.840	$TSN^{+}_{L-\text{type}}$ 0.840	0.840	4	$TSN^{-}_{L-\text{type}}$ -0.102	$TSN^{-}_{L-\text{type}}$ -0.102	-0.102
5	$TSN^{+}_{S-\text{type}}$ 0.449	$TSN^{+}_{S-\text{type}}$ 0.449	0.449	6	$TSN^{-}_{S-\text{type}}$ -0.723	$TSN^{-}_{S-\text{type}}$ -0.723	-0.723
7	$TSN^{+}_{N-\text{type}}$ 0.322	$TSN^{-}_{N-\text{type}}$ -0.317	0.006	8	$TSN^{+}_{N-\text{type}}$ 0.322	$TSN^{+}_{L-\text{type}}$ 0.840	0.211
9	$TSN^{+}_{N-\text{type}}$ 0.322	$TSN^{-}_{L-\text{type}}$ -0.102	0.313	10	$TSN^{+}_{N-\text{type}}$ 0.322	$TSN^{+}_{S-\text{type}}$ 0.449	0.389
11	$TSN^{+}_{N-\text{type}}$ 0.322	$TSN^{-}_{S-\text{type}}$ -0.723	-0.122	12	$TSN^{-}_{N-\text{type}}$ -0.317	$TSN^{+}_{L-\text{type}}$ 0.840	0.347
13	$TSN^{-}_{N-\text{type}}$ -0.317	$TSN^{-}_{L-\text{type}}$ -0.102	-0.154	14	$TSN^{-}_{N-\text{type}}$ -0.317	$TSN^{+}_{S-\text{type}}$ 0.449	0.299
15	$TSN^{-}_{N-\text{type}}$ -0.317	$TSN^{-}_{S-\text{type}}$ -0.723	-0.327	16	$TSN^{+}_{L-\text{type}}$ 0.840	$TSN^{-}_{L-\text{type}}$ -0.102	0.613
17	$TSN^{+}_{L-\text{type}}$ 0.840	$TSN^{+}_{S-\text{type}}$ 0.449	0.749	18	$TSN^{+}_{L-\text{type}}$ 0.840	$TSN^{-}_{S-\text{type}}$ -0.723	0.096
19	$TSN^{-}_{L-\text{type}}$ -0.102	$TSN^{+}_{S-\text{type}}$ 0.449	0.408	20	$TSN^{-}_{L-\text{type}}$ -0.102	$TSN^{-}_{S-\text{type}}$ -0.723	-0.411
21	$TSN^{+}_{S-\text{type}}$ 0.449	$TSN^{-}_{S-\text{type}}$ -0.723	-0.300				

The Expanded Derivation of the Convolutions of Three Truncated Normal Random Variables

$$f_{Z_3}(s)=\int_{-\infty}^{\infty} f_{X_{T_3}}(s-z)f_{Z_2}(z)dz$$

$$=\int_{-\infty}^{\infty}\frac{\frac{1}{\sigma_3\sqrt{2\pi}}\exp^{-\frac{1}{2}\left(\frac{s-z-\mu_3}{\sigma_3}\right)^2}}{\int_{x_{l_3}}^{x_{u_3}}\frac{1}{\sigma_3\sqrt{2\pi}}\exp^{-\frac{1}{2}\left(\frac{v-\mu_3}{\sigma_3}\right)^2}dv} I_{[x_{l_3},x_{u_3}]}(s-z)\,f_{Z_2}(z)dz$$

$$=\int_{-\infty}^{\infty}\frac{\frac{1}{\sigma_3\sqrt{2\pi}}\exp^{-\frac{1}{2}\left(\frac{s-z-\mu_3}{\sigma_3}\right)^2}}{\int_{x_{l_3}}^{x_{u_3}}\frac{1}{\sigma_3\sqrt{2\pi}}\exp^{-\frac{1}{2}\left(\frac{v-\mu_3}{\sigma_3}\right)^2}dv} I_{[x_{l_3},x_{u_3}]}(s-z)\left(\int_{-\infty}^{\infty}\frac{\frac{1}{\sigma_2\sqrt{2\pi}}\exp^{-\frac{1}{2}\left(\frac{z-x-\mu_2}{\sigma_2}\right)^2}}{\int_{x_{l_2}}^{x_{u_2}}\frac{1}{\sigma_2\sqrt{2\pi}}\exp^{-\frac{1}{2}\left(\frac{p-\mu_2}{\sigma_2}\right)^2}dp}\cdot\right.$$

$$\left.\frac{\frac{1}{\sigma_1\sqrt{2\pi}}\exp^{-\frac{1}{2}\left(\frac{x-\mu_1}{\sigma_1}\right)^2}}{\int_{x_{l_1}}^{x_{u_1}}\frac{1}{\sigma_1\sqrt{2\pi}}\exp^{-\frac{1}{2}\left(\frac{h-\mu_1}{\sigma_1}\right)^2}dh} I_{[z-x_{u_2},z-x_{l_2}]}(x)\,I_{[x_{l_1},x_{u_1}]}(x)dx\right)dz$$

$$=\int_{-\infty}^{\infty}\int_{-\infty}^{\infty}\frac{\frac{1}{\sigma_3\sqrt{2\pi}}\exp^{-\frac{1}{2}\left(\frac{s-z-\mu_3}{\sigma_3}\right)^2}}{\int_{x_{l_3}}^{x_{u_3}}\frac{1}{\sigma_3\sqrt{2\pi}}\exp^{-\frac{1}{2}\left(\frac{v-\mu_3}{\sigma_3}\right)^2}dv}\frac{\frac{1}{\sigma_2\sqrt{2\pi}}\exp^{-\frac{1}{2}\left(\frac{z-x-\mu_2}{\sigma_2}\right)^2}}{\int_{x_{l_2}}^{x_{u_2}}\frac{1}{\sigma_2\sqrt{2\pi}}\exp^{-\frac{1}{2}\left(\frac{p-\mu_2}{\sigma_2}\right)^2}dp}\cdot$$

$$\frac{\frac{1}{\sigma_1\sqrt{2\pi}}\exp^{-\frac{1}{2}\left(\frac{x-\mu_1}{\sigma_1}\right)^2}}{\int_{x_{l_1}}^{x_{u_1}}\frac{1}{\sigma_1\sqrt{2\pi}}\exp^{-\frac{1}{2}\left(\frac{h-\mu_1}{\sigma_1}\right)^2}dh} I_{[x_{l_1},x_{u_1}]}(x)\,I_{[z-x_{u_2},z-x_{l_2}]}(x)\,I_{[s-x_{u_3},s-x_{l_3}]}(z)dxdz.$$

It is noted that $I_{[x_{l_3},x_{u_3}]}(s-z)$ can be written as $I_{[s-x_{u_3},s-x_{l_3}]}(z)$.

The Expanded Derivation of the Convolutions of Three Truncated Skew Normal Random Variables

$$f_{Z_{TS_3}}(s)=\int_{-\infty}^{\infty} f_{Y_{TS_3}}(s-z)f_{Z_{TS_2}}(z)dz$$

$$=\int_{-\infty}^{\infty}\frac{\frac{2}{\sigma_3}\frac{1}{\sqrt{2\pi}}e^{-\frac{1}{2}\left(\frac{s-z-\mu_3}{\sigma_3}\right)^2}\int_{-\infty}^{\alpha_3\frac{s-z-\mu_3}{\sigma_3}}\frac{1}{\sqrt{2\pi}}e^{-\frac{1}{2}t^2}dt}{\int_{y_{l_3}}^{y_{u_3}}\frac{2}{\sigma_3}\frac{1}{\sqrt{2\pi}}e^{-\frac{1}{2}\left(\frac{v-\mu_3}{\sigma_3}\right)^2}\left(\int_{-\infty}^{\alpha_3\frac{v-\mu_3}{\sigma_3}}\frac{1}{\sqrt{2\pi}}e^{-\frac{1}{2}t^2}dt\right)dv} I_{[y_{l_3},y_{u_3}]}(s-z)\,f_{Z_2}(z)dz$$

$$=\int_{-\infty}^{\infty}\frac{\frac{2}{\sigma_3}\frac{1}{\sqrt{2\pi}}e^{-\frac{1}{2}\left(\frac{s-z-\mu_3}{\sigma_3}\right)^2}\int_{-\infty}^{\alpha_3\frac{s-z-\mu_3}{\sigma_3}}\frac{1}{\sqrt{2\pi}}e^{-\frac{1}{2}t^2}dt}{\int_{y_{l_3}}^{y_{u_3}}\frac{2}{\sigma_3}\frac{1}{\sqrt{2\pi}}e^{-\frac{1}{2}\left(\frac{v-\mu_3}{\sigma_3}\right)^2}\left(\int_{-\infty}^{\alpha_3\frac{v-\mu_3}{\sigma_3}}\frac{1}{\sqrt{2\pi}}e^{-\frac{1}{2}t^2}dt\right)dv}I_{[y_{l_3},y_{u_3}]}(s-z)\cdot$$

$$\left(\int_{-\infty}^{\infty}\frac{\frac{2}{\sigma_2}\frac{1}{\sqrt{2\pi}}e^{-\frac{1}{2}\left(\frac{z-x-\mu_2}{\sigma_2}\right)^2}\int_{-\infty}^{\alpha_2\frac{z-x-\mu_2}{\sigma_2}}\frac{1}{\sqrt{2\pi}}e^{-\frac{1}{2}t^2}dt}{\int_{y_{l_2}}^{y_{u_2}}\frac{2}{\sigma_2}\frac{1}{\sqrt{2\pi}}e^{-\frac{1}{2}\left(\frac{p-\mu_2}{\sigma_2}\right)^2}\left(\int_{-\infty}^{\alpha_2\frac{p-\mu_2}{\sigma_2}}\frac{1}{\sqrt{2\pi}}e^{-\frac{1}{2}t^2}dt\right)dp}\cdot\right.$$

$$\left.\frac{\frac{2}{\sigma_1}\frac{1}{\sqrt{2\pi}}e^{-\frac{1}{2}\left(\frac{x-\mu_1}{\sigma_1}\right)^2}\int_{-\infty}^{\alpha_1\frac{x-\mu_1}{\sigma_1}}\frac{1}{\sqrt{2\pi}}e^{-\frac{1}{2}t^2}dt}{\int_{y_{l_1}}^{y_{u_1}}\frac{2}{\sigma_1}\frac{1}{\sqrt{2\pi}}e^{-\frac{1}{2}\left(\frac{h-\mu_1}{\sigma_1}\right)^2}\left(\int_{-\infty}^{\alpha_1\frac{h-\mu_1}{\sigma_1}}\frac{1}{\sqrt{2\pi}}e^{-\frac{1}{2}t^2}dt\right)dh}I_{[z-y_{u_2},z-y_{l_2}]}(x)\,I_{[y_{l_1},y_{u_1}]}(x)dx\right)dz$$

$$=\int_{-\infty}^{\infty}\int_{-\infty}^{\infty}\frac{\frac{2}{\sigma_3}\frac{1}{\sqrt{2\pi}}e^{-\frac{1}{2}\left(\frac{s-z-\mu_3}{\sigma_3}\right)^2}\int_{-\infty}^{\alpha_3\frac{s-z-\mu_3}{\sigma_3}}\frac{1}{\sqrt{2\pi}}e^{-\frac{1}{2}t^2}dt}{\int_{y_{l_3}}^{y_{u_3}}\frac{2}{\sigma_3}\frac{1}{\sqrt{2\pi}}e^{-\frac{1}{2}\left(\frac{v-\mu_3}{\sigma_3}\right)^2}\left(\int_{-\infty}^{\alpha_3\frac{v-\mu_3}{\sigma_3}}\frac{1}{\sqrt{2\pi}}e^{-\frac{1}{2}t^2}dt\right)dv}\cdot$$

$$\frac{\frac{2}{\sigma_2}\frac{1}{\sqrt{2\pi}}e^{-\frac{1}{2}\left(\frac{z-x-\mu_2}{\sigma_2}\right)^2}\int_{-\infty}^{\alpha_2\frac{z-x-\mu_2}{\sigma_2}}\frac{1}{\sqrt{2\pi}}e^{-\frac{1}{2}t^2}dt}{\int_{y_{l_2}}^{y_{u_2}}\frac{2}{\sigma_2}\frac{1}{\sqrt{2\pi}}e^{-\frac{1}{2}\left(\frac{p-\mu_2}{\sigma_2}\right)^2}\left(\int_{-\infty}^{\alpha_2\frac{p-\mu_2}{\sigma_2}}\frac{1}{\sqrt{2\pi}}e^{-\frac{1}{2}t^2}dt\right)dp}\cdot$$

$$\frac{\frac{2}{\sigma_1}\frac{1}{\sqrt{2\pi}}e^{-\frac{1}{2}\left(\frac{x-\mu_1}{\sigma_1}\right)^2}\int_{-\infty}^{\alpha_1\frac{x-\mu_1}{\sigma_1}}\frac{1}{\sqrt{2\pi}}e^{-\frac{1}{2}t^2}dt}{\int_{y_{l_1}}^{y_{u_1}}\frac{2}{\sigma_1}\frac{1}{\sqrt{2\pi}}e^{-\frac{1}{2}\left(\frac{h-\mu_1}{\sigma_1}\right)^2}\left(\int_{-\infty}^{\alpha_1\frac{h-\mu_1}{\sigma_1}}\frac{1}{\sqrt{2\pi}}e^{-\frac{1}{2}t^2}dt\right)dh}I_{[x_{l_1},x_{u_1}]}(x)I_{[z-y_{u_2},z-y_{l_2}]}(x)I_{[s-y_{u_3},s-y_{l_3}]}(z)dxdz.$$

Since $s = z + k$, $I_{[y_{l_3},y_{u_3}]}(s-z)$ can be written as $I_{[s-y_{u_3},s-y_{l_3}]}(z)$.

The Expanded Derivation of Sums of Two Truncated Normal Random Variables and One Truncated Skew Normal Random Variable

Let $Z_2 = X_{T_1} + X_{T_2}$ and $Z_3 = Z_2 + Y_{TS_3}$. Therefore, the probability density function of Z_3 is:

$$f_{Z_3}(s) = \int_{-\infty}^{\infty} f_{Y_{TS_3}}(s-z) f_{Z_2}(z)dz$$

$$= \int_{-\infty}^{\infty} \frac{\frac{2}{\sigma_3}\frac{1}{\sqrt{2\pi}} e^{-\frac{1}{2}\left(\frac{s-z-\mu_3}{\sigma_3}\right)^2} \int_{-\infty}^{\alpha_3\frac{s-z-\mu_3}{\sigma_3}} \frac{1}{\sqrt{2\pi}} e^{-\frac{1}{2}t^2} dt}{\int_{y_{l_3}}^{y_{u_3}} \frac{2}{\sigma_3}\frac{1}{\sqrt{2\pi}} e^{-\frac{1}{2}\left(\frac{v-\mu_3}{\sigma_3}\right)^2} \left(\int_{-\infty}^{\alpha_3\frac{v-\mu_3}{\sigma_3}} \frac{1}{\sqrt{2\pi}} e^{-\frac{1}{2}t^2} dt\right) dv} I_{[y_{l_3}, y_{u_3}]}(s-z) f_{Z_2}(z)dz$$

$$= \int_{-\infty}^{\infty} \frac{\frac{2}{\sigma_3}\frac{1}{\sqrt{2\pi}} e^{-\frac{1}{2}\left(\frac{s-z-\mu_3}{\sigma_3}\right)^2} \int_{-\infty}^{\alpha_3\frac{s-z-\mu_3}{\sigma_3}} \frac{1}{\sqrt{2\pi}} e^{-\frac{1}{2}t^2} dt}{\int_{y_{l_3}}^{y_{u_3}} \frac{2}{\sigma_3}\frac{1}{\sqrt{2\pi}} e^{-\frac{1}{2}\left(\frac{v-\mu_3}{\sigma_3}\right)^2} \left(\int_{-\infty}^{\alpha_3\frac{v-\mu_3}{\sigma_3}} \frac{1}{\sqrt{2\pi}} e^{-\frac{1}{2}t^2} dt\right) dv} I_{[y_{l_3}, y_{u_3}]}(s-z) \cdot$$

$$\left(\int_{-\infty}^{\infty} \frac{\frac{1}{\sigma_2\sqrt{2\pi}} \exp^{-\frac{1}{2}\left(\frac{z-x-\mu_2}{\sigma_2}\right)^2}}{\int_{x_{l_2}}^{x_{u_2}} \frac{1}{\sigma_2\sqrt{2\pi}} \exp^{-\frac{1}{2}\left(\frac{p-\mu_2}{\sigma_2}\right)^2} dp} \frac{\frac{1}{\sigma_1\sqrt{2\pi}} \exp^{-\frac{1}{2}\left(\frac{x-\mu_1}{\sigma_1}\right)^2}}{\int_{x_{l_1}}^{x_{u_1}} \frac{1}{\sigma_1\sqrt{2\pi}} \exp^{-\frac{1}{2}\left(\frac{h-\mu_1}{\sigma_1}\right)^2} dh} I_{[z-x_{u_2}, z-x_{l_2}]}(x) I_{[x_{l_1}, x_{u_1}]}(x)dx \right) dz$$

$$= \int_{-\infty}^{\infty}\int_{-\infty}^{\infty} \frac{\frac{2}{\sigma_3}\frac{1}{\sqrt{2\pi}} e^{-\frac{1}{2}\left(\frac{s-z-\mu_3}{\sigma_3}\right)^2} \int_{-\infty}^{\alpha_3\frac{s-z-\mu_3}{\sigma_3}} \frac{1}{\sqrt{2\pi}} e^{-\frac{1}{2}t^2} dt}{\int_{y_{l_3}}^{y_{u_3}} \frac{2}{\sigma_3}\frac{1}{\sqrt{2\pi}} e^{-\frac{1}{2}\left(\frac{v-\mu_3}{\sigma_3}\right)^2} \left(\int_{-\infty}^{\alpha_3\frac{v-\mu_3}{\sigma_3}} \frac{1}{\sqrt{2\pi}} e^{-\frac{1}{2}t^2} dt\right) dv} \frac{\frac{1}{\sigma_2\sqrt{2\pi}} \exp^{-\frac{1}{2}\left(\frac{z-x-\mu_2}{\sigma_2}\right)^2}}{\int_{x_{l_2}}^{x_{u_2}} \frac{1}{\sigma_2\sqrt{2\pi}} \exp^{-\frac{1}{2}\left(\frac{s-\mu_2}{\sigma_2}\right)^2} ds} \cdot$$

$$\frac{\frac{1}{\sigma_1\sqrt{2\pi}} \exp^{-\frac{1}{2}\left(\frac{x-\mu_1}{\sigma_1}\right)^2}}{\int_{x_{l_1}}^{x_{u_1}} \frac{1}{\sigma_1\sqrt{2\pi}} \exp^{-\frac{1}{2}\left(\frac{h-\mu_1}{\sigma_1}\right)^2} dh} I_{[x_{l_1}, x_{u_1}]}(x) I_{[z-x_{u_2}, z-x_{l_2}]}(x) I_{[s-y_{u_3}, s-y_{l_3}]}(z)dxdz.$$

The Expanded Derivation of Sums of One truncated Normal Random Variable and Two Truncated Skew Normal Random Variables

When $Z_2 = Y_{TS_1} + Y_{TS_2}$ and then $Z_3 = Y_{TS_1} + Y_{TS_2} + X_{T_3} = Z_2 + X_{T_3}$. Therefore, the probability density function of Z_3 is expressed as

$$f_{Z_3}(s) = \int_{-\infty}^{\infty} f_{X_{TS_3}}(s-z) f_{Z_2}(z)dz$$

$$= \int_{-\infty}^{\infty} \frac{\frac{1}{\sigma_3\sqrt{2\pi}} \exp^{-\frac{1}{2}\left(\frac{s-z-\mu_3}{\sigma_3}\right)^2}}{\int_{x_{l_3}}^{x_{u_3}} \frac{1}{\sigma_3\sqrt{2\pi}} \exp^{-\frac{1}{2}\left(\frac{v-\mu_3}{\sigma_3}\right)^2} dv} I_{[x_{l_3}, x_{u_3}]}(s-z) f_{Z_2}(z)dz$$

$$= \int_{-\infty}^{\infty} \frac{\frac{1}{\sigma_3\sqrt{2\pi}} \exp^{-\frac{1}{2}\left(\frac{s-z-\mu_3}{\sigma_3}\right)^2}}{\int_{x_{l_3}}^{x_{u_3}} \frac{1}{\sigma_3\sqrt{2\pi}} \exp^{-\frac{1}{2}\left(\frac{v-\mu_3}{\sigma_3}\right)^2} dv} I_{[x_{l_3}, x_{u_3}]}(s-z) \cdot$$

$$\left(\int_{-\infty}^{\infty} \frac{\frac{2}{\sigma_2}\frac{1}{\sqrt{2\pi}} e^{-\frac{1}{2}\left(\frac{z-x-\mu_2}{\sigma_2}\right)^2} \int_{-\infty}^{\alpha_2 \frac{z-x-\mu_2}{\sigma_2}} \frac{1}{\sqrt{2\pi}} e^{-\frac{1}{2}t^2} dt}{\int_{y_{l_2}}^{y_{u_2}} \frac{2}{\sigma_2}\frac{1}{\sqrt{2\pi}} e^{-\frac{1}{2}\left(\frac{p-\mu_2}{\sigma_2}\right)^2} \left(\int_{-\infty}^{\alpha_2 \frac{p-\mu_2}{\sigma_2}} \frac{1}{\sqrt{2\pi}} e^{-\frac{1}{2}t^2} dt \right) dp} \cdot \right.$$

$$\left. \frac{\frac{2}{\sigma_1}\frac{1}{\sqrt{2\pi}} e^{-\frac{1}{2}\left(\frac{x-\mu_1}{\sigma_1}\right)^2} \int_{-\infty}^{\alpha_1 \frac{x-\mu_1}{\sigma_1}} \frac{1}{\sqrt{2\pi}} e^{-\frac{1}{2}(t)^2} dt}{\int_{y_{l_1}}^{y_{u_1}} \frac{2}{\sigma_1}\frac{1}{\sqrt{2\pi}} e^{-\frac{1}{2}\left(\frac{h-\mu_1}{\sigma_1}\right)^2} \left(\int_{-\infty}^{\alpha_1 \frac{h-\mu_1}{\sigma_1}} \frac{1}{\sqrt{2\pi}} e^{-\frac{1}{2}(t)^2} dt \right) dh} I_{[z-y_{u_2}, z-y_{l_2}]}(x) I_{[y_{l_1}, y_{u_1}]}(x)dx \right) dz$$

$$= \int_{-\infty}^{\infty}\int_{-\infty}^{\infty} \frac{\frac{1}{\sigma_3\sqrt{2\pi}} \exp^{-\frac{1}{2}\left(\frac{s-z-\mu_3}{\sigma_3}\right)^2}}{\int_{x_{l_3}}^{x_{u_3}} \frac{1}{\sigma_3\sqrt{2\pi}} \exp^{-\frac{1}{2}\left(\frac{v-\mu_3}{\sigma_3}\right)^2} dv} \frac{\frac{2}{\sigma_2}\frac{1}{\sqrt{2\pi}} e^{-\frac{1}{2}\left(\frac{z-x-\mu_2}{\sigma_2}\right)^2} \int_{-\infty}^{\alpha_2 \frac{z-x-\mu_2}{\sigma_2}} \frac{1}{\sqrt{2\pi}} e^{-\frac{1}{2}t^2} dt}{\int_{y_{l_2}}^{y_{u_2}} \frac{2}{\sigma_2}\frac{1}{\sqrt{2\pi}} e^{-\frac{1}{2}\left(\frac{p-\mu_2}{\sigma_2}\right)^2} \left(\int_{-\infty}^{\alpha_2 \frac{p-\mu_2}{\sigma_2}} \frac{1}{\sqrt{2\pi}} e^{-\frac{1}{2}t^2} dt \right) dp} \cdot$$

$$\frac{\frac{2}{\sigma_1}\frac{1}{\sqrt{2\pi}} e^{-\frac{1}{2}\left(\frac{x-\mu_1}{\sigma_1}\right)^2} \int_{-\infty}^{\alpha_1 \frac{x-\mu_1}{\sigma_1}} \frac{1}{\sqrt{2\pi}} e^{-\frac{1}{2}t^2} dt}{\int_{y_{l_1}}^{y_{u_1}} \frac{2}{\sigma_1}\frac{1}{\sqrt{2\pi}} e^{-\frac{1}{2}\left(\frac{h-\mu_1}{\sigma_1}\right)^2} \left(\int_{-\infty}^{\alpha_1 \frac{h-\mu_1}{\sigma_1}} \frac{1}{\sqrt{2\pi}} e^{-\frac{1}{2}t^2} dt \right) dh} \cdot$$

$$I_{[y_{l_1}, y_{u_1}]}(x) I_{[z-y_{u_2}, z-y_{l_2}]}(x) I_{[s-z-x_{u_3}, s-z-x_{l_3}]}(z)dxdz.$$

Appendix B

Supporting Matlab code for Chapter 2

The following base MATLAB code was used to generate contour plots for a Bivariate Normal Distribution and calculate DPMOs by changing various values:

```
format shortG
%corr. coeff.
rho=0.9;
%starting standard deviations
sigma1=.5;
sigma2=1;
%starting means
mu1=5;
mu2=1;
%mean shifts
k11=3.363345;
k12=3.363345;
%standard deviation shifts
k21=1;
k22=1;
%Limits
lowerx=mu1-6*sigma1+k11*sigma1;
lowery=mu2-6*sigma2+k12*sigma2;
upperx=mu1+6*sigma1+k11*sigma1;
uppery=mu2+6*sigma2+k12*sigma2;
XL=[lowerx lowery];
XU=[upperx uppery];
a=(sigma1/k21).^2;
b=(rho*sigma1*sigma2)/(k21*k22);
c=(sigma2/k22).^2;
MU = [mu1 mu2];
SIGMA = [a b;b c];
x1 = lowerx-sigma1:.2: upperx+sigma1; x2 = lowery-sigma2:.2:
uppery+sigma2;
[X1,X2] = meshgrid(x1,x2);
F = mvnpdf([X1(:) X2(:)],MU,SIGMA);
F = reshape(F,length(x2),length(x1));
%contour(X1,X2,F,);
Y=mvncdf(XL,XU,MU,SIGMA);
DPMO=(1-Y)*10.^6
%contour(x1,x2,F,[.0001 .001 .01 .05:.2:.95 .99 .999 .9999]);
contour(x1,x2,F,[.0000000000001 .000000000001 .00000000001 .0000000001
.000000001 .00000001 .0000001 .000001 .00001 .0001 .001 .01 .05:.1:.95
.99 .999 .9999 .99999 .999999 .9999999 .99999999 .999999999 .9999999999
.99999999999 .999999999999 .9999999999999]);
[C h]=contour(x1,x2,F,[.0000000000001 .000000000001 .00000000001
.0000000001 .000000001 .00000001 .0000001 .000001 .00001 .0001 .001 .01
.05:.1:.95 .99 .999 .9999 .99999 .999999 .9999999 .99999999 .999999999
.9999999999 .99999999999 .999999999999 .9999999999999]);
clabel(C,h)
```

```
xlabel('x1'); ylabel('x2');
line([lowerx upperx upperx lowerx lowerx],[lowery lowery uppery uppery
lowery],'linestyle','--','color','k');
```

The following base MATLAB code was used to calculate a matrix DPMOs output to an excel spreadsheet by changing various values for the mean shifts, standard deviation shifts and correlation coefficients for a Bivariate Normal Distribution:

```
format shortG
rho=-0.5;
sigma1=1;
sigma2=1;
mu1=0;
mu2=0;
row=1;
column=1;
DPMOmatrix=zeros(3);
for k21=0.5:0.5:1.5
    for k22=0.5:0.5:1.5
        k11=0;
        k12=0;
        XL=[mu1-6*sigma1+k11*sigma1 mu2-6*sigma2+k12*sigma2];
        XU=[mu1+6*sigma1+k11*sigma1 mu2+6*sigma2+k12*sigma2];
        MU = [mu1 mu2];
        a=(sigma1/k21).^2;
        b=(rho*sigma1*sigma2)/(k21*k22);
        c=(sigma2/k22).^2;
        SIGMA = [a b;b c];
        Y = mvncdf(XL,XU,MU,SIGMA);
        DPMO=(1-Y)*10.^6;
        % disp(DPMO);
    DPMOmatrix([row,column])=DPMO;
    row=row+1;
    column=column+1;
    end
end
DPMOmatrix
%filename = 'Problem4A.xlsx';
%xlswrite(filename,DPMOmatrix,1,'B2:D4')
```

Appendix C

Supporting Julia code for Chapter 5

The two-stage stochastic optimization model was solved and output to an excel file using the following two Julia files in conjunction with each other:

Model-CentralLoop.jl

```
function createandsolvemodel_CT(sd, Nr_SC,  ksi, psi, L1, L2, L3, L4, a, b, c, d,
pi_USL, pi_LSL, pi_UGB, pi_LGB,target1)

m_rand = Array{Float64}(Nr_SC)
c_rnd = Array{Float64}(Nr_SC)

#   all_quad_lazy = 0

  #m = Model(solver=CplexSolver(CPX_PARAM_MIPEMPHASIS=1,
CPX_PARAM_VARSEL=4, CPX_PARAM_PRELINEAR=0,
CPX_PARAM_REDUCE=1))
  #m = Model(solver=CplexSolver(CPX_PARAM_BARDISPLAY=1,
CPX_PARAM_MIPSEARCH=1, CPX_PARAM_PRELINEAR=0,
CPX_PARAM_REDUCE=1))
  #m = Model(solver=CplexSolver(CPX_PARAM_PREIND=0,
CPX_PARAM_EPGAP=0.00, CPX_PARAM_SCRIND=0)) #Switch off CPLEX
presolver
  #m = Model(solver=CplexSolver(CPX_PARAM_EPGAP=0.00,
CPX_PARAM_SCRIND=0)) #Switch off CPLEX presolver
  #m = Model(solver=GurobiSolver(MIPGap=0.01))
  #m = Model(solver=CouenneNLSolver())
  m = Model(solver=IpoptSolver(print_level=0))


  # Continuous Variables
  @variable(m, USL >=0)
  @variable(m, LSL >=0)
  @variable(m, UGB >=0)
  @variable(m, LGB >=0)
  @variable(m, PA >=0)
  @variable(m, PB >=0)
  @variable(m, PC >=0)
  @variable(m, Vs[1:Nr_SC] >=0)
  @variable(m, Ws[1:Nr_SC] >=0)
  @variable(m, Us[1:Nr_SC] >=0)
```

```
  @variable(m, Js[1:Nr_SC] >=0)
  @variable(m, Ls[1:Nr_SC] >=0)
  @variable(m, Gs[1:Nr_SC] >=0)
  @variable(m, Ks[1:Nr_SC] >=0)
  @variable(m, Fs[1:Nr_SC] >=0)
##################################################################
srand(sd)
for i in 1:Nr_SC
	if rand() <= 0.3
		m_rand[i] = 10000
		c_rnd[i] = 5
	else
		m_rand[i] = 5000
		c_rnd[i] = 2
	end
end
#################################################################
  # Objective
  @NLobjective(m, Max, sum{(1/Nr_SC)*((m_rand[i] - c_rnd[i]*(4*PA+PB+PC))*(PA-
q) + (m_rand[i] - c_rnd[i]*(PA+2*PB+PC))*(PB-q) + (m_rand[i] -
c_rnd[i]*(PA+PB+4*PC))*(PC-q)), i=1:Nr_SC}
 -((1/a)*(L1/(UGB - target1)) + (1/b)*(L2/(LGB - target1)) +(1/c)*(L3/(USL - target1))
+(1/d)*(L4/(LSL - target1)))
 -(pi_USL*sum{Ws[s], s=1:Nr_SC}  + pi_LSL*sum{Us[s], s=1:Nr_SC} +
pi_UGB*sum{Gs[s], s=1:Nr_SC} + pi_LGB*sum{Fs[s], s=1:Nr_SC})) # ask about
comment in simulationmodel.jl, seems this is subtracted twice when should be added
back

# -((1/a)*L1/(UGB - target1) + (1/b)*L2/(LGB - target1) +(1/c)*L3/(USL - target1)
+(1/d)*L4/(LSL - target1))
# -((1/a)*L1 + (1/b)*L2 +(1/c)*L3 +(1/d)*L4)
  # Constraints
  @NLconstraint(m, c1[s=1:Nr_SC], USL + Vs[s] - Ws[s] ==  ksi[s])
  @NLconstraint(m, c2[s=1:Nr_SC], LSL + Us[s] - Js[s] ==  ksi[s])
  @NLconstraint(m, c3[s=1:Nr_SC], UGB + Ls[s] - Gs[s] ==  psi[s])
  @NLconstraint(m, c4[s=1:Nr_SC], LGB + Ks[s] - Fs[s] ==  psi[s])
  @NLconstraint(m, c5, UGB - (USL-prec) <= 0)
  @NLconstraint(m, c6, LSL - (LGB-prec) <= 0)
  @NLconstraint(m, c7, LSL - USL <= 0)
  @NLconstraint(m, c8, LGB - UGB <= 0)
  @NLconstraint(m, c9, q - (PA-err) <= 0) #marginal profit per unit must be strictly
positive
  @NLconstraint(m, c10, q - (PB-err) <= 0)
  @NLconstraint(m, c11, q - (PC-err) <= 0)
```

```
  @NLconstraint(m, c12, target1 - (UGB-prec) <= 0)
        @NLconstraint(m, c14, LGB - (target1-prec)<= 0)
        @NLconstraint(m, c16, 5*(4*PA+PB+PC)<= 10000-err)#demand must be
greater than zero case 1
        @NLconstraint(m, c17, 5*(PA+2*PB+PC)<= 10000-err)
        @NLconstraint(m, c18, 5*(PA+PB+4*PC)<= 10000-err)
        @NLconstraint(m, c19, 2*(4*PA+PB+PC)<= 5000-err)#demand must be greater
than  zero case 2
        @NLconstraint(m, c20, 2*(PA+2*PB+PC)<= 5000-err)
        @NLconstraint(m, c21, 2*(PA+PB+4*PC)<= 5000-err)


  tic()
  status = solve(m)

  if (status == :Optimal)
                println("Status 1:", status)
                Obj = getobjectivevalue(m)
                USL_opt = getvalue(USL)
                LSL_opt = getvalue(LSL)
                UGB_opt = getvalue(UGB)
                LGB_opt = getvalue(LGB)
                PA_opt = getvalue(PA)
                PB_opt = getvalue(PB)
                PC_opt = getvalue(PC)
                Vs_opt = getvalue(Vs)
                Ws_opt= getvalue(Ws)
                Us_opt = getvalue(Us)
                Js_opt = getvalue(Js)
                Ls_opt= getvalue(Ls)
                Gs_opt= getvalue(Gs)
                Ks_opt= getvalue(Ks)
                Fs_opt= getvalue(Fs)
                T_cpu = toq()
   elseif (status == :UserLimit)
      println("Status 2:", status)
                Obj = getobjectivevalue(m)
                USL_opt = getvalue(USL)
                LSL_opt = getvalue(LSL)
                UGB_opt = getvalue(UGB)
                LGB_opt = getvalue(LGB)
                PA_opt = getvalue(PA)
                PB_opt = getvalue(PB)
                PC_opt = getvalue(PC)
```

```
            Vs_opt = getvalue(Vs)
            Ws_opt= getvalue(Ws)
            Us_opt = getvalue(Us)
            Js_opt = getvalue(Js)
            Ls_opt= getvalue(Ls)
            Gs_opt= getvalue(Gs)
            Ks_opt= getvalue(Ks)
            Fs_opt= getvalue(Fs)
            T_cpu = toq()
        else
            println("Status 3:", status)
            Obj = 0
            Obj = getobjectivevalue(m)
            USL_opt = 0
            LSL_opt = 0
            UGB_opt = 0
            LGB_opt = 0
            PA_opt = 0
            PB_opt = 0
            PC_opt = 0
            Vs_opt = 0
            Ws_opt= 0
            Us_opt = 0
            Js_opt = 0
            Ls_opt= 0
            Gs_opt= 0
            Ks_opt= 0
            Fs_opt= 0
            T_cpu = toq()
  end

 #print(m)
 #writeLP(m,"Model.lp")
 # println("******************************************")
  #println("Objective value: ", Obj)
  #println("***Run time = : ",T_cpu)
  #println("******************************************")

  return Obj, USL_opt, LSL_opt, UGB_opt, LGB_opt, PA_opt, PB_opt, PC_opt,
Vs_opt,Ws_opt,Us_opt,Js_opt,Ls_opt,Gs_opt,Ks_opt,Fs_opt

end
```

SimulationModelLoop.jl

```
# ----------------------------------------
# Tolerance Optimization PROBLEM
# ----------------------------------------
using JuMP,  MathProgBase, CPLEX,  Gurobi, MAT, GLPKMathProgInterface, JLD,
Distributions, MathProgBase, AmplNLWriter,Ipopt, Gurobi, CPLEX, MAT, Graphs,
JLD,  GLPKMathProgInterface
#CoinOptServices
include("Model-CentralLoop.jl")


#############CONSTANTS######################
Scenarios = 30
SeedMax = 30
beta = 0.1 #upper spec limit max vio chance
alpha = 0.1 #lower spec limit max vio chance
gamma = 0.4 #upper GB max vio chance
delta = 0.4 #lower GB max vio chance
eps = 0.001
err= 0.0001
prec= 0.05 # max precision
q = 230 # production cost
M = 0 #fixed counter
N = 0 #fixed counter
K = 0 #fixed counter
L = 0 #fixed counter
mu1=24
sd1=2 #alpha beta gamma delta are production dependent, change standard deviation
together with alpha beta delta gamma.
mu2=24
sd2=2
l = 165 #upper guard band cost psi
e = 135 #lower guard band cost psi
f = 230 #upper spec limit ksi
k = 230 #lower spec limit ksi 3,10,30,60,90 (orig 2)
target1 = 25
Last_Obj = 0
Last_USL = 0
Last_LSL = 0
Last_UGB = 0
Last_LGB = 0
Last_PA = 0
Last_PB = 0
```

```
Last_PC = 0
##############DECALRATIONS####################

 ksi = Array{Float64}(Scenarios)
 psi = Array{Float64}(Scenarios)
 t_ksi = Array{Float64}(Scenarios)
 t_psi = Array{Float64}(Scenarios)

######Generating truncated normal random variables###################
for seed in 1:SeedMax
 srand(seed)
 psi = rand(Normal(mu1,sd1), Scenarios)
 t_psi =psi
  #Truncated(psi,lb,ub)-----check this
 srand(seed)
 ksi = rand(Normal(mu2,sd2), Scenarios)


 a = 0
 L1 = 0
 b = 0
 L2 = 0
 for i in 1:Scenarios
          @printf(" seed=%d \t tpsi[%d]=%1.2f \n",seed,i, t_psi[i])
          if t_psi[i] > target1
                    a = a +1
                    L1 = L1 + l*(t_psi[i] - target1)
          else
                    b = b +1
                    L2 = L2 + e*(t_psi[i] - target1)
          end
 end



 for i in 1:Scenarios
          if t_ksi[i] < 0
                    t_ksi[i] = 0
          else
                    t_ksi[i] = ksi[i]
          end
 end

 c = 0
```

```
 L3 = 0
 d = 0
 L4 = 0
 for i in 1:Scenarios
        if t_ksi[i] > target1
                c = c +1
                L3 = L3 + f*(t_ksi[i] - target1)
        else
                d = d +1
                L4 = L4 + k*(t_ksi[i] - target1)
        end
 end

##########Running the model######################
pi1 = 1000000000
pi2 = 1000000000
pi3 = 1000000000
pi4 = 1000000000

Max_pi1 = 1000000
Max_pi2 = 1000000
Max_pi3 = 1000000
Max_pi4 = 1000000

Min_pi1 = 0
Min_pi2 = 0
Min_pi3 = 0
Min_pi4 = 0

        while (abs(pi1 - (Min_pi1 + Max_pi1)/2) >= eps || abs(pi2 - (Min_pi2 +
Max_pi2)/2) >= eps)
                @printf("absolute value calculation: %1.2f %1.2f %1.2f \n",abs(pi1 -
(Min_pi1 + Max_pi1)/2), abs(pi2 - (Min_pi2 + Max_pi2)/2), delta)
                @printf("pi1 = %1.2f \n",pi1)
                @printf("pi2 = %1.2f \n",pi2)
                pi1 = (Min_pi1 + Max_pi1)/2
                pi2 = (Min_pi2 + Max_pi2)/2
                pi3 = (Min_pi3 + Max_pi3)/2
                pi4 = (Min_pi4 + Max_pi4)/2

                Obj, USL, LSL, UGB, LGB, PA, PB, PC, Vs, Ws, Us, Js, Ls, Gs, Ks, Fs
= createandsolvemodel_CT(seed, Scenarios, t_psi, t_ksi, L1, L2, L3, L4, a, b, c, d, pi1,
pi2,pi3,pi4, target1)
                for i in 1:Scenarios
```

```
		if t_psi[i] > USL
			t_psi[i] = USL
		elseif t_psi[i] < LSL
			t_psi[i] = LSL
		end

	end

	M = 0
	N = 0
	K = 0
	L = 0

	for s in 1:Scenarios
		if Ws[s] > 0
			M = M + 1
		end
		if Us[s] > 0
			N = N + 1
		end
		if Gs[s] > 0
			K = K + 1
		end
		if Ks[s] > 0
			L = L + 1
		end
	end
	@printf("[%d %d] beta*sc = %1.2f eps= %1.2f\n",M,N, beta*Scenarios,
eps)
	if (M >= beta*Scenarios + eps)
		Min_pi1 =(Min_pi1 + Max_pi1)/2
		#@printf("Min_pia updated to = %1.2f \n", Min_pia)
	elseif (M <= beta*Scenarios - eps)
		Max_pi1 =(Min_pi1 + Max_pi1)/2
		#@printf("Max_pia updated to = %1.2f \n", Max_pia)
	end
	if (N >= alpha*Scenarios + eps)
		Min_pi2 =(Min_pi2 + Max_pi2)/2
		#@printf("Min_pit updated to = %1.2f \n", Min_pit)
	elseif (N <= alpha*Scenarios - eps)
		Max_pi2 =(Min_pi2 + Max_pi2)/2
		#@printf("Max_pit updated to = %1.2f \n", Max_pit)
	end
```

```
		if (K >= gamma*Scenarios + eps)
			Min_pi3 =(Min_pi3 + Max_pi3)/2
			#@printf("Min_pia updated to = %1.2f \n", Min_pia)
		elseif (M <= gamma*Scenarios - eps)
			Max_pi1 =(Min_pi3 + Max_pi3)/2
			#@printf("Max_pia updated to = %1.2f \n", Max_pia)
		end
		if (L >= delta*Scenarios + eps)
			Min_pi4 =(Min_pi4 + Max_pi4)/2
			#@printf("Min_pit updated to = %1.2f \n", Min_pit)
		elseif (L <= delta*Scenarios - eps)
			Max_pi4 =(Min_pi4 + Max_pi4)/2
			#@printf("Max_pit updated to = %1.2f \n", Max_pit)
		end

 ###############Printing##################################

 for i in 1:Scenarios
	Obj = Obj + pi1*Ws[i] + pi2*Us[i] + pi3*Gs[i] + pi4*Fs[i] # should this be
adding these values instead of subtracting?
 end

 EdemandA= .3*(10000-5(4*PA+PB+PC))+.7*(5000-2(4*PA+PB+PC))
 EdemandB= .3*(10000-5(PA+2*PB+PC))+.7*(5000-2(PA+2*PB+PC))
 EdemandC= .3*(10000-5(PA+PB+4*PC))+.7*(5000-2(PA+PB+4*PC))

  @printf("Obj value = %1.2f \n", Obj)
  @printf("USL value = %1.2f \n", USL)
  @printf("LSL value = %1.2f \n", LSL)
  @printf("UGB value = %1.2f \n", UGB)
  @printf("LGB value = %1.2f \n", LGB)
  @printf("PA value = %1.2f \n", PA)
  @printf("PB value = %1.2f \n", PB)
  @printf("PC value = %1.2f \n", PC)
 @printf("EdemandA value = %1.2f \n", EdemandA)
 @printf("EdemandB value = %1.2f \n", EdemandB)
 @printf("EdemandC value = %1.2f \n", EdemandC)

 outputfilename1 = "ToleranceOptSol.xls"
 outputfile1 = open(outputfilename1, "a")
#labeling columns and rows
 #@printf(outputfile1, "Scenarios \n",)
 # rounding solutions printline
```

```
# @printf(outputfile1,"%f\t %f\t %f\t %f\t %f\t %f\t %f\t %f\t %f\t %f\t \n", Scenarios,
seed, round(Obj,0), round(USL,2), round(LSL,2), round(UGB,2), round(LGB,2),
round(PA,2), round(PB,2), round(PC,2))
#@printf(outputfile1,"%f\t %f\t %f\t %f\t %f\t %f\t %f\t %f\t %f\t %f\t \n", Scenarios,
seed, Obj, USL, LSL, UGB, LGB, PA, PB, PC )
Last_Obj = Obj
Last_USL = USL
Last_LSL = LSL
Last_UGB = UGB
Last_LGB = LGB
Last_PA = PA
Last_PB = PB
Last_PC = PC
 end
 outputfilename1 = "FiveSuppliers.xls"
 outputfile1 = open(outputfilename1, "a")
 @printf(outputfile1,"%f\t %f\t %f\t %f\t %f\t %f\t %f\t %f\t %f\t %f\t %f\t %f\t %f\t
%f\t %f\t %f\t %f\t %f\t %f\t %f\t \n",beta, alpha, gamma, delta, prec, q, l, e, f, k,
Scenarios, seed, Last_Obj, Last_USL, Last_LSL, Last_UGB, Last_LGB, Last_PA,
Last_PB, Last_PC )
 close(outputfile1)
end
```

Boxplots for the results of the output of the solution to the model were generated with the following MATLAB code:

```
format ShortG;
sheet = 1;
CostRange= 'A2:A151';
ObjRange = 'B2:B151';
filename='Cost Sensitivity Plots.xlsx';
costdata = xlsread(filename);
Cost = xlsread(filename,sheet,CostRange);
ObjectiveValue=xlsread(filename,sheet,ObjRange);
figure
boxplot(ObjectiveValue,Cost,'Notch','on')
box on;
grid on;
title('Profit vs. Production Cost')
xlabel('Production Cost')
ylabel('Profit')
```

Boxplots with sublplots were generated with the following MATLAB code:

```
%basic data extraction
format ShortG;
sheet = 1;
```

```
CostRange= 'A2:A151';
PaRange = 'B2:B151';
PbRange = 'C2:C151';
PcRange = 'D2:D151';
filename='CostvsPricePlots.xlsx';
costdata = xlsread(filename);
Cost = xlsread(filename,sheet,CostRange);
Pa=xlsread(filename,sheet,PaRange);
Pb=xlsread(filename,sheet,PbRange);
Pc=xlsread(filename,sheet,PcRange);
%data input formating for boxplot2 function
a=transpose(Pa);
b=transpose(Pb);
c=transpose(Pc);
d=Pa(2:31);
e=Pb(2:31);
g=Pc(2:31);
h=Pa(32:61);
%i=Pb(32:61);
j=Pc(32:61);
x = [50 100 200 300 325];
y = randn(5, 3, 100);
figure
box on;
grid on;
subplot(1,3,1)
boxplot(Pa,Cost, 'notch', 'on')
title('Subplot 1:Pa')
ylabel('Selling Price')
subplot(1,3,2)
boxplot(Pb,Cost, 'notch', 'on')
title('Subplot 2:Pb')
xlabel('Production Cost')
subplot(1,3,3)
boxplot(Pc,Cost, 'notch', 'on')
title('Subplot 3:Pc')
suptitle('Selling Price vs. Production Cost')
```

REFERENCES

Aggarwal, O. P., Guttman, I. (1960). Truncation and tests of hypotheses. *The Annals of Mathematical Statistics, 31*(4), 1213.

Alhyari, S., Alazab, M., Venkatraman, S., Alazab, M., & Alazab, A. (2012). Quality in E-Services: An Empirical Study in Jordan. *International Journal of Electronic Government Research*, *8*(2), 57-74. doi:10.4018/jegr.2012040103

Allen, F. M., Braswell, R. N., & Rao, P. V. (1974). Distribution-Free Approximations for Chance Constraints. *Operations Research, 22*(3), 610-621.

Antony, J. (2004). Some pros and cons of six sigma: an academic perpective. *The TQM Magazine, 16*(4), 4. doi:10.1108/0954478041054195

Arellano-Valle, R. B., del Pino, G., San Martin, E. . (2002). Definition and probabilistic of skew-distributions. *Statistics and Probability Letters, 58*(2), 111-121.

Azzalini, A. (1985). A class of distributions which includes the normal ones. *Scandinavian Journal of Statistics, 12*(2), 171-178.

Azzalini, A. (1986). Further results on a class of distributions which includes the normal ones. *Statistica, 46*, 199-208.

Azzalini, A. (2005). The skew-normal distribution and related mulitvariate families (with discussion). *Scandinavian Journal of Statistics, 32*, 159-188.

Azzalini, A., Capitanio, A. (1999). Statistical applications of the multivariate skew normal distribution. *Journal of Royal Statistical Society Series B, 61*(3), 579-602.

Azzalini, A., Valle, D. (1996). The multivariate skew-normal distribution. *Biometrika, 83*(4), 715-726.

Barr, D. R., & Sherrill, E. T. (1999). Mean and Varience of Truncated Normal Distributions. *The American Statistician, 53*(4), 357-361.

Birge, J., & Louveaux, F. (1997). *Introduction to Stochastic Programming*.

Birnbaum, Z. W. a. A., F.C. (1949). On Sums of Symmetrically Truncated Normal Random Variables. *The Annals of Mathematical Statistics, 20*(3), 458-461.

Bissell, A. F. (1990). How Reliable Is Your Capability Index? *Applied Statistics*, *39*(3), 331-340.

Bjørke, Ø. (1989). *Computer-Aided Tolerancing* (Second Edition ed.). New York, N.Y.: ASME Press.

Bothe, D. R. (2002) "Statistical Reason for the 1.5 Sigma Shift." *Quality Engineering* Vol. 14 No. 3, pp. 479-487.

Box, G. E. P., & Cox, D. R. (1964). An Analysis of Transformations. *Journal of the Royal Statistical Society, Series B*(26), 211-252.

Boyles, R. A. (1991). The Taguchi Capability Index. *Journal of Quality Technology, 23*(2), 107-126.

Cao, Y., Mao, J., & Yang, J. (2009). A robust tolerance optimization method based on fuzzy quality loss. *Proceedings of the Institute of Mechanical Engineers, Part C: Journal of Mechanical Engineering Science, 223*, 2647-2653.

Carrigan, M. D. and D. Kujawa. (2006) "Six Sigma in health care management and strategy." *The Health Care Manager* Vol. 25 No. 2, pp. 133-141.

Ceglarek, D., & Shi, J. (1995). Dimensional Variation Reduction for Automotive Body Assembly. *Manufacturing Review, 8*(2), 139-154.

Cha, Jinho, "Re-Establishing the Theoretical Foundations of a Truncated Normal Distribution: Standardization Statistical Inference, and Convolution" (2015).All Dissertations. Paper 1793. http://tigerprints.clemson.edu/cgi/viewcontent.cgi?article=2794&context=all_dissertations

Cha, J., Cho, B.R. (2014). Classical Statistical Inference Extended to Truncated Populations for Continuous Process Improvement: Test Statistics, P-values, and Confidence Intervals. *Quality and Reliability Engineering International*. doi:10.1002/qre.1719

Cha, J., Cho, B.R., Sharp, J.L. (2014). Rethinking the truncated normal distribution. *Experimental Design and Process Optimisation*, *3*(4), 327-363.

Chan, L. K., Cheng, S. W., & Spiring, F. A. (1988). A New Measure of Process Capability: Cpm. *Journal of Quality Technology, 20*(3), 160-175.

Chang, B.-W., & Maghsoodloo, S. (1995). Optimization of Mechanical Assembly Tolerances by Incorporating Taguchi's Quality Loss Function. *Journal of Manufacturing Systems, 14*(4), 264-276.

Charnes, A., & Cooper, W. W. (1959). Chance-Constrained Programming. *Management Science, 6*(1), 73-79.

Charnes, A., & Cooper, W. W. (1962). Chance Constraints and Normal Deviates. *Journal of the American Statistical Association, 57*(297), 134-148.

Charnes, A., & Cooper, W. W. (1963). Deterministic Equivalents for Optimizing and Satisficing under Chance Constraints. *Operations Research, 11*(1), 18-39.

Chase, K. W., Loosli, B. G., Greenwood, W. H., & Hauglund, L. F. (1990). Least Cost Tolerance Allocation for Mechanical Assemblies with Automated Process Selection. *Manufacturing Review, 3*(1), 49-59.

Chattinnawat, W. (2015). Statistical tolerance design to minimize dual-responses of APFA height deviations with tolerance cost quality loss model. *International Journal of Quality and Reliability Management, 32*(5).

Chen, M.-C. (2001). Tolerance synthesis by neural learning and nonlinear programming. *International Journal of Production Economics, 70*, 55-65.

Chiao, T. C. (2006) "Strategic quality competitiveness management." *International Journal of Information Technology and Management* Vol. 5 No. 2-3, pp. 197-211.

Cho, B. R., & Hong, S. H. (2007). Joint optimization of process target mean and tolerance limits with measurement errors under multi-decision alternatives. *European Journal of Operational Research, 183*, 327-335.

Cox, N. D. (1986). *Volume 11: How to Perform Statistical Tolerance Analysis.* Milwaukee, Wisconsin: American Society for Quality Control.

Das, P. (2005) "Reduction in procurement of materials using Six Sigma philosophy." *Total Quality Management & Business Excellence* Vol. 16 No. 5, pp. 645-656.

Das, R., & Jones, R. (2015). Characteristics of the design surface of damage tolerance parameters and their relation to shape optimisation. *International Journal of Fatigue, 70*, 490-502.

Dong, Z., Hu, W., & Xue, D. (1994). New Production Cost-Tolerance Models for Tolerance Synthesis. *Journal of Engineering for Industry, 116*(2), 199-206.

Elder, B. L. (2008) "Six Sigma in the Microbiology Laboaratory." *Clinical Microbiology Newsletter* Vol. 30 No. 19 pp. 243-147.

English, J. R., & Taylor, G. D. (1993). Process Capability Analysis: A Robustness Study. *International Journal of Production Research, 31*(7), 1621-1635.

Erdogan, E. (2006). *Ambiguous Chance Contrained Programs: Algorithms and Applications.* (Doctor of Industrial Engineering and Operations Research), Columbia University, New York.

Euler, L. (1748). *Introductio in analysin infinitorum, tomus I.* Lausanne: Bousquet.

Euler, L. (1750). Lausanne: Bousquet. *Commentarii Academiae Scientiarum Petropolitanae, 11*, 32-81.

Evans, D. H. (1975). Statistical Tolerancing: the state of the art. Part III. shifts and drifts. *Journal of Quality Technology, 7*, 72-76.

Flecher C., A. D., Naveau P. (2010). Truncated skew-normal distributions: moments, estimation by weighted moments and application to climatic data. *International Journal of Statistics, LXVIII*(3), 331-345.

Fortini, E. T. (1967). *Dimensioning for Interchangeable Manufacture*. New York, N. Y.: Industrial Press Inc.

Francis, V. J. (1946). On the distribution of the sum of n sample values drawn from a truncated normal distribution. *Supplement to the Journal of the Royal Statistical Society, 8*(2), 223-232.

Geetha, K., Ravindran, D., Kumar, M. S., & Islam, M. N. (2013). Multi-objective optimization for optimum tolerance synthesis with process and machine selection using a genetic algorithm. *International Journal of Advanced Manufacturing Technology, 67*, 2439-2457.

Gijo, E. V., & Sarkar, A. (2012). Application of Six Sigma to improve the quality of the road for wind turbine installation. *The TQM Journal, 25*(3), 244-258. doi:10.1108/17542731311307438

Gilson, J. (1951). *A New Approach to Engineering Tolerances: a critical presentation of the considerations necessary for the allocation and maintenance of realistic tolerances in modern economic production* (First ed.). London: Machinery Publishing Company.

Goethals, P. L., & Cho, B. R. (2011). Solving the optimal process target problem using response surface designs in heteroscedastic conditions. *International Journal of Production Research, 49*(12), 3455-3478.

Greenwood, W. H., & Chase, K. W. (1987). A new tolerance analysis method for design and manufacturers. *Transactions of the American Society of Mechanical Engineers: Journal of Engineering for Industry, 109*(2), 112-116.

Gupta, A. K., Chen, J.T. (2004). A class of multivaraiate skew-normal models. *Annals of The Institute of Statistical Mathematics, 56*(2), 305-315.

Henzold, G. (1995). *Handbook of Geometrical Tolerancing, Design, Manufacturing and Inspection*. New York, N. Y.: John Wiley and Sons.

Hernandez, F., & Johnson, R. A. (1980). The Large-Sample Behavior of Transformations to Normality. *Journal of the American Statistical Association, 75*(372), 855-861.

Huang, X. (2007). Chance-constrained programming models for capital budgeting with NPV as fuzzy parameters. *Journal of Computational and Applied Mathematics, 198*(1), 149-159. Retrieved from http://www.sciencedirect.com/science/article/pii/S0377042705007120

Jamalizadeh, A., Behboodian, J., Balakrishnan, N. . (2008). A two-parameter generalized skew-normal distribution. *Statistics and Probability Letters, 78*(13), 1722-1726.

Jawitz, J. W. (2004). Moments of truncated continuous univariate distributions. *The Advanced in Water Resources, 27*(3), 269-281.

Kamberi, M., H. Garcia, D. P. Feder, R. J. Rapoza. (2011) "Setting acceptance criteria for validation of analytical methods of drug eluting stents: Minimum requirements for analytical variability." *European Journal of Phamaceutical Science* Vol. 42 No. 3, pp. 230-237.

Kataoka, S. (1963). A Stochastic Programming Model. *Econometrica, 31*(1 2), 181-196.

Kazemi, M. R., Haghbin, H., Behboodian, J. (2011). Another generation of the skew normal distribution. *World Applied Science Journal, 12*(7), 1034-1039.

Khasawneh, M., Bowling, S.R., Kaewkuekool, S. and Cho, B.R. (2005). Tables of a truncated standard normal distribution: a doubly truncated case. *Quality Engineering, 17*(2), 227-241.

Khasawneh, M., Bowling, S.R., Kaewkuekool, S. and Cho, B.R. (2005(a)). Tables of a truncated standard normal distribution: a singly truncated case. *Quality Engineering, 17*(1), 33-50.

Kim, T. M. a. T., T. . (2003). Computational Improvement for Expected Sliding Distance of a Caisson-Type Breakwater by Introduction of a Doubly-Truncated Normal Distribution. *Coastal Engineering, 45*(3), 387-419. doi:10.1142/S0578563403000816

Kirschling, G. (1988). *Qualit¨atssicherung und Toleranzen*. Berlin, Germany: Springer-Verlag.

Kotz, S., & Lovelace, C. R. (1998). *Process Capability Indices in Theory and Practice*. London: Arnold.

Kratuengarn, R. (1973). *Distribution of sums of truncated normal variables.* (Master of Science Dissertations & Theses), University of Strathclyde (United Kingdom), Ann Arbor (United States).

Krenek, R., Cha J., Cho, B.R. and J. L. Sharp (2017) 'Development of statistical convolutions of truncated normal and truncated skew normal distributions with applications', Journal of Statistical Theory and Practice, Vol. 11,No. 1, pp.1-25.

Krenek, R., Cha, J. and Cho, B.R. (2015) 'Zipping and re-zipping methods to improve the precision and accuracy of manufacturing processes', Int. J. Experimental Design and Process Optimisation, Vol. 4, Nos. 3/4, pp.256–289

Krenek, R. and Cho, B.R. (2015) 'The expanded DPMO interface for capturing the compounding effect of process mean and variability as a new paradigm for process evaluation and improvement', Int. J. Six Sigma and Competitive Advantage, Vol. 9, Nos. 2/3/4, pp.174–207.

Kushler, R. H., & Hurley, P. (1992). Confidence Bounds for Capability Indices. *Journal of Quality Technology, 24*(4), 188-195.

Lanier, F. H., C. L. I. Godniez, S. D. Aguirre, and D. A. Garcia. (2012) "Design methodology of the reverse supply chain for the management of the solid waster in Cuba." *International Journal of Environmental Engineering*, Vol. 4 No. 3-4, pp. 283-306.

Lanza, G., Haefner, B., & Kraemer, A. (2015). Optimization of selective assembly and adaptive manufacturing by means of cyber-physical system based matching. *CIRP Annals- Manufacturing Technology, 64*(1), 399-402.

Laureani, A., Antony, J., & Douglas, A. (2010). Lean six sigma in a call centre: a case study. *International Journal of Productivity and Performance Management*, *59*(8), 757-768. doi:10.1101/17410401011089454

Levlzow, C. B. and M. S. Willis. (2013) "Reducing laboratory billing defects using Six Sigma principles. *Lab Medicine*, Vol. 44, pp. 358-371.

Li, S. (1995). An Insurance and Investment Portfolio Model Using Chance Constrained Programming. *Omega*, *23*(5), 577-585.

Lichensteiger, S., & Bickford, J. P. (2013). Using Selective Voltage Binning to Maximize Yield. *IEEE Transactions on Semiconductor Manufacturing, 26*(4), 436-441.

Lipow, M., Mantel, N., Wilkinson, J. W. (1964). The Sum of Values from a Normal and a Truncated Normal Distribution. *Technometrics, 6*(4), 469-471.

Lou, X. Y. (2015). Research on Green Manufacturing Technology for Electromechanical Products. *Applied Mechanics and Materials, 722*, 426-429.

Lu, C., Zhao, W.-H., & Yu, S.-J. (2012). Concurrent tolerance design for manufacture and assembly with a game theoretic approach. *International Journal of Advanced Manufacturing Technology, 62*, 303-316.

Luceño, A. (1996). A Process Capability Ratio with Reliable Confidence Intervals. *Communications in Statistics-Simulation and Computation, 25*(1), 235-246.

Luo, Y., Wu, X., Zhou, M., & Wang, M. Y. (2014). Simultaneous parameter and tolerance optimization of structures via probability-interval mixed reliability model. *Structural and Multidisciplinary Optimization*.

MacGregor, J.F., and T. Kourti. (1995) "Statistical Process Control of Multivariate Processes." *Control Engineering Practice* Vol. 3 No. 3, pp. 403-414.

Makarov, Y. V., Loutan, C., Ma, J., & Mello, P. d. (2009). Operational Impacts of Wind Generation on California Power Systems. *IEEE Transactions on Power Systems, 24*(2), 1039-1050.

Maleyeff, J. and D. E. Krayenvenger (2004) "Goal setting with Six Sigma mean shift determination." *Aircraft Engineering and Aerospace Technology*

Mansoor, E. M. (1963). *The application of probability to tolerances used in engineering designs*.

Mease, D., Nair, V. N., & Sudjianto, A. (2004). Selective Assembly in Manufacturing: Statistical Issues and Optimal Binning Strategies. *Technometrics, 24*(2), 165-175.

Miller, B. L., & Wagner, H. M. (1965). Chance Constrained Programming with Joint Constraints. *Operations Research, 13*(6), 930-945.

Montgomery, D. C. (2013) *Introduction to Statistical Quality Control*, Hoboken, New Jersey, John Wiley & Sons.

Montgomery, D. C., & Woodall, W. H. (2008). An Overview of Six Sigma. *International Statistical Review, 76*(3), 18. doi:10.1111

Nadarajah, S., Kotz, S. (2006). Skew distributions generated from different families. *Acta Applicandae Mathematicae, 91*(1), 1-37.

Nemirovski, A., & Shapiro, A. (2006). Convex Approximations of Chance Constrained Programs. *SIAM Journal of Optimization, 17*(4), 969-996.

Ngaile, G., Wang, J., & Gau, J.-T. (2015). Challenges in teaching modern manufacturing technologies. *European Journal of Engineering Education*, 1-18.

Nigam, S. D., & Turner, J. U. (1995). Review of statistical approaches to tolerance analysis. *Computer-Aided Design, 27*(1), 6-15.

Pagnoncelli, B. K., Ahmed, S., & Shapiro, A. (2009). Sample Average Approximation Method for Chance Constrained Programming: Theory and Applications. *Journal of Optimization Theory and Applications, 142*(2), 399-416.

Pearn, W. L., Kotz, S., & Johnson, N. L. (1992). Distributional and Inferential Properties of Process Capability Indices. *Journal of Quality Technology, 24*(4), 216-231.

Pocha, C. (2010). "Lean Six Sigma in Health Care and Challenge of Implementation of Six Sigma Methodologies at a Veterans Affairs Medical Center." *Quality Management in Health Care* Vol.19 No. 4, pp. 312-318.

Prabhaharan, G., Asokan, P., & Rajendran, S. (2005). Sensitivity-based conceptual design and tolerance allocation using the continuous ants colony algorithm. *International Journal of Advanced Manufacturing Technology, 25*, 516-526.

Pugh, G. A. (1986). Partitioning for Selective Assembly. *Computers and Industrial Engineering, 11*(1-4), 175-179.

Pugh, G. A. (1992). Selective Assembly with Components of Dissimilar Variance. *Computers and Industrial Engineering, 23*(1-4), 487-491.

Roberts, C. (1966). A correlation model useful in the study of twins. *Journal of the American Statistical Association, 61*(316), 1184-1190.

Santos, D. L., R. B. Raj, M. Lane, and D. Sissenstein. (1997) "Defect reduction in PCB contract manufacturing operations." *Computers & Industrial Engineering*, Vol.33 No. 3-4, pp. 381-384.

Scholz, F. W. (1995). *Tolerance stack analysis methods, a critical review*. Retrieved from the Research and Technology group of Boeing Information and Support Services

Shin, S., & Cho, B. R. (2009). Studies on a biobjective robust design optimization problem. *IIE Transactions, 41*, 957-968.

Singh, P. K., Jain, P. K., & Jain, S. C. (2009). Important issues in tolerance design of mechanical assemblies. Part 2: tolerance synthesis. *Proceedings of the Institute of Mechanical Engineers, Part B: Journal of Engineering Manufacture, 223*(10), 1249-1287.

Singh, P. K., Jain, S. C., & Jain, P. K. (2004). A genetic algorithm based solution to optimum tolerance synthesis of mechanical assemblies with alternate manufacturing process-benchmarking with the exhaustive search method using the Lagrange multiplier. *Proceedings of the Institute of Mechanical Engineers, Part B: Journal of Engineering Manufacture, 218*(7), 765-778.

Sivakumar, K., Balamurugan, C., & Ramabalan, S. (2011). Concurrent multi-objective tolerance allocation of mechanical assemblies considering alternative manufacturing process selection. *International Journal of Advanced Manufacturing Technology, 53*, 711-732.

Somerville, S. E., & Montgomery, D. C. (1996). Process Capability Indices and Nonnormal Distributions. *Quality Engineering, 9*(2), 305-316.

Stevenson, J. R. (2009). *Detecting the Process' 1.5 Sigma Shift: A Quantitative Study.* (Doctor of Industrial Technology), University of Northern Iowa, Cedar Falls.

Symonds, G. H. (1967). Deterministic Solutions for a Class of Chance-Constrained Problems. *Operations Research, 15*(3), 495-512.

Taner, M. T., Kagan, G., Celik, S., Erbas, E., & Kagan, M. K. (2013). Formation of Six Sigma Infrastructure for the Coronary Stenting Process. *International Review of Management and Marketing, 3*(4), 232-242.

Taner, M. T., Sezen, B., & Atwat, K. M. (2011). Application of Six Sigma methodology to a diagnostic imaging process. *International Journal of Healthcare Quality Assurance, 25*(4), 274-290. doi:10.1108/09526861211221482

Thore, S. (1987). Chance-constrained activity analysis. *European Journal of Operational Research, 30*(3), 267-269. Retrieved from http://www.sciencedirect.com/science/article/pii/0377221787900701

Tsai, J. C. a. K., C.H. (2012). A novel statistical tolerance analysis method for assembled parts. *International Journal of Production Research, 50*(12), 3498-3513.

Vernic, R. (2006). Multivariate skew-normal distributions with applications in insurance. *Mathematics and Economics, 38*(2), 413-426.

Wächer, A. (2002). *An Interior Point Algorithm for Large-Scale Nonlinear Optimization with Applications in Process Engineering.* (Doctor of Chemical Engineering), Carnegie Mellon University, Pittsburgh.

Wade, O. R. (1967). *Tolerance Control in Design and Manufacturing*. New York, N.Y.: Industrial Press Inc.

Wu, C.-C., Chen, Z., & Tang, G.-T. (1998). Component tolerance design for minimum quality loss and manufacturing cost. *Computers in Industry, 35*, 223-232.

Yang, L., Y.-R.Wang, and S. Pai. (2009) "On-line SPC with consideration of learning curve." *Computers & Industrial Engineering*, Vol. 57 No. 3, pp.1089-1095.

Zhang, N. F., Stenback, G. A., & Wardrop, D. M. (1990). Interval Estimation of Process Capability Index Cpk. *Communications in Statistics-Theory and Methods, 19*(12), 4455-4470.